

In compliance with the
Canadian Privacy Legislation
some supporting forms
may have been removed from
this dissertation.

While these forms may be included
in the document page count,
their removal does not represent
any loss of content from the dissertation.

University of Alberta

The Life Cycle of the Conjugative Plasmid

by

Trevor D. Lawley 

A thesis submitted to the Faculty of Graduate Studies and Research in partial fulfillment
of the requirements for the degree of Doctor of Philosophy in Microbiology and
Biotechnology.

Department of Biological Sciences

Edmonton, Alberta

Fall 2003



National Library
of Canada

Bibliothèque nationale
du Canada

Acquisitions and
Bibliographic Services

Acquisitons et
services bibliographiques

395 Wellington Street
Ottawa ON K1A 0N4
Canada

395, rue Wellington
Ottawa ON K1A 0N4
Canada

Your file *Votre référence*
ISBN: 0-612-88009-5
Our file *Notre référence*
ISBN: 0-612-88009-5

The author has granted a non-exclusive licence allowing the National Library of Canada to reproduce, loan, distribute or sell copies of this thesis in microform, paper or electronic formats.

L'auteur a accordé une licence non exclusive permettant à la Bibliothèque nationale du Canada de reproduire, prêter, distribuer ou vendre des copies de cette thèse sous la forme de microfiche/film, de reproduction sur papier ou sur format électronique.

The author retains ownership of the copyright in this thesis. Neither the thesis nor substantial extracts from it may be printed or otherwise reproduced without the author's permission.

L'auteur conserve la propriété du droit d'auteur qui protège cette thèse. Ni la thèse ni des extraits substantiels de celle-ci ne doivent être imprimés ou autrement reproduits sans son autorisation.

Canada

University of Alberta

Library Release Form

Name of Author: Trevor D. Lawley

Title of Thesis: The Life Cycle of the Conjugative Plasmid

Degree: Doctor of Philosophy

Year this Degree Granted: 2003

Permission is hereby granted to the University of Alberta Library to reproduce single copies of this thesis and to lend or sell such copies for private, scholarly, or scientific purposes only.

The author reserves all other publication and other rights in association with the copyright in this thesis, and except as herein before provided, neither the thesis nor any substantial portion thereof may be printed or otherwise reproduced in any material form without the author's prior written permission.

Date:

June 30, 2003

University of Alberta

Faculty of Graduate Studies and Research

The undersigned certify that they have read, and recommended to the Faculty of Graduate Studies and Research for acceptance, a thesis entitled "The Life Cycle of the Conjugative Plasmid" submitted by Trevor D. Lawley in partial fulfillment of the requirements for the degree of Doctor of Philosophy, in Microbiology and Biotechnology.

✓

Dr. Brett B. Finlay

Date: June 30, 2003

Abstract

The conjugative plasmid backbone comprises the conserved plasmid survival components, consisting of replication, active partitioning and conjugation functions, which collectively determine the maintenance and spread of a conjugative plasmid within a bacterial community. Replication and partitioning ensure the plasmid molecule is transmitted vertically, whereas conjugation transmits the plasmid molecule horizontally. The backbone component functions specify overlapping stages of the plasmid life cycle, which includes both the vegetative cycle (vertical transmission) and the conjugative cycle (horizontal transmission). This thesis uses molecular genetic and cell biology techniques to define the conjugation and partitioning systems of the IncHI1 plasmid R27 and elucidate the key cellular localizations and movements of the plasmid which occur during the life cycle, using both R27 and the IncP β plasmid R751.

The complete conjugative transfer system (20 genes) of R27 from *Salmonella enterica* serovar Typhi was functionally characterized using bioinformatics, mutagenesis, genetic complementation and an H-pilus assay. Bioinformatic analysis demonstrated that the R27 transfer system is a chimera of IncF-like and IncP-like transfer systems. The DNA transfer replication functions of R27 are ancestrally related to that of IncP plasmids, such as RP4 and R751, whereas the mating pair formation (Mpf)/type IV secretion system (T4SS) encoded by R27 contains an equivalent to each of the essential components of F-like plasmids.

The *lacO*/GFP-LacI system was used to visualize both R27 and R751 foci residing at the mid- and quarter-cell regions of *Escherichia coli*. The partitioning systems of R27 were shown to be responsible for maintaining plasmids in clusters at these positions throughout the cell cycle. R27 foci duplicated at either the mid- or quarter-cell

regions, reflecting the progression of the plasmid vegetative cycle. Comparisons of R751 during conjugative and non-conjugative conditions identified the key localizations and movements associated with the conjugative cycle, including the initiation of conjugative transfer in the donor and the establishment of R751 in the recipient. A survey of successful mating pairs demonstrated that close physical contact between donor and recipient bacteria is required for DNA transfer and that regions of intimate contact can occur at any location on the donor or recipient cell membrane. The transferred DNA is targeted to the recipient replisome for DNA replication prior to plasmid establishment.

A functional and bioinformatic study of the conjugative system combined with the cellular localizations and movements of plasmid DNA during transfer are used to develop the concept of the conjugative cycle.

Acknowledgements

I would like to thank my supervisor Dr. Diane Taylor for her generosity, guidance and support. These qualities have made my PhD and my time in Edmonton positive and memorable. I also thank my co-supervisor Dr. Laura Frost for always having time to listen to my ideas and share hers. Many of these conversations have played an important role in the development of this thesis. I acknowledge the support from both Drs. John Elliott and Brenda Leskiw, as members of my committee, and would like to thank Drs. Brett Finlay and Marcus Stein for participating in my PhD defense.

The members of the Taylor lab have always made coming to the lab interesting and fun and I would like to thank each of them for the lessons taught and the great memories: Dave Rasko, Michelle Rooker, Qin Jiang, Cathy Trieber, Sean Connell, Trinh Ngo, Monica Keelan, Amera Gibreel, Bing Ma, Lisa Nonaka, Trevor Wilson, Dave Kelley, Joanne Simala-Grant and Ge Wang. I would like to particularly thank Matt Gilmour, James Gunton and Dobryan Tracz, who collaborated with me and significantly contributed to Chapter 2 of this thesis. Throughout this project we have not only made major advancements in the InCHI1 project, but I think we all now understand the power of collaboration.

Drs. Andrew Wright and Scott Gordon have played an instrumental role in Chapters 3 and 4 by teaching me how to label DNA with GFP and visualize it with fluorescence microscopy, during the summer of 1999. Elizabeth Joyce and Stephen Popper facilitated this collaboration through their kindness.

I am grateful to the Canadian Institute of Health Research and Alberta Heritage Foundation for Medical Research for the financial support.

My Edmonton friends have played an central role in my PhD by keeping me in touch with the real world and sharing many amazing times: Lauchie, Currie, Michelle, Laura, Tim, Dave, Jeff, Andrea, Kevin, Rob, Jack, Susan, Mike, Adam, Adam and Mary Jane.

My Mom (Josepha), Dad (Dave), brother (Darcy) and niece (April) have been my roots over the years, and I thank them for their unconditional support.

I would especially like to thank Bronwyn, a fellow scientist and my best friend, as I have learned the most from her.

Table of Contents

1	General Introduction	2
1.1	Gram-Negative Bacterial Plasmids	2
1.2	Plasmid Backbone	3
1.2.1	Replication	4
1.2.2	Active Partitioning	5
1.2.3	Conjugation	6
1.3	Model Conjugative Plasmids	8
1.3.1	IncF plasmids	8
1.3.2	IncP Plasmids	9
1.3.3	IncW Plasmids	10
1.3.4	IncQ Plasmids	11
1.3.5	IncHI Plasmids	12
1.4	Bacterial Cell Biology	14
2	Functional and Mutational Analysis of the Complete Conjugative Transfer System of the IncHI1 Plasmid R27	18
2.1	Introduction	18
2.2	Experimental Procedures	18
2.2.1	Bacterial Strains, Growth Conditions and Plasmids	18
2.2.2	DNA Manipulations	22
2.2.3	Computer Analysis	22
2.2.4	Mutagenesis	22
2.2.5	Cloning of Transfer Genes	23
2.2.6	Conjugation Assay	24
2.2.7	Phage Plaque Assays	24
2.2.8	Cloning of Origin of Transfer	24
2.3	Results	25
2.3.1	Nucleotide Sequence Analysis of Tra1 Region	25
2.3.2	Tra1 Gene Disruptions and Identification of Transfer Mutants	30
2.3.3	Genetic Complementation of Tra1 Transfer-Deficient Mutants	33
2.3.4	Hgal Plaque Assay of R27 Tra1 Transfer-Deficient Mutants	34
2.3.5	Identification and Cloning of the R27 Origin of Transfer within Tra1	34
2.3.6	Nucleotide Sequence Analysis of Tra2 Region	37
2.3.7	Tra2 Gene Disruptions and Identification of Transfer Mutants	49
2.3.8	Genetic Complementation of Tra2 Transfer-Deficient Mutants	49
2.3.9	Hgal Plaque Assay of Tra2 Transfer-Deficient Mutants	50
2.4	Discussion	51
3	Characterization of the Double Partitioning Modules of R27: Correlating Plasmid Stability with Plasmid Localization	58
3.1	Introduction	58
3.2	Experimental Procedures	59
3.2.1	Bacterial Strains and Plasmids	59
3.2.2	Growth Conditions	60
3.2.3	Nucleotide Sequence and Statistical Analysis	60
3.2.4	Cloning of Par1 and Par2	60
3.2.5	Construction of <i>parB</i> and <i>parR</i> Mutants	61

3.2.6	Pulsed-Field Gel Electrophoresis.....	61
3.2.7	Stability Assay	62
3.2.8	R27:: <i>lacO</i> Construction	62
3.2.9	Microscopy and Photography	63
3.3	Results.....	63
3.3.1	Nucleotide Sequence Analysis of Par1 and Par2.....	63
3.3.2	Stability of Par1 and Par2 Clones and R27 <i>parB</i> and <i>parR</i> Mutants.....	66
3.3.3	Double Partitioning Mutant of R27	69
3.3.4	Localization of R27:: <i>lacO</i> in <i>E. coli</i>	72
3.3.5	Time-Lapse Observations of R27:: <i>lacO</i> Foci Duplication	72
3.3.6	Localization of R27 Partitioning Mutants in <i>E. coli</i>	79
3.3.7	Statistical Analysis of R27 Localization.....	79
3.4	Discussion.....	80
4	Bacterial Conjugative Transfer: Visualization of Successful Mating Pairs and Plasmid Establishment in live <i>Escherichia coli</i>	84
4.1	Introduction.....	84
4.2	Experimental Procedures	86
4.2.1	Bacterial Strains and Plasmids.....	86
4.2.2	Growth Conditions.....	86
4.2.3	R751:: <i>lacO</i> Construction	87
4.2.4	Construction of R751:: <i>lacO</i> Transfer Mutants	87
4.2.5	Microscopy and Photography	88
4.3	Results.....	88
4.3.1	Localization of R751 in <i>E. coli</i>	88
4.3.2	Establishment of R751:: <i>lacO</i> in Recipient (Transconjugant) After Conjugative Transfer	94
4.3.3	Time-lapse Observations of Plasmid Appearance and Duplication in Recipient Cells.....	98
4.3.4	Spatial Relationship between Donor and Transconjugant during Conjugative Transfer.	103
4.4	Discussion.....	106
5	General Discussion	110
5.1	T4SS.....	111
5.1.1	Mpf System of R27 and F Define a T4SS Subfamily.....	111
5.1.2	H/F-Like T4SS Components.....	111
5.1.2.1	H/F-Like T4SS Propilin Processing.....	117
5.1.2.2	H/F-Like T4SS Pilus Assembly.....	118
5.1.2.2.1	Pilus Tip Formation	118
5.1.2.2.2	Pilus Extension.....	120
5.1.2.3	H/F-Like T4SS Mating Pair Stabilization.....	122
5.1.3	Relationships between H/F and P T4SS	123
5.1.4	The Core of the Conjugative Pore	126
5.2	Plasmid Behaviour	127
5.2.1	Vegetative Cycle vs. Conjugative Cycle	127
5.2.2	Relaxosomes and the Initiation of Transfer.....	129
5.2.3	Relaxosomes and the Termination of Transfer.....	132

5.2.4	Conjugative Junctions and the Site of Transfer	140
5.2.5	Establishment of Transferred Strand	140
5.3	The Conjugative Cycle	141
5.4	Conclusions and Future Directions	145
6	Bibliography	148

List of Figures

Figure 2-1. Open reading frame map of Tra1 of R27	26
Figure 2-2. Alignment of Walker A and Walker B boxes from coupling proteins	31
Figure 2-3. Origin of transfer.....	35
Figure 2-4. Open reading frame map of Tra2 of R27	38
Figure 2-5. Alignment of T4SS secretin-like protein	44
Figure 2-6. Alignment of proceeded pilin subunits from IncHI and IncP transfer systems	46
Figure 2-7. Comparison of R27, F and RP4 transfer systems	52
Figure 3-1. Genetic organization of the Par1 and Par2 modules of R27	64
Figure 3-2. Partitioning stability assay results.....	67
Figure 3-3. Pulsed-field gel electrophoresis of R27 double partitioning mutant.....	70
Figure 3-4. Representative micrographs of R27 and R27 partitioning mutants localized in live <i>E. coli</i>	73
Figure 3-5. Summary of data for R27 and R27 partitioning mutants localization in <i>E. coli</i>	75
Figure 3-6. Time-lapse fluorescence microscopy of R27 foci duplication.....	77
Figure 4-1. Intracellular localization of R751 in <i>E. coli</i> donors	90
Figure 4-2. Localization of R751 as a function of cell length in donor and transconjugant cells	92
Figure 4-3. Fluorescence and phase-contrast micrographs differentiating donors, recipients and transconjugants	95
Figure 4-4. Time-lapse fluorescence microscopy demonstrating appearance of R751 in recipient cells	99
Figure 4-5. Time-lapse fluorescence microscopy demonstrating appearance and duplication of R751 in recipient cells	101
Figure 4-6. Combined fluorescence/DIC micrographs of successful mating pairs	104
Figure 5-1. Comparison of H/F-like T4SS with each other and with P- and I-like T4SS	112
Figure 5-2. A representation of the H/F-like conjugative pore.....	114

Figure 5-3. Model 1 for DNA transfer and termination of conjugation in gram-negative bacteria.....	133
Figure 5-4. Model 2 for DNA transfer and termination of conjugation in gram-negative bacteria.....	135
Figure 5-5. Model 3 for DNA transfer and termination of conjugation in gram-negative bacteria.....	137
Figure 5-6. Model representing the conjugative cycle of a gram-negative bacterial plasmid transferring between <i>E. coli</i> donor and recipient cells	142

List of Tables

Table 2-1. Bacterial strains and plasmids used for Tra1 and Tra2 study.....	19
Table 2-2. Summary of the computer analysis of Tra1	28
Table 2-3. Effect of mutations in Tra1 on R27 conjugation.....	29
Table 2-4. Summary of the computer analysis of Tra2 of R27	40
Table 2-5. Effect of mutations in Tra2 on R27 conjugation.....	42
Table 5-1. Summary of conserved H/F-like T4SS components	116

List of Abbreviations

Ap	ampicillin
bp	base pairs
CAT	chloramphenicol acetyltransferase cassette
Cm	chloramphenicol
DNA	deoxyribonucleic acid
Dtr	DNA transfer replication
FISH	fluorescence <i>in situ</i> hybridization
GFP	green fluorescent protein
Inc	Incompatibility plasmid group
Kn	kanamycin
kb	kilobase pairs
Mpf	mating pair formation
Mps	mating pair stabilization
ml	millilitres
Nal	nalidixic acid
nm	nanometers
ORF	open reading frame
PCR	polymerase chain reaction
PSI-BLAST	position specific interactive basic local alignment search tool
PFGE	pulsed-field gel electrophoresis
RCR	rolling circle replication
ssDNA	single-stranded DNA
Tc	tetracycline
T-strand	transferred strand
Tp	trimethoprim
Tra1 (or 2)	Transfer region 1 (or 2)
T4SS	Type IV Secretion System
μl	microliters
μm	microns
UV	ultraviolet

Chapter 1

General Introduction

1 General Introduction

1.1 Gram-Negative Bacterial Plasmids

The bacterial genome consists of the entire genetic composition within a bacterium. The chromosome is the main source of genetic information, containing the general housekeeping genes essential for growth and division. Mobile DNA elements, such as plasmids, insertion sequences, transposons, integron gene cassettes and phages, can constitute the remainder of the genome and encode a variety of accessory functions; functions that are not essential for bacterial survival but confer a selective advantage under certain growth conditions (203). Accessory functions include, but are not limited to, resistance mechanisms, virulence traits and metabolic pathways. Mobile elements are capable of exchanging accessory genes with the prokaryotic gene pool. Due to their mobile nature, they can rapidly provide a host with a novel phenotype and allow the host to adapt to a new or changing environment. Mobile elements are therefore seen as a mechanism of innovation for bacterial evolution, the power of which is highlighted by the rapid and widespread dissemination of antibiotic resistance (198).

Bacterial plasmids are frequently circular molecules of double-stranded DNA that exist autonomously from the bacterial chromosome. Conjugative plasmids, which are the focus of this thesis, are able to transfer between bacteria and are the most complex bacterial plasmids. They are generally quite large, 30-300 kb, and can represent up to 5% of the bacterial genome. Plasmids are often classified into incompatibility (Inc) groups, where incompatibility is defined as the inability of related plasmids to coexist in the same host cell (35, 40, 196). Incompatibility between two plasmids is determined by shared replication (152) and/or partitioning functions (8), which suggests a shared evolutionary history. Approximately 28 incompatibility groups in Gram-negative bacteria have been recognized (196, 198).

Interestingly, bacterial plasmids have been referred to as organisms, according to the strict definition: “a unit of continuous lineage with an individual evolutionary history” (39). This comparison creates a new perspective when thinking about the biology of conjugative plasmids and means one must consider both the life cycle of the plasmid and

the environment within which the plasmid resides. The life cycle possesses two modes of reproduction: one mode is the vertical inheritance from mother to daughter cell, which is due to vegetative replication and partitioning functions, and the other is the horizontal inheritance which disseminates the plasmid intercellularly, which is due to the conjugative functions. Both modes are replicative, as the plasmid is duplicated, therefore creating continuous vertical and horizontal lineages. The life cycle of a conjugative plasmid therefore contains both vertical and horizontal transmission and is dependent upon three principal functions: replication, partitioning and conjugation.

A conjugative plasmid's environment is the host cell. The host-range of a conjugative plasmid can vary significantly from narrow (i.e. IncHI1, IncFI) (128) to broad (i.e. IncP, IncW) (74). Gram-negative narrow host-range plasmids are generally confined to *Enterobacteriaceae* or other genus such as *Pseudomonas*, whereas broad host-range plasmids are readily transferred and maintained between *Enterobacteriaceae* and *Pseudomonas* (74) and in some cases between gram-negative and gram-positive bacteria (61, 68, 136). The host-range of a plasmid is dependent upon the interplay of replication, partitioning and conjugation functions (73).

The replication, partitioning and conjugative transfer determinants of a conjugative plasmid are collectively referred to as the plasmid backbone (201). Although these processes were once viewed as separate stages, it is now becoming clear that backbone functions are continuous and overlapping phases of the plasmid life cycle (17). An understanding of the plasmid backbone functions is therefore required to understand the plasmid's life cycle, which includes both the vegetative cycle (vertical inheritance) and the conjugative cycle (horizontal inheritance).

1.2 Plasmid Backbone

The concept of a plasmid backbone was first used to describe the IncP backbone, as determined by comparing the genomes of R751 (IncP β) and RP4 (IncP α) (158, 201). As replication, partitioning and conjugation functions are required for plasmid survival within a bacterial community, they are highly conserved compared to accessory functions, such as resistance, properties which are only occasionally required (203).

Therefore closely related plasmids can contain backbone genes that are all closely related. However, it should be noted that genetic loci for replication, active partitioning and conjugation are modular (i.e. independent genetic units) and are therefore subject to genetic exchange between plasmids. For example, IncHI1 plasmids contain multiple replicons and active partitioning modules (187). Therefore, it should be stated that the concept of a plasmid backbone is not the basis of a formal classification scheme, but rather collectively identifies the central processes of the conjugative plasmid life cycle. A brief overview of replication, active partitioning and conjugation will be given here as, they will be referred to throughout the thesis and ultimately linked together to provide a comprehensive model of the plasmid life cycle.

1.2.1 Replication

Plasmid replication is the best understood aspect of the plasmid backbone functions. Initiation of replication controls plasmid copy number, which is measured as a fixed number of plasmid molecules per chromosomal origin (51). Copy number control is important for plasmid maintenance because if the number of plasmids vastly increases above the copy number then the plasmid may create a metabolic burden for the host, whereas if the number of plasmids drops below the copy number then plasmid inheritance will be compromised (43). Plasmids from gram-negative bacteria generally use a theta replication mechanism, whereas gram-positive plasmids generally use a rolling circle replication (RCR) mechanism (43).

Both plasmids used in this thesis, R27 (IncHI1) and R751 (IncP β), employ a theta-type mechanism for replication. This type of replication was named theta because the replication intermediates resemble the Greek letter θ (51). The basic theta replicon generally does not exceed 3 kb and consists of a replication initiator protein (Rep) and an origin of vegetative replication (*oriV*) that is flanked by several repeated DNA sequences, termed iterons (51). Replication is initiated when a critical concentration of Rep proteins bind to the iterons, which results in local melting of the *oriV*, and separation of the DNA strands to create a replication bubble. The host-encoded replisome (DNA Pol III holoenzyme) is loaded and assembled into the replication bubble for priming and for leading and lagging strand DNA synthesis (43). Control of initiation is exerted at two

levels: firstly, the Rep proteins are autoregulated so that the concentration of Rep protein is maintained at a relatively constant level. For example, if the concentration of Rep proteins is excessive then Rep will bind to the promoter region found near or within the iteron sequences and decrease Rep expression, creating a negative feedback loop. If the Rep concentration is low then the expression level of Rep is increased due to the reduced binding of Rep to the promoter region (51). The second mechanism for initiation control is a model referred to as “handcuffing”; the coupling of multiple origins via iteron-bound Rep proteins which blocks origin function. This model proposes that as plasmid number reaches the appropriate copy number “handcuffing” causes steric hindrance to initiation and thereby controls the copy number (29).

It is notable that RCR replication and DNA transfer replication (Dtr), which produces the transfer strand intermediate for conjugation, are functionally similar (43, 49, 106). In each process an initiator protein nicks, or relaxes, the DNA at the origin to produce a free 3'OH which serves as a primer for DNA synthesis. Replacement strand synthesis is coupled with 5' to 3' strand displacement, which results in a single-stranded DNA (ssDNA) intermediate. In RCR the ssDNA undergoes complementary strand synthesis, whereas in conjugation the ssDNA is first transferred into the recipient prior to complementary strand synthesis. The parallels between RCR and Dtr will be discussed in more detail within Chapter 4 and Chapter 5 (General Discussion).

1.2.2 Active Partitioning

Random segregation of plasmids at cell division results in a plasmid loss rate of 2^{-n} per generation, where n is the plasmid copy number (59). For plasmids such as the IncQ plasmid R1162, which has a high copy number (10-16) and lacks an active partitioning mechanism, plasmid loss due to random segregation at cell division (resulting in plasmidless daughter cells) is minimal (rate of $\sim 10^{-5}$ per generation) (13). In theory, low-copy number plasmids such as R27 and F (1-2 copies) should have plasmid loss rates of 0.25-0.5 per generation. However, plasmid loss rates are 10^{-4} - 10^{-5} per generation for such plasmids, rates which are comparable to that of the chromosome loss in *E. coli* (67). The stability of low copy number plasmids is due to the presence of an active partitioning system that segregates plasmid molecules in a non-random fashion at

cell division. In the past few years great strides have been made in understanding the mechanism by which partitioning modules stabilize plasmids. Active partitioning modules (2-5 kb) consist of two genes and an adjacent centromere region that act by placing plasmids within each daughter cell at division (67). Active partitioning is a key aspect of the plasmid life cycle and will be the focus of Chapter 3.

1.2.3 Conjugation

Bacterial conjugation is a special type of DNA replication during which one strand of the plasmid molecule is transferred from donor to recipient in the 5' to 3' direction, while the second strand is retained in the donor (218). The host-encoded replisome (DNA PolIII) is responsible for complementary strand synthesis of both the transferred and retained DNA strands (100). Horizontal DNA transfer is directed by the conjugation apparatus which consists of three multi-protein complexes: the membrane-associated mating apparatus (Mpf)/Type IV secretion system (T4SS) and the cytoplasmic relaxosome, both which are coupled together by the inner membrane-associated coupling protein (218). The Mpf apparatus consists of 11-13 different proteins, the relaxosome contains 1-4 different proteins and the coupling protein contains one type of protein.

A working model of conjugation suggests that the Mpf proteins form a membrane-associated apparatus that functions in synthesizing and assembling mature conjugative pili on the cell surface. The conjugative pilus facilitates the initial contact with the recipient cell; a prerequisite for the formation of stable mating pairs (54). For the IncF-like Mpf apparatus, the transfer proteins are believed to function in pilus extension, pilus retraction, formation of stable mating pairs, and formation of a lumen through which plasmid transfer occurs (56). In other model systems, such as the IncP system, the exact role of the P-pili remains to be determined, although conjugative pili are essential and donors containing IncP plasmids also form stable mating pairs (177). The exact role of the Mpf proteins remains poorly understood.

The relaxosome is a specific DNA-protein complex that is composed of a relaxase and accessory protein(s). Relaxases initiate and terminate conjugation by catalysing site- and strand- specific nicking and rejoining reactions at the plasmid encoded *nic* site within the origin of transfer (*oriT*). Nicking results in a covalent bond between the 5' end of the

cleaved strand and the relaxase, forming a complex known as the transferred strand (T-strand) intermediate. Genetic evidence suggests that the transferring intermediate is connected to the mating apparatus via the plasmid encoded coupling protein (26, 77). Based on an analysis of the crystal structure of TrwB, the coupling protein from the IncW plasmid R388, it has been proposed that coupling proteins may serve as a conduit through which the single-stranded DNA transfers (64, 65). The Mpf/T4SS and the coupling protein are referred to as the conjugative pore.

At the molecular level, our understanding of relaxosomes and conjugal DNA processing is well developed, whereas much remains to be understood about the conjugative pore. The conjugative apparatus will be discussed in Chapter 2 and Chapter 5 (General Discussion).

Although conjugation was first recognized to occur between enteric bacteria, conjugation is now known to be a universal characteristic of both gram-negative and gram-positive bacteria where it drives gene flow throughout the eubacterial domain. As such, conjugation can be viewed as a powerful mechanism of evolution. Notably, conjugation can mediate DNA transfer between distantly-related bacteria (61, 68, 136), between bacteria and *Saccharomyces cerevisiae* (lower eukaryote) (84) and between bacteria and mammalian cells (higher eukaryote) (207). In these studies a limiting factor in *trans* domain DNA transfer was the inability of the incoming DNA to become established in the new host. These observations imply that replication and partitioning functions can be a barrier for interdomain transfer and highlight the importance of a functional plasmid backbone for DNA transfer.

Bacterial pathogens are now known to utilize secretion pathways which are ancestrally related to the Mpf apparatus. Genomic comparisons between the IncP transfer system and the VirB system of the Ti plasmid (Tumor inducing) of *Agrobacterium tumefaciens*, which injects oncogenic DNA into plant genomes, lead to the realization that conjugation-like secretion systems are widespread in the bacterial world (116, 118, 208). The components of the conjugative pore are now classified with ancestrally-related secretion systems into the T4SS (30, 31).

1.3 Model Conjugative Plasmids

Listed and briefly described below are five important model conjugative plasmids, which have been characterized primarily in *Escherichia coli*, and will be referred to throughout this thesis. Each model system provides valuable insights into different aspects of the multi-stage process of conjugation and our understanding of the conjugative cycle. Since there appears to be a generally conserved mechanism for conjugative transfer in gram-negative bacteria, knowledge from each system can be applied to a general model of conjugation. It should be noted that by studying several model systems it is also becoming evident that diversity, or variation, of key aspects of conjugation exists. This point will be discussed further in Chapter 2 and within Chapter 5 (General Discussion).

1.3.1 IncF plasmids

F-like plasmids, typified by the F factor, are narrow host-range mobile elements, which are generally confined to *Enterobacteriaceae* (38). Under laboratory conditions, transfer of F-like plasmids is very efficient at 37°C and poor at temperatures at or below 30°C (128). F-like plasmids encode for the resistance to a wide range of antibiotics and heavy metals as well as the ability to utilize lactose (90). In addition, certain F-like plasmids are important for the pathogenesis of *Salmonella typhimurium* (pSLT) (99) and enteropathogenic *E. coli* (pB171) (202).

The F factor transfer system, as the first to be described, is a paradigm for bacterial conjugation and has provided invaluable insight into the transfer mechanism (213). Systematic mutagenesis and complementation analysis of the F factor were used to identify essential conjugation genes. Subsequently, F-pilus specific bacteriophages were used to identify those conjugation genes which are involved in conjugative pilus biosynthesis (90).

The transfer region is now known to be a continuous 33 kb region of the F factor, which consists of ~40 transfer genes and is flanked by the *oriT* (56). Of the 40 genes, 19 are essential for transfer under laboratory conditions. These include 12 Mpf genes, two mating pair stabilization (Mps) genes, four DNA metabolism genes/regulatory genes and a coupling protein gene. In addition, two genes that are not essential for transfer, *traS*

and *traT*, are involved in entry exclusion, a property that prevents donor to donor mating (2). Careful analysis of transfer gene mutants provided the foundation for initially describing the general stages of conjugation: i) donor pilus identification of a suitable recipient, ii) mating pair/aggregate formation, iii) mating pair stabilization, iv) DNA transfer and v) disaggregation of mating pairs/aggregates (56).

In a landmark study, Kingsman and Willetts (100) demonstrated that conjugative pili were required for triggering DNA transfer and replacement strand synthesis (conjugal DNA synthesis). They proposed that after the conjugative pilus contacted a suitable recipient, a “mating signal” was propagated through the conjugative pilus and into the donor where it initiated conjugal DNA synthesis and transfer. The “mating signal” still remains unknown. Furthermore, this work demonstrated that conjugal DNA synthesis requires the host replisome (DNA PolIII holoenzyme) and is uncoupled and separate from DNA transfer. Therefore, conjugal DNA synthesis does not provide the motive force for transfer of DNA into the recipient.

1.3.2 IncP Plasmids

IncP plasmids are of particular interest because of their broad host range, or promiscuous nature, and therefore their ability to promote gene dissemination among diverse bacterial species (74). IncP plasmids also have the amazing ability to transfer very efficiently under a wide range of temperatures (14-37°C) (128). Well-studied plasmids belonging to the IncP group include RP4 (RK2), a member of the IncP α group, and R751, a member of the IncP β group. RP4 (53 kb) was originally isolated from *Pseudomonas aeruginosa* from a burn patient (158) and R751 (60 kb) was isolated from *Klebsiella aerogenes* (201).

Both RP4 and R751 have been completely sequenced and compared to one another (158, 201). IncP plasmids share a conserved backbone of replication, stable maintenance and conjugation functions. In addition, the global regulation system, controlled by KorA and KorB, which co-ordinates the backbone functions, appears to be completely conserved. The main difference between RP4 and R751 was the insertion of phenotypic markers and transposons (201). The transfer genes of both plasmids are contained within two transfer regions, Tra1 and Tra2. Tra1 is 6 kb and contains the *oriT*,

3 essential relaxosome genes, the coupling protein gene and a Mpf gene, *traF*, which is required for pilus subunit processing. The Tra2 region is 11 kb and contains 10 essential Mpf genes (115, 117). The Mpf proteins and coupling protein, which collectively constitutes the conjugative pore, of RP4 and R751 are interchangeable (115), whereas the DNA processing genes, the relaxosome components, are not interchangeable, indicating the specificity of these systems (156).

Although the 11 Mpf components and the coupling protein of RP4 have been identified, little is known about their functions, individually or collectively (76). The Mpf proteins and the coupling protein are membrane associated and possibly form a membrane complex (69). Research from Erich Lanka's group has provided detailed insight into the mechanism by which conjugation is initiated and terminated by relaxosomes. Relaxosomes catalyze a site- and strand-specific cleavage at the *nic* site within the *oriT* contained on double-stranded supercoiled DNA. Cleavage results in a covalent bond between the 5' end of the *nic* and a tyrosine residue on the relaxase. Cleavage likely represents an earlier stage of conjugation (156, 161, 162). Relaxases are also capable of cleaving and rejoining single-stranded DNA containing the *nic* region, likely reflecting the termination of a conjugation event (157, 160). An important observation from the latter study was that the 5' bound relaxase molecule was incapable of performing a second cleavage reaction, which is required to release the T-strand from the replacement strand. The authors therefore concluded that two relaxase molecules would be required per conjugation event (157). The relevant details of these experiments will be described in the Chapter 5 (General Discussion).

1.3.3 IncW Plasmids

The IncW plasmid R388 is a 33 kb broad-host range plasmid that was originally isolated from *E. coli* (121). Similarly to IncP plasmid, IncW plasmids are capable of efficient transfer under a wide range of temperatures (14-37°C) (128). The complete transfer region of this plasmid is contained within a 14.9 kb region (19). The conjugative apparatus is coded by 11 Mpf, 3 relaxosome genes and a coupling protein gene. Although no work has been performed on the Mpf system of R388, important information on the relaxosome and coupling protein are available.

Biochemical and genetic analysis of the relaxosome of R388 have demonstrated that the general mechanism of strand cleavage is conserved with the relaxosome of IncP plasmids. That is, after nicking, a tyrosine residue becomes covalently bound to the 5' end of the transferring strand. One important difference between the proposed termination mechanism of IncW and IncP plasmids exists. TrwC, the R388 relaxase, contains two pairs of active tyrosine residues, whereas the IncP relaxase, TraI, contains only one. TrwC has been shown to cleave at a second *nic* site when bound to the 5' end of the T-strand (70). This observation implies that only one TrwC molecule is required per conjugation event. Substitution mutations of each tyrosine residue are each transfer proficient, indicating catalytic redundancy of the double tyrosine motif. The biological relevancy of the two tyrosine residues in these conjugative relaxases is therefore unclear. Both models, the one and two relaxase molecules per conjugation event, will be discussed in detail within Chapter 5 (General Discussion).

Every gram-negative bacterial conjugation system encodes a coupling protein (122). Recently, the X-ray crystal structure of the soluble portion of TrwB, the coupling protein from the IncW plasmid R388, has been solved. TrwB exists as an integral inner membrane homohexamer with a central channel that may serve as the conduit for single stranded DNA transfer (65). In addition, the structure of TrwB resembles DNA ring helicases and F1 ATPases. These observations suggest that coupling proteins utilize the energy derived by hydrolysis of ATP to pump single stranded DNA out of the donor and into the recipient during transfer (122).

1.3.4 IncQ Plasmids

IncQ plasmids are not conjugative plasmids, but rather are mobilizable plasmids. Mobilizable plasmids encode their own relaxosome and provide their own Dtr functions, but utilize the conjugative pore encoded by a co-resident plasmid for transfer. IncP, W, N and Ti plasmids can mobilize IncQ plasmids very well (171); in contrast the F factor mobilizes IncQ plasmids poorly (178), and R27 does not mobilize IncQ plasmids at all (personal observation). IncQ plasmids are small (8.6 to 14 kb), have a high copy number (10-16) and have an extremely broad host range (171). The only backbone functions encoded by IncQ plasmids are the conjugative (relaxosome) and vegetative replication

functions. The vegetative replication functions include initiation (RepA), helicase (RepB) and primase (RepC). The possession of the helicase and primase functions has been proposed to promote the broad host range of R1162 by minimizing the dependence upon host factors for replication (85, 171).

IncQ plasmids have been useful for studying the initiation and termination of transfer. The relaxase of R1162, MobA, contains one tyrosine residue in its active site and behaves biochemically as the relaxase of IncP plasmids (15). Genetic and mutational analysis of the *oriT* region has demonstrated that the DNA sequence downstream of the *nic* site is important for cleavage and the region upstream of the *nic* site is important for termination (49). Termination is defined as the rejoining of the 5' and 3' ends of the T-strand. The region upstream, the termination region, is last to enter the recipient and contains an inverted repeat. The inverted repeat possibly forms a loop, or "peg", structure, that is recognized by the relaxosome, for rejoining of the 5' and 3' ends to terminate transfer (14). The presence of inverted repeats in all characterized *oriT* regions suggests that the termination mechanism may be conserved.

1.3.5 IncHI1 Plasmids

Plasmid-mediated resistance to chloramphenicol in *Salmonella enterica* serovar Typhi (*S. typhi*) was first identified in the 1970's. Strains of *S. typhi* containing IncHI1 plasmids resulted in typhoid fever epidemics throughout Mexico, India, Vietnam and Thailand (191). *S. typhi* has remained endemic in the Indian subcontinent and IncHI1 plasmids have contributed to the pathogen's persistence by conferring resistance to multiple antibiotics (53, 138, 165, 185, 186). Harnett *et al.* (79) have recently reported that strains of *S. typhi*, resistant to up to nine antibiotics, were isolated from travelers returning to Ontario, Canada from South Asia. Resistance is encoded by IncHI1 plasmids and highlights the importance of these plasmids in the emergence of multidrug-resistant *S. typhi*. IncHI1 plasmids are a major public health concern and their replication, maintenance and transfer systems deserve additional study.

IncHI1 plasmids are some of largest plasmids identified in *Enterobacteriaceae* (196). R27, the prototypical IncHI1 plasmid, was originally isolated from *S. typhi* in the 1960's. Recently, the complete nucleotide sequence of R27 was determined and

analyzed (187). R27 is 180 kbp and contains 210 open reading frames (ORFs), including those that code for the tetracycline-resistance transposon *Tn10* (107). Replication of R27 is dependent on one of two IncH-specific replicons, RepHI1A or RepHI1B (57, 58). A third replicon is responsible for one-way incompatibility with the F factor and has been designated RepFIA (58). R27 also contains two unrelated active partitioning modules, which are believed to facilitate the faithful segregation of plasmid molecules to daughter cells upon host cell division (175). The possession of both multiple replication and partitioning modules, so far, appears to be unique to IncHI1 plasmids. The conjugative transfer genes of R27 are located within two regions of R27 which are separated by 63 kb (187).

IncHI1 plasmids are characterized by an unusual thermosensitive mode of transfer, which occurs between 14-28°C (optimally 22-28°C), but is inhibited at 37°C (199). R27 is capable of transferring between *Enterobacteria* during conjugation experiments (128). Although the mechanism of thermosensitive transfer remains unknown, it has been proposed that IncHI1 plasmids are potential vectors in the dissemination of antibiotic resistance among pathogenic and indigenous bacteria in water and soil environments (128).

One of the objectives of this thesis was to identify all of the conjugative transfer and active partitioning genes on R27 using bioinformatic and functional analyses. This work, combined with previous analysis of R27 replication (146, 147), would provide information on each component of the IncHI1 backbone. Furthermore, a detailed bioinformatic analysis of the R27 conjugative transfer components should provide insight into the evolutionary relationship to other conjugative systems. Such an analysis is timely due to the rapidly expanding genomic databases and the advances in bioinformatic tools. One important improvement in bioinformatic analysis is PSI-BLAST (Position Specific Iterative Basic Local Alignment Search Tool) (5), an updated version of BLAST (4). PSI-BLAST is more sensitive to weak but biologically relevant protein similarities than BLAST and can therefore identify homologies that may have been missed in previous bioinformatic analysis of conjugative transfer proteins (30, 56).

1.4 Bacterial Cell Biology

Due to their small size (1-3 μm), lack of cytoskeletal structures and specialized organelles, such as a nucleus, bacteria were once viewed as amorphous bags of macromolecules. However, in the past few years, the application of high-resolution cell biology methods, such as Green Fluorescent Protein (GFP) and fluorescent microscopy, to *E. coli* and *Bacillus subtilis* has transformed our view of the bacterial cell significantly. Listed below are several important examples. DNA Pol III, and therefore the replisome, is localized to specific sub-cellular locations at the mid- and quarter-cell (113). These observations were vital in creating a model for bacterial chromosome replication in which a stationary replisome extrudes newly replicated DNA towards opposite cell poles (114). Three chemotaxis proteins have been found to co-localize to the cell pole, suggesting a macromolecular receptor (192). Conjugative pilus synthesis proteins were found to randomly localize as clusters in the inner membrane, suggesting they co-localize with conjugative pili and/or mating pores (63). In some cases protein localization patterns are dynamic, as demonstrated by the cell division protein MinD, which oscillates from pole to pole within seconds (170). The localization patterns for each of these proteins has functional relevance and has provided valuable mechanistic insights.

Cell biology techniques adapted for visualizing the localizations and movements of DNA in living cells has drastically altered the understanding of DNA segregation in prokaryotes. Specific regions of the circular chromosome are now known to have specific sub-cellular locations and move in predictable patterns that are synchronized with the cell cycle (66, 148, 210). For example, at the beginning of the cell cycle in *E. coli*, the chromosome is positioned so that the origin of vegetative replication (*oriC*) and the terminus are at opposite ends of the cell. As the cell cycle progresses, the *oriC* and terminus each migrate to the mid cell to undergo replication at a centrally located replisome. Replication results in the two daughter *oriCs* moving rapidly towards opposite poles, whereas the two termini remain at the mid cell. Cell division at the mid cell results in two daughter cells each with the chromosomal *oriC* and terminus at opposite poles (66, 86). In many respects, these types of observations have revitalized our view of the bacterial cell so that one should perhaps refer to the study of “Bacterial Cell Biology”.

One of the major cell biology tools used in these studies was GFP, originally isolated from the jelly fish *Aequorea victoria* where it is involved in bioluminescence (28). Now a valuable reporter system for the labeling of protein and DNA (204), GFP is used to label proteins at either the N- or C-terminal ends and label DNA via a DNA binding protein-GFP fusion (described below). GFP fluoresces in live bacteria (and eukaryotes) in a non-invasive manner without the addition of substrates (28). Fluorescent images of labeled macromolecules within living cells can be captured digitally in real time, thus enabling time-lapse experiments to be performed. The enhanced GFP variant used in the experiments described above and those experiments in this thesis is commonly referred to as S65T, which contains a serine to threonine mutation at residue 65 (83). GFP absorbs UV light at a wavelength of 488 nm and emits at 512 nm (28).

The method used in this thesis to label bacterial DNA was originally developed to visualize chromosome segregation in *S. cerevisiae* (194). The method was adapted for visualizing chromosomes in *B. subtilis* (210) and *E. coli* (66) in the laboratories of Drs. Richard Losick and Andrew Wright, respectively. The system consists of two parts: i) a *lacO* cassette and ii) an expression vector containing a GFP-LacI fusion. The *lacO* cassette, consisting of 256 tandem repeats of the lactose operator and the kanamycin resistance gene flanked by Tn7 inverted repeats, is introduced into the target DNA. Expression of GFP-LacI results in GFP-LacI binding to the tandem operators and causes the hybrid repressor molecules to cluster as a fluorescent focus. The foci can be visualized by fluorescence microscopy and represent the location of the plasmid molecules. The accuracy of the localized patterns obtained with this method has been verified with fluorescence *in situ* hybridization (FISH), a highly sensitive DNA labeling technique (166).

A major objective of this thesis was to describe the plasmid life cycle, consisting of the vegetative cycle (vertical inheritance) and conjugative cycle (horizontal inheritance) of the conjugative plasmids R27, an IncHI1 plasmid from *S. typhi*, and R751, an IncP β plasmid from *K. aerogenes*, using the GFP-LacI/*lacO* system as a plasmid specific reporter system and fluorescent microscopy. Key localizations and movements of these plasmids during vegetative growth and during conjugative transfer were

correlated with the plasmid backbone functions in the context of the host cell. These observations are combined to present an overview of the plasmid life cycle.

Chapter 2

Functional and Mutational Analysis of the Complete Conjugative Transfer System of the IncHI1 Plasmid R27

Portions of this work have been published in the following manuscripts:

Lawley, T.D., M.W. Gilmour, J.E. Gunton, D.M. Tracz, and D.E. Taylor. 2003. Functional and mutational analysis of conjugative transfer region 2 (Tra2) from the IncHI1 plasmid R27. *J. Bacteriol.* **185**(2): 581-591.

Lawley, T.D., M.W. Gilmour, J.E. Gunton, L.J. Standeven, and D.E. Taylor. 2002. Functional and mutational analysis of conjugative transfer region 1 (Tra1) from the IncHI1 plasmid R27. *J. Bacteriol.* **184**(8):2173-2180

2 Functional and Mutational Analysis of the Complete Conjugative Transfer System of the IncHI1 Plasmid R27

2.1 Introduction

Conjugative plasmids belonging to the Incompatibility group HI1 (IncHI1) encode for multiple-antibiotic resistance in *S. typhi* and therefore contribute to the persistence of typhoid fever worldwide (53, 165). IncHI1 plasmids are low copy number, self-transmissible plasmids that have an unusual mode of conjugation which is thermosensitive for transfer, with transfer occurring optimally between 22°C and 30°C, but which is negligible at 37°C (199). Recent evidence indicates that at least one transfer gene, *trhC*, is not expressed at non-permissive transfer temperatures, suggesting that transfer thermosensitivity may be imposed at the transcriptional level (63).

R27, the prototype IncHI1 plasmid, was recently sequenced and analysed (187). The transfer genes of R27 are contained within two separate regions, designated Tra1 and Tra2. Since mutations in either transfer region abolishes transfer, both transfer regions contribute to the R27 conjugative apparatus (175, 187). A preliminary analysis of the Tra2 region has indicated that this region codes for Mpf and H-pili synthesis phenotypes. Protein homology led us to conclude that the R27 Tra2 region is ancestrally related to the transfer region of the F factor (175).

The objective of this work was to characterize both the Tra1 and Tra2 regions of R27 using DNA sequence analysis, mutagenesis, genetic complementation and an H-pilus specific phage assay. The ultimate goal was to identify IncHI1 conjugal transfer genes and to determine any evolutionary relationships to other conjugative transfer systems, especially T4SS.

2.2 Experimental Procedures

2.2.1 Bacterial Strains, Growth Conditions and Plasmids

E. coli strains and plasmids used in this study are listed in Table 2-1. *E. coli* was grown at 27°C or 37°C in LB broth (Difco Laboratories, Detroit, Mich.) with shaking or

Table 2-1. Bacterial strains and plasmids used for Tra1 and Tra2 study

Strain or Plasmid	Relevant genotype, phenotype, or characteristic(s) ^a	Cloning or Gene Disruption Primers (5' to 3') ^b	Source or reference
<i>E. coli</i>			
DH5α	<i>supE44 lacU169 (80lacZM15) hsdR17 recA1 endA1 gyrA96 thi-1 relA1</i>		(176)
DY330	W3110 Δ <i>lacU169 gal490 λcl857 Δ(cro-bioA)</i>		(217)
DY330N	temperature resistant revertant; Nal ^r		
DY330R	temperature resistant revertant; Rif ^r		
DT1942	RG192 (Rif ^r) with pDT1942		
RG192	<i>ara leu lac</i>		
Plasmids			
R27	IncIII plasmid, Tc ^r		(187)
pDT1942	derepressed R27; R27::TnlacZ		
pMS119EH/HE	IPTG inducible expression vector; Amp ^r		
pBAD24	P _{BAD} expression vector; Amp ^r		(75)
pBAD30	P _{BAD} expression vector; Amp ^r		(75)
pGEM	cloning vector; Amp ^r		Promega
Tra1			
pAT22	<i>traI</i> cloned into pMS119EH; Amp ^r	F:TATATGGATCCATGAATTCAGGGCACTCTTC R:TATATCTGCAGTTAATGGTGATGGTGATGGTGCGCCAGATCCCGACCTCTTTTAG	
pJEG31	R27 with CAT in ORF115; Tc ^r Cm ^r	F:GATGGTGTGGCGAGTGATAGGAATCAGCATTATTGTCCTACTGTGACGGGAAGATCACTTC R:CGCTCAGAAGCCCTTCTGCATCATCAGGCAGGTATATTTCTTATTTCAGGGCGTAGCACCAG	
pJEG36	ORF122 cloned into pMS119EH; Amp ^r	F:TATAGGATCCATGTCTAAATCGAAGCTATTAAG R:TATAGAATCTTAAATGGTGATGGTGATGGTGTTGTGCCACCTCTGATTTTGAG	
pJEG51	pDT1942 with CAT in ORF117; Tc ^r Km ^r Cm ^r	F:TGCTTTTACTAGGGATGATGCTTATCTTATTTATAGTCTCTGTGACGGGAAGATCACTTC R:AGTAGCCTCACTATTTGCAATAACAGATAACCACCGGTCAATTATTCAGGGCGTAGCACCAG	
pJEG52	pDT1942 with CAT in ORF118; Tc ^r Km ^r Cm ^r	F:CAGTGCATCTCTGAAAGTAAGTAAAAGCCGCTCGCTCGTTCTGTGACGGGAAGATCACTTC R:TGTCATGGCAAAATTGCCCCACACATTTCAAAGCACCTTTTATTTCAGGGCGTAGCACCAG	
pJEG85	ORF128 cloned into pMS119EH; Amp ^r	F:TATATGAATTC AATGGATTACAACATCTATAC R:TATATGGATCCCTTAAATGGTGATGGTGATGGTGCGCCTTCTATTTTCATTTCAGCCAG	
pJEG94	pDT1942 with CAT in ORF123; Tc ^r Km ^r Cm ^r	F:TCACGCGTAATTTACTCGGTAAACTATTACGTACCGAGATCTGTGACGGGAAGATCACTTC R:TCCAAATCCATTACCAAAATAGTCGGCGTTGGAGGAGTGGTTTATTTCAGGGCGTAGCACCAG	
pJEG104	pDT1942 with CAT in ORF122; Tc ^r Km ^r Cm ^r	F:CTAAATCGAAGCTATTAAGTCAATTTGGAGATTTACGTACCTGTGACGGGAAGATCACTTC R:GCTATCCCTGGGTAATTCCTCTCAATGTGATTCCGTTCTTATTTCAGGGCGTAGCACCAG	
pJEG105	pDT1942 with CAT in ORF125; Tc ^r Km ^r Cm ^r	F:TTCACAGCCCTTTCAGGGCTTTCTAGTAGTCACATTTACTGTGACGGGAAGATCACTTC R:GGTATTAACGTTAATCGAGTCATTTACCGATCTCCTCATGTTTATTTCAGGGCGTAGCACCAG	
pJEG115	pDT1942 with CAT in ORF124; Tc ^r Km ^r Cm ^r	F:CGCTACAAAAACGATGTCTCTTGGTGCCAATAAAAACTCCCTGTGACGGGAAGATCACTTC R:CCCTGCGGTTATCCGTGCGGCGACTCCACCCACGAATCCCTTATTTCAGGGCGTAGCACCAG	
pJEG123	ORF124 cloned into pMS119EH; Amp ^r	F:TGAATTC AATGGCTAAAGTCGATCAAACAAAG R:TGGATCCCTTAAATGGTGATGGTGATGGTGATCTAACTCTCCTGGGAATAC	
pLJS4	ORF123 cloned into pMS119EH; Amp ^r	F:GGATCCATGTCAGAATCAGATAACATC R:GAATTCCTTAAATGGTGATGGTGATGGTGATAATCCTTCAAGAGCACTTTA	
pLJS33	ORF117 cloned into pMS119EH; Amp ^r	F:TATATGAATTC AATGGCTGCGGATAATTTCTGCTC R:TATATGGATCCCTTAAATGGTGATGGTGATGGTGCGCCATAAGTTTTTGAAAGTTAG	
pLJS36	ORF119 cloned into pMS119EH; Amp ^r	F:TATATGAATTC AATGACAAAATCAAAAAGAAC R:TATATGGATCCCTTAAATGGTGATGGTGATGGTGCGCATGCAATTCCTTAGATATT	
pLJS42	ORF127 cloned into pMS119EH; Amp ^r	F:TATATGAATTC AATGCGCGCTGATTTCCATGTTTG R:TATATGGATCCCTTAAATGGTGATGGTGATGGTGCGCGTTACCTGTGCCACGAAGAC	

pDT1942	derepressed R27; R27::TnlacZ; Tc ^r Km ^r	
pDT2956	pDT1942 with mini::Tn10 inserted into <i>traG</i> ; Tc ^r Km ^r Cm ^r	
pDT2984	pDT1942 with mini::Tn10 inserted into ORF127; Tc ^r Km ^r Cm ^r	
pDT2987	pDT1942 with mini::Tn10 inserted into ORF126; Tc ^r Km ^r Cm ^r	
pDT2991	pDT1942 with mini::Tn10 inserted into ORF128; Tc ^r Km ^r Cm ^r	
pDT2995	pDT1942 with mini::Tn10 inserted into <i>traI</i> ; Tc ^r Km ^r Cm ^r	
pMWG137	pDT1942 with mini::Tn10 inserted into ORF121; Tc ^r Km ^r Cm ^r	F:TATAGGATCCATGACCGATGTAACAATGAATG R:TATAGAATTCCTTAATGGTGATGGTGATGGTGCCGGCGTTACCAGACAGTTC F:TATATGAATTC AATGACTCGATTAACGTTAATAC R:TATATGGATCCCTTAATGGTGATGGTGATGGTGCGCGCGGCATATGCACCTCCTAAAC
pMWG189	ORF126 cloned into pBAD24; Amp ^r	
pTL138	1.3 kbp OriT <i>KpnI-SnaBI</i> fragment into pBAD30; Amp ^r	
pTL139	1.6 kbp OriT <i>SnaBI-XbaI</i> fragment into pBAD30; Amp ^r	
pOriT1.1	794 bp sub-clone of <i>oriT</i> region from pTL138; not mobilized by R27.	F: ATATGGTACCTACGGCTATTATCGGACG R: ATATAAGCTTTCAGATCACGATCTCAGC F: ATATGGTACCTTGCTGAGATCGTGATCTG R: ATATAAGCTTTCACACACTTAGAACGT F: ATATGGTACCTTGCTGAGATCGTGATCTG R: ATATAAGCTTAAACCCCTGACCTGCTAACG F: ATATGGTACCGGTTATTGCTACTTAATGCCGA R: ATATAAGCTTATCTGATTCTGACATGTGCC
pOriT1.2	977 bp sub-clone of <i>oriT</i> region from pTL138; mobilized by R27	
pOriT2.1	360 bp sub-clone of <i>oriT</i> region from pOriT1.2; not mobilized by R27.	
pOriT2.2	285 bp sub-clone of <i>oriT</i> region from pOriT1.2; mobilized by R27.	
Tra2		
pGUN110	pDT1942 with <i>cat</i> inserted into <i>trhA</i> ; Tc ^r Kan ^r Cm ^r	F:AACTGACATTGAATACTAACGTTGAAAGAGTAAAACTAAATGTGACGGAAGATCACTTC R:GATATCGCCGAAGGCTCCATCATCGGAACCCGCGTACGCAATTATTCAGGCGTAGCACCAG F:TATAGAATTC AATGGAAGTACATGAATAAC R: TATAGGATCCCTTAATGGTGATGGTGATGGTGAGGAAATACCAGCATCCAG F: AGTACGAGATACCGCCACATACATATCGCTTCCATACAGCTGTGACGGAAGATCACTTC R:CGCCACAACACTACCGAAGTTATAAAGAAATCAAAAATATTAATTATTCAGGCGTAGCACCAG F: TATAGAATTC AATGACAAGCCAGTACGAGATAC R: ATATGGATCCCTTAATGGTGATGGTGATGGTGAGAATAGAGGTTTCTGATAAATG
pGUN205	<i>trhA</i> cloned into pMS119EH; Amp ^r	
pMWG253	pDT1942 with <i>cat</i> inserted into <i>trhL</i> ; Tc ^r Kan ^r Cm ^r	
pMWG270	<i>trhL</i> cloned into pMS119EH; Amp ^r	
pDT2970	pDT1942 with mini-Tn10 inserted into <i>trhE</i> ; Tc ^r Cm ^r Kan ^r	
pTDL242	<i>trhE</i> cloned into pMS119EH; Amp ^r	F:TATAGAATTC AATGAACTTCTCAGCAGGTT (175) R:TATAGGATCCCTTAATGGTGATGGTGATGGTGTTACCTATTGACGGCGG
pDT2981	pDT1942 with mini-Tn10 inserted into <i>trhK</i> ; Tc ^r Cm ^r Kan ^r	
pTDL243	<i>trhK</i> cloned into pMS119EH; Amp ^r	F:TATAGAATTC AATGACTTCAAAAAAGGTTTTTC (175) R:TATAGGATCCCTTAATGGTGATGGTGATGGTGTCTTTTAAATCAGGCTTGCGC F:TAGTTGTCTTTTGGGTACCAGTTATTACTACCAAATACTGTGACGGAAGATCACTTC R:ATCCGCAAGCGTTGGTTCGCTTATAACAATCGTGCTTTTCTTATTCAGGCGTAGCACCAG
pDOB3	pDT1942 with <i>cat</i> inserted into <i>orf030</i> ; Tc ^r Kan ^r Cm ^r	
pDT2971	pDT1942 with mini-Tn10 inserted into <i>trhB</i> ; Tc ^r Cm ^r Kan ^r	
pTDL42	<i>trhB</i> cloned into pMS119EH; Amp ^r	F:ATATGAATTCATGGACATTAATAAAGGCGCTC R:TATAGGATCCCTCAGTGATGGTGATGGTGATGTGCGCGGCTTGTCAGGTTTG F: GAGTGAGTCTGCTGATAGCTTAAATATCGACGCGGCTAAACTGTGACGGAAGATCACTTC R:TGTATCCATAGATCACGATAAGAAGTCCAGGCTGCGACTTATTCAGGCGTAGCACCAG F:AACGAAAACCTTTAGACGGTGTATTGGCGAAAATGAAAAGCCTGTGACGGAAGATCACTTC R:CGCGGTGACCACTGACGGACGGTATACAATCACGGGGGGGATTATTCAGGCGTAGCACCAG F: GTTATTTTCAGCGCTCTGGTTGTTGGTTCATCTCATACCTGTGACGGAAGATCACTTC R: GAGAGATCATACGATTGTTCTGTCAGTCCATAACTTCACTTATTCAGGCGTAGCACCAG F: TATAGAATTC AATGAACATTAATAAAGTTATTTTCAG R: ATATGGATCCCTTAATGGTGATGGTGATGGTGAGTGTCTCAACAATACCG F:CTGCCAGACTGCAAGTGCTTACCCTTATCGCATTTACTCTGTGACGGAAGATCACTTC R:ACATTTGAAATCCGAAAGTTGATCCAGCTTACGATTGCTTATTCAGGCGTAGCACCAG
pMWG263	pDT1942 with <i>cat</i> inserted into <i>orf028</i> ; Tc ^r Kan ^r Cm ^r	
pMWG264	pDT1942 with <i>cat</i> inserted into <i>orf027</i> ; Tc ^r Kan ^r Cm ^r	
pMWG265	pDT1942 with <i>cat</i> inserted into <i>trhV</i> ; Tc ^r Kan ^r Cm ^r	
pMWG296	<i>trhV</i> cloned into pMS119EH; Amp ^r	
pGUN141	pDT1942 with <i>cat</i> inserted into <i>trhZ</i> ; Tc ^r Kan ^r Cm ^r	

pGUN206	<i>trhZ</i> cloned into pMS119EH; Amp ^r	F:ATATGAATTCAATGAAATATATATTGACCG R:ATATGGATCCTTATTGAACAGGGTGATGGGC	
pGUN139	pDT1942 with <i>cat</i> inserted into <i>017</i> ; Tc ^r Kan ^r Cm ^r	F:GAGTTTCAGCATTATTCTTACCTTACTTGTGACTGGATGCTGTGACGGAAGATCACTTC R:CTGAACCTCAATCAGAAAAGTAACTTTCCGTCGGGTAGTTATTCAGGCGTAGCACCAG	
pGUN142	pDT1942 with <i>cat</i> inserted into <i>016</i> ; Tc ^r Kan ^r Cm ^r	F:GAACTGATAATTTTGCCGTTGCTGGCATTMTTAGGTCCATCTGTGACGGAAGATCACTTC R:ATTCGGTTGACGTAATTTGCAGCAATAGTAATAAATTCATTTATTCAGGCGTAGCACCAG	
pGUN144	pDT1942 with <i>cat</i> inserted into <i>trhO</i> ; Tc ^r Kan ^r Cm ^r	F:TCCGAGCACGTCAGACAATTGATCTGACTAATTTTCAGCTGTGACGGAAGATCACTTC R:AAGAGATTTCCCTGTGGAGAAAACGATCAACTCCCTCATCAGTTATTCAGGCGTAGCACCAG	
pGUN77	<i>trhO</i> cloned into pMS119EH; Amp ^r	F:ATATGAATTCAATGGCATCCGAGCACGTCAG R:ATATGGATCCTTATAATGTGGCCTCTATATTATTATC	
pTDL205	pDT1942 with <i>cat</i> inserted into <i>htdA</i> ; Tc ^r Kan ^r Cm ^r	F:GCCCCAATTTTCATCGCTTAAAGTACGACTGGGAGTGGGCTCTGTGACGGAAGATCACTTC R:GCAGGCGGAATGACCACTTCGATGAGTATTGTATCAATTGTTATTCAGGCGTAGCACCAG	
pTDL244	<i>htdA</i> cloned into pMS119EH; Amp ^r	F:TATAAAGCTTATGTTATCACGCAACTCACT R:TATACTAGATTAAATGGTGATGGTGATGGTGACTTTCCTCCAGTTCC	
pTDL218	pDT1942 with <i>cat</i> inserted into <i>htdF</i> ; Tc ^r Kan ^r Cm ^r	F:TCTTACTCGATCTTTAACGCAAAACCGTCGAAGCCTGACTCTGTGACGGAAGATCACTTC R:ACAGAAGTGGTTTTAAGAACCTTGCCAGTAAAATCGTACATTATTCAGGCGTAGCACCAG	
pTDL206	pDT1942 with <i>cat</i> inserted into <i>htdK</i> ; Tc ^r Kan ^r Cm ^r	F:CAATCTGTGCGGATGGCATTCGAAGTAAATCTCGACAAAACGTGACGGAAGATCACTTC R:TTGAGTCTCAGTTACAAACGCCGAATTATCAGCAGAGCGATTATTCAGGCGTAGCACCAG	
pDOB7	pDT1942 with <i>cat</i> inserted into <i>orf009</i> ; Tc ^r Kan ^r Cm ^r	F:GTCGAGTACTCGAAGAACCGACTATGCGAACCGTTGATACTGTGACGGAAGATCACTTC R:TTATAGCGGCAACAGACACCTTCAATGGCAATCCATCGTTATTCAGGCGTAGCACCAG	
pGUN58	pDT1942 with <i>cat</i> inserted into <i>trhP</i> ; Tc ^r Kan ^r Cm ^r	F:ACGTGCCAATAAATCTCGGAATCCTGATACTGGTTATGTTTGTGACGGAAGATCACTTC R:AGCTATGATAATCCCTGACCTTACCGATTTATCCTTCAGATTATTCAGGCGTAGCACCAG	
pMWG114	<i>trhP</i> cloned into pMS119EH; Amp ^r	F:TATAGAATTCATGAGAGAATACATACCTAAG R:TATAGGATCCTTAATGGTGATGGTGATGGTGCGCAAAGATCGCATATGTTTTTC	(175)
pDT2985	pDT1942 with mini-Tn10 inserted into <i>trhW</i> ; Tc ^r Cm ^r Kan ^r	F:TATAGAATTCATGGGACTCACGTTTTTGG R:TATAGGATCCTTAATGGTGATGGTGATGGTGATTCTCCTCTGCCGCGATT	(175)
pTDL245	<i>trhW</i> cloned into pMS119EH; Amp ^r	F:TATAAAGCTTATGCTGTGCTCTCGCTG R:TATACTAGATTAAATGGTGATGGTGATGGTGGTGGTATATACCTGACGC	(175)
pDT2953	pDT1942 with mini-Tn10 inserted into <i>trhU</i> ; Tc ^r Cm ^r Kan ^r	F:TATAAAGCTTATGCTGTGCTCTCGCTG R:TATACTAGATTAAATGGTGATGGTGATGGTGGTGGTATATACCTGACGC	(175)
pTDL246	<i>trhU</i> cloned into pMS119EH; Amp ^r	F:TATAAAGCTTATGCTGTGCTCTCGCTG R:TATACTAGATTAAATGGTGATGGTGATGGTGGTGGTATATACCTGACGC	(175)
pDT2988	pDT1942 with mini-Tn10 inserted into <i>trhN</i> ; Tc ^r Cm ^r Kan ^r	F:TATAAAGCTTATGAAACATAGAAAAATAATTTCTTC R:TATACTAGATTAAATGGTGATGGTGATGGTGATATTTGGTATTTCTTACCTG	
pTDL247	<i>trhN</i> cloned into pMS119EH; Amp ^r	F:GTTTCAGCTTTAGTTGCAAGTGCCTCTCTGGTAGGGTGTGCCTGTGACGGAAGATCACTTC R:CAAACCGGCCAGAGAGTAAGCATTTTTGGCTACAGAATCTTATTCAGGCGTAGCACCAG	
pDOB5	pDT1942 with <i>cat</i> inserted into <i>orf004</i> ; Tc ^r Kan ^r Cm ^r	F:CAACAGATGAGCAAAGGGTCAATGAAAAATGCAAATGCCGTGACGGAAGATCACTTC R:CGGGTAAATGTGACCATCCCCACTTTGGCATAAGGGAACTTATTCAGGCGTAGCACCAG	
pDOB6	pDT1942 with <i>cat</i> inserted into <i>trhI</i> ; Tc ^r Kan ^r Cm ^r	F:CAACAGATGAGCAAAGGGTCAATGAAAAATGCAAATGCCGTGACGGAAGATCACTTC R:CGGGTAAATGTGACCATCCCCACTTTGGCATAAGGGAACTTATTCAGGCGTAGCACCAG	

^a Abbreviations: Nal^r, Nalidixic acid resistance; Rif^r, Rifampicin resistance; Tc^r, tetracycline resistance; Km^r, kanamycin resistance; Amp^r, ampicillin resistance.

^b Underlined regions of cloning primers designate restriction endonuclease cleavage sites; bold bases designate a His-tag and an engineered stop codon. Underlined regions of disruption primers designate *cat* specific bases.

on LB agar plates. Antibiotics were added at the following concentration when appropriate: ampicillin 100 µg/ml, tetracycline 10µg/ml, nalidixic acid 50 µg/ml, rifampicin 50 µg/ml and chloramphenicol 16 µg/ml. X-Gal (5-bromo-4-chloro-3-indolyl-β-D-galactopyranoside) and IPTG (isopropyl-β-D-thiogalactoside) were each used at 50 µg/ml.

2.2.2 DNA Manipulations

R27 DNA was isolated using either ultracentrifugation in a CsCl-ethidium bromide gradient (212) or with the Qiagen Large-Construct Kit (Qiagen Inc., Mississauga, Ont.). Expression and cloning vectors were purified using Qiagen Midi-preps (Qiagen Inc.). Standard recombinant DNA methods were performed as described in Sambrook et al. (176). Restriction endonucleases were used according to the manufacturer's instructions and digested DNA was analysed by agarose gel electrophoresis.

2.2.3 Computer Analysis

Laser gene software (DNASTAR Inc., Madison, WI) was used for nucleotide sequence analysis. Repeated nucleotide sequences were identified with GeneQuest. The predicted protein sequence for each ORF was compared to the GenBank non-redundant database using PSI-BLAST. Conserve motifs were identified manually or with ScanProsite (<http://ca.expasy.org/tools/scnpsite.html>) and obtained predictions for molecular weight and pI values with Compute pI/Mw (http://ca.expasy.org/tools/pi_tool.html).

2.2.4 Mutagenesis

Mutants of *traG*, *traI*, *trhF*, *trhH* and *trhG* in Tra1 and *trhE*, *trhK*, *trhB*, *trhC*, *trhW*, *trhU* and *trhN* in Tra2 were created prior to this study using random mini-Tn10 mutagenesis (145) as described previously (175). Mini-Tn10 consists of a chloramphenicol resistance cassette flanked by Tn10 inverted repeats (101). To identify the insertion position for each mutant, the region flanking the mini-Tn10 insertions was sequenced using the dideoxy method (Sequenase version 2; United States Biochemical

Co., Cleveland, Ohio) with primers PNE11 (5'TATTCTGCCTCCCAGAGCCT) and PNE12 (5'TGGTGCCTAACGGCAAAAAGC). Sequence results were compared to the complete nucleotide sequence of R27 (ACCESSION NC_002305). All remaining Tra1 genes (*115*, *116*, *traJ*, *118*, *121*, *traH*, *trhR*, *trhY* and *trhX*) and Tra2 genes (*trhA*, *trhL*, *orf030*, *orf028*, *orf027*, *trhV*, *trhZ*, *orf017*, *orf016*, *trhO*, *htdA*, *htdF*, *htdK*, *orf009*, *trhP*, *orf004*, and *trhI*) were mutated by gene disruption using the *E. coli* recombination system recently described by Yu and colleagues (217). This method utilizes *E. coli* strain DY330, containing a defective lambda prophage that serves to protect and recombine an electroporated linear DNA substrate *in vivo*. Gene disruptions were created by insertion of a chloramphenicol-resistance cassette (CAT; *cat* from mini-Tn10) into each of the above mentioned ORFs in a sequence-specific fashion. DNA substrates were generated through PCR with primers (~60nt) that produced a linear CAT cassette with 40 bp terminal arms homologous to the desired target site (Table 2-1). DNA substrates were introduced by electroporation into DY330 harboring R27 that was grown according to Yu et al. (217). Cells were plated on agar plates containing both tetracycline, to select for R27, and chloramphenicol, to select for the desired insertions. To screen presumptive colonies, the target gene was PCR amplified (using cloning primers as described below) and analyzed with 1% agarose gel electrophoresis. An increase in the size of the ORF by ~900 bp demonstrated that the CAT cassette had been inserted into the target gene. The insertion location of the CAT cassette into *traJ* was confirmed by sequencing with primers GIL86 (5'CAGTTATTGGTGCCCTTAAAC) and GIL87 (5'GGTATCAACAGGGACACCAG), verifying the precision of this method.

2.2.5 Cloning of Transfer Genes

The primer sequences used for cloning Tra1 and Tra2 transfer genes are listed in Table 2-1. PCR products, which included terminal *Bam*HI and *Eco*RI (*Bam*HI and *Pst*I for *traI*) or *Hind*III and *Xba*I restriction endonuclease sites, were cloned into pGEM-T (Promega) and then subcloned into either pMS119EH, pMS119HE or pBAD24. A His₆-tag was engineered into the C-terminus of each protein to facilitate the detection of the recombinant protein by immunoblot analysis with anti-His₆ antibodies in future studies.

2.2.6 Conjugation Assay

Conjugal transfer of R27 was performed as previously described (199). For complementation experiments, *E. coli* donors (DY330R) which contained the R27 transfer mutant and an expression vector encoding the appropriate transfer protein were mated with recipients (DY330N). To determine the effect of over-expressing transfer proteins on the transfer frequency, each transfer protein was expressed *in trans* within a donor containing R27 during conjugation experiments. Transfer frequencies were expressed as transconjugants per donor.

2.2.7 Phage Plaque Assays

Hgal RNA bacteriophage was prepared as previously described (126). Phage spot tests were performed to determine Hgal infectivity of TraI mutants. A 50 μ L sample of mid-logarithmic phase cultures was suspended in 8 mL of brain heart infusion (BHI) broth (Difco Laboratories, Detroit, Mich.) containing 0.6% agar that was incubated at 48°C. The suspension was overlaid onto a fresh BHI plate. After solidification of the overlay 10 μ L of Hgal stock (10^9 Pfu/mL) was spotted on the overlay. Plates were incubated at 27°C overnight and analyzed for zones of clearing in the Hgal-spotted regions.

2.2.8 Cloning of Origin of Transfer

Two intergenic regions from the TraI region were considered likely to harbor the *oriT*, a 757 bp region between *traH* and *trhR* and a 400 bp region between *trhY* and *trhX*. Since the *oriT* is the only element required *in cis* on a DNA molecule for transfer (106), each of these regions was cloned to determine if either could be mobilized by R27. A 1.3 kbp *KpnI-SnaBI* region containing the 757 bp intergenic region was cloned into the *KpnI* and *SmaI* sites of pBAD30 (75) and a 1.5 kbp *HindIII-XbaI* fragment containing the 400 bp intergenic region was cloned into the same sites of pBAD30 (Figure 2-3). The 1.3 kbp fragment was mobilized by R27 at a frequency of 10^{-3} transconjugants/donor, whereas both the 1.5 kbp *HindIII-XbaI* clone and pBAD30 were not mobilized.

To systematically identify the minimal *oriT*, regions of the 1.3 kbp clone were PCR amplified, cloned and tested in mobilization experiments. The strategy is outlined

in Figure 2-3. Two overlapping regions of the 1.3 kbp fragment were PCR amplified using primers which incorporated *Kpn*I and *Hind*III sites to the ends. These products were cloned into pBAD30 using the *Kpn*I and *Hind*III sites, resulting in clones of *oriT* 1.1 (977 bp) and *oriT* 1.2 (794 bp). The primers for amplifying *oriT* 1.1 were oritclone1 and nicprimer3 and the primers for amplifying *oriT* 1.2 were orit2 and nicprimer5 (Table 2-1). The *oriT* 1.2 clone was mobilized by R27, whereas the *oriT* 1.1 clone and pBAD30 alone were not mobilized under the same conditions. Two overlapping regions of the of the *oriT* 1.2 clone were subcloned as described above, resulting in clones of *oriT* 2.1 (360 bp) and *oriT* 2.2 (285 bp). The primers for amplifying *oriT* 2.1 were Trev3000 and Trev3002 and the primers for amplifying *oriT* 2.2 were Trev3001 and Trev3004 (Table 2-1). The *oriT* 2.2 clone was mobilized by R27 at a frequency of 10^{-3} transconjugants/donor, whereas the *oriT* 2.1 clone and pBAD30 alone were not mobilized.

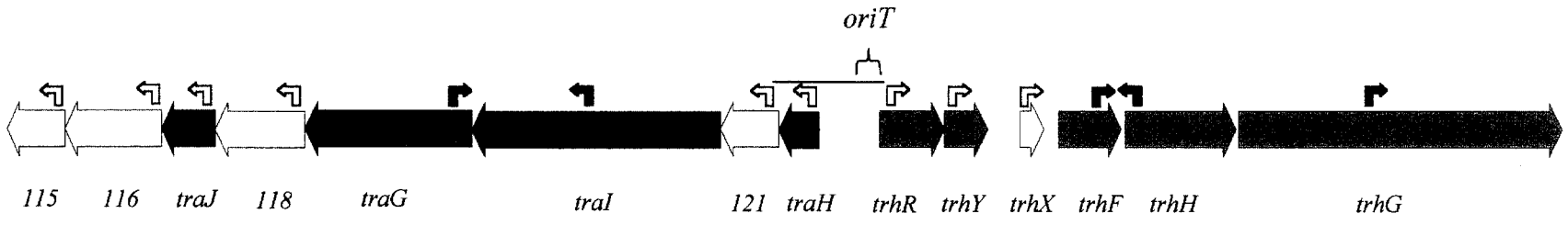
2.3 Results

Transfer 1 Region

2.3.1 Nucleotide Sequence Analysis of Tra1 Region

The location of the Tra1 region in R27 was originally identified by using random transposon mutagenesis and screening for transfer-deficient mutants (145). The completion of the nucleotide sequence of R27 allowed the precise mapping of the insertion location of 15 mini-Tn10 transfer mutants into 5 genes: *traG*, *traI*, *trhF*, *trhH* and *trhG* (Figure 2-1; Table 2-3 and 2-3) (187). R27 transfer genes have been named, *trh* (mating pair formation), *tra* (relaxosome or coupling) or *htd* (H transfer determinant). The genetic organization of this region suggests that these genes are contained within transfer operons, an organization that is commonly seen in other transfer systems, such as those from IncF (56) and IncP plasmids (158, 201). The ends of these putative operons were used to define the Tra1 region as a starting point for this study. Therefore, the Tra1 region was defined as being between the coordinates 98 and 117 kb on R27 and contains 14 ORFs. The ORFs are organized into three operon units, using the operon structure defined by Ermolaeva *et al.* (50), consisting of 8, 2 and 4 ORFs, which are separated by

Figure 2-1. Open reading frame (ORF) map of the transfer region 1 of R27. Red ORFs indicate essential Mpf genes, blue ORFs indicate relaxosome genes and the green ORF indicates the coupling protein gene. Light grey genes are not essential for conjugative transfer. The mating pair formation genes have been designated *trh* and the relaxosome and coupling genes have been designated *tra*. Black bent arrows represent the insertion location of mini-Tn10 and direction of CAT transcription. White bent arrows represent the insertion location of CAT cassette and direction of transcription. *oriT* indicates a 285 bp region of TraI that has been cloned and is mobilized by R27. Black horizontal line indicates *KpnI-SnaBI* fragment used to identify *oriT*. ORF map corresponds to coordinates 98 to 117 kbp and ORF115 to ORF128 on R27 (187).



1 kbp

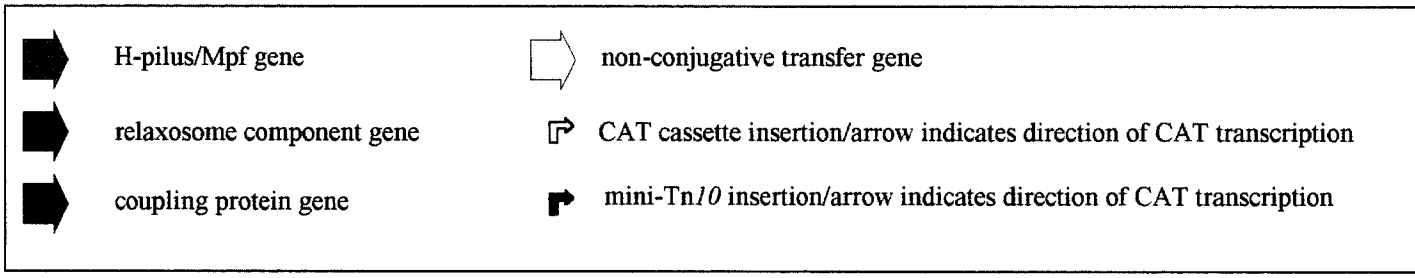


Table 2-2. Summary of computer analysis of nucleotide sequence of transfer region 1 from R27

Gene/ ORF ^a	Length (aa)	Mol Wt ^b	Motif ^c	PSI-BLAST results (protein/source/length of homolog)	Degree of relatedness (identical residues/range of identity=% identity)	Accession no. of homolog
<i>orf115</i>	242	27.9	none	Orf8 of <i>B. uniformis</i> NBU element (246aa)	46/210=21%	AF238367
<i>orf116</i>	393	42.9	Type IV protease (191-325)	Proteinase IV of <i>V.</i> <i>chloraea</i> (616aa)	69/343=20%	H82130
<i>traJ</i>	220	25.4	AraC motif (8-48) and leucine zipper (182-202)	none		
<i>orf118</i>	367	42.2	none	none		
<i>traG</i>	694	80.0	Walker A (205-212) and B (504-514)	TraG from R751 (637aa)	70/539=12% C-terminus	S22992
<i>traI</i>	1011	113.0	Relaxase and Zinc carboxypeptidase (588-598)	none		
<i>orf121</i>	240	27.9	none	none		
<i>traH</i>	161	19.2	none	none		
<i>trhR</i>	266	30.3	none	none		
<i>trhY</i>	170	19.4	none	none		
<i>trhX</i>	95	11.0	none	none		
<i>trhF</i>	348	39.6	none	TraF from R100 (247aa)	46/231=19%	AAB61943
<i>trhH</i>	470	48.1	none	TraH from R100 (460aa)	108/419=25%	BAA78879
<i>trhG</i>	1329	140.9	none	TraG from F factor (938aa)	121/682=17% N-terminus	AAC44184

^a Gene designation and coordinates as in Sherburne et al. (187).

^b Molecular weight predicted with EditSeq program of Lasergene (DNASar, Inc.)

^c Conserved Domain Database and ScanProsite (<http://ca.expasy.org/tools/scnpsite.html>)

Table 2-3. Effect of mutations in *TraI* on R27 conjugation.

R27 mutant ^a in the donor strain	Transfer ^b phenotype of mutant ^c	Relative conjugation frequency of R27 mutant (%) ^d	Relative conjugation frequency during complementation (%) ^e	Relative conjugation frequency of R27 with over- expressed transfer protein ^f (%)	Plaque with Hgal ^g
<i>115</i>	+	120	N/D	N/D	+
<i>116</i>	+	130	N/D	N/D	+
<i>traJ</i>	-	0	24	23	+
<i>118</i>	+	100	N/D	N/D	+
<i>traG</i>	-	0	5	30	+
<i>traI</i>	-	0	5	100	+
<i>121</i>	+	14	N/D	N/D	+
<i>traH</i>	-	0	83	97	+
<i>trhR</i>	-	0	221	177	-
<i>trhY</i>	-	0	0.2	217	-
<i>trhX</i>	+	16	N/D	N/D	+
<i>trhF</i>	-	0	0.5	65	-
<i>trhH</i>	-	0	0.3	79	-
<i>trhG</i>	-	0	136	77	-

^a Gene designation according to complete sequence of R27 (187) or this study. Donor strain was DY330R.

^b Ability of mutant to transfer via conjugation. Detectable matings scored as “+” and non-detectable (<10⁻⁸ transconjugants/donor) scored as “-”.

^c CAT cassette introduced into gene by either random transposon mutagenesis or homologous recombination as described in Materials and Methods.

^d Transfer frequency of R27 mutant relative to R27 [(R27 mutant frequency / R27 frequency) x 100%]. Due to the inherent variation of R27 transfer frequency, relative frequency was determined using the R27 transfer frequency for each experiment. R27 transferred with an average frequency of 5 x 10⁻¹ transconjugants/donor. Values represent the average values of two independent experiments.

^e Restoration of conjugation by complementation *in trans* using a cloned gene (see Table 1); N/D, not determined. Transconjugants/donor cell after 18 hr liquid mating with recipient DY330N, as described in Materials and Methods.

^f Designated transfer protein was over-expressed in donor containing R27 during conjugation assay. Relative transfer frequency of R27 with transfer protein / R27 for each experiment. Values represent the average value of two independent experiments.

^g Ability of H-pilus specific RNA bacteriophage to form plaques with *E. coli* harboring designated mutant of R27 (agar spot test). *E. coli* containing R27 forms plaques when infected with H-gal.

two intergenic regions of 757 and 400 bp. The putative transcriptional units are transcribed away from the 757 bp intergenic region (Figure 2-1).

To identify potential transfer genes and to determine any evolutionary relationship to other conjugative systems, the predicted protein sequence from each TraI ORF was compared against the GenBank database using PSI-BLAST. Only six of the protein sequences had significant hits in the database (Table 2-2). ORF115 shares identity with ORF8 from the *Bacteriodes uniformis* mobile element NBU1 (189). ORF116 is homologous to a putative proteinase IV from *Vibrio cholerae*. TraG shares a low identity with TraG from the IncP β plasmid R751 (201), but also shares homology to coupling proteins from several other conjugative systems, such as IncW and IncF. TrhF, TrhH and TrhG share identity with TraF, TraH, and TraG, respectively, from IncF plasmids (7).

To identify conserved sequence motifs, the predicted amino acid sequence from each ORF from TraI was compared to the Prosite database. The ORF116 sequence contains a motif characteristic of Type IV proteases, which is consistent with the BLAST analysis. TraJ contains a helix-turn-helix motif at residues 8-48, which is characteristic of transcriptional regulators belonging to the AraC family, and a leucine zipper motif at 182-202, which is a common dimerization domain. TraG contains a Walker A ATP binding motif at position 205-212 (Figure 2-2). An alignment of TraG (IncHI1) with TrwB (IncW) and TraG (IncP β) has identified a conserved Walker B ATP binding domain at position 504-514 (Figure 2-2), although the importance of this motif has yet to be demonstrated (64). TraI, which has previously been shown to contain all three relaxase domains (187), contains a Zinc carboxypeptidase motif at position 588-598, although the significance of this is unknown.

2.3.2 TraI Gene Disruptions and Identification of Transfer Mutants

To supplement the mini-Tn10 transfer mutants, and to identify a role for ORFs 115, 116, traJ, 118, 121, traH, trhR, trhY and trhX in the conjugative transfer of R27, gene disruptions of each of these ORFs were systematically created. A CAT cassette (chloramphenicol-resistance gene) was inserted within the first 120 bp of the predicted start codon of each ORF using the methods of Yu et al (217). Each plasmid mutant was then tested for its ability to transfer (Table 2-3). Gene disruptions in traJ, traH, trhR and

Figure 2-2. Alignment of A) Walker A and B) Walker B boxes from coupling proteins from R27 (TraG; accession NP_058332), R388 (TrwB; accession CAA44852), and R751 (TraG; accession S22992). Numbers represent the number of amino acid residues preceding the motif. Motifs were aligned in MegAlign (DNASTAR Inc.) and shaded in GeneDoc using conservative mode and 2 levels.

A)

		Walker A
R27	TraG (200)	H T L I T G N V G T G K T V L
R388	TrwB (125)	H L L V N G A T G T G K S V L
R751	TraG (177)	H V L T Y A P T R S G K G V G

B)

		Walker B
R27	TraG (504)	R I S I F V D E A H S
R388	TrwB (350)	R L W L F I D E L A S
R751	TraG (444)	R L L M M L D E F P S

trhY abolished conjugative transfer of R27. A disruption of *trhX* reduced the conjugation frequency of R27 10-fold, whereas disruptions of *orf115*, *116*, *118* and *121* had no effect on the conjugation frequency. These data, combined with that from the random transposon mutagenesis experiments, indicate that nine of the fourteen genes within the Tra1 region are essential for conjugative transfer of R27 (Table 2-3; Figure 2-1).

2.3.3 Genetic Complementation of Tra1 Transfer-Deficient Mutants

The wild-type gene corresponding to each of the transfer-deficient mutants was cloned into the expression vectors pMS119EH, pMS119HE or pBAD24 (Table 2-1). Each clone was transformed into the strain containing the appropriate R27 mutant. When the wild-type version was expressed *in trans*, conjugative transfer of R27 was restored for each of the nine transfer-deficient mutants (Table 2-3), demonstrating that each of these genes is essential for conjugative transfer.

During complementation experiments, the conjugation frequency varied between 221% (*trhR*) and 0.2% of wild-type levels (*trhY*) (Table 2-3). Two explanations for the variation could be due to transcriptional polar effects and/or that the over-expressed transfer proteins affects wild-type conjugation frequencies. To address these possibilities, the complementation frequencies for each mutant were compared to the transfer frequency of R27 when the corresponding transfer protein was over-expressed in donors during conjugation experiments (Table 2-3). Any difference in the conjugation frequency between the complementation and the over-expression experiments may reflect polar effects on downstream genes.

Over-expression of either TraI or TraH had no effect on the transfer frequency of R27, whereas the *traI* and *traH* mutants were complemented to 5% and 83% of wild-type levels. This indicates that the *traI* and *traH* mutants are partially polar. When either TrhR or TrhY were over-expressed the transfer frequency increased to 177% and 152% of wild-type levels, respectively. The *trhR* mutant complemented to 221% of wild-type levels, whereas the *trhY* mutant was complemented to 0.2% of wild-type levels. This indicates that the *trhY* mutant is partially polar. When TraJ, TraG, TrhF, TrhH or TrhG were over-expressed individually in donors the transfer frequencies were reduced to 23%, 30%, 65%, 79% and 77% of wild-type levels, respectively. In the case of both TraJ and

TrhG, these frequencies were comparable to their respective complementation frequencies (Table 2-3). This suggests that the reduced transfer frequency of *traJ* and *trhG* during complementation experiments is due to the over-expression of these transfer proteins and not because of polarity, as would be expected for mutants at the ends of transfer operons. Since over-expression of TraG, TrhF or TrhH cannot account for the low levels of complementation, these mutants are likely partially polar.

These results suggest that both mini-Tn10 and CAT cassette insertions resulted in partially polar transfer mutants of *traG*, *traI*, *traH*, *trhY*, *trhF* and *trhH*. Nevertheless, these mutants allowed for the identification of nine essential transfer genes within the Tra1 region of R27.

2.3.4 Hgal Plaque Assay of R27 Tra1 Transfer-Deficient Mutants

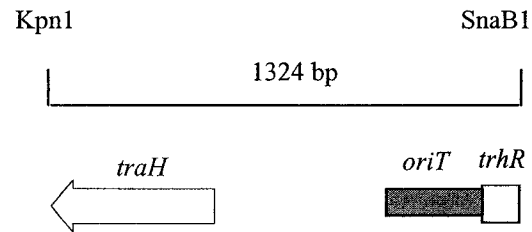
Hgal is an H-pilus specific bacteriophage that lyses *E. coli* harbouring R27 to form distinctive plaques. Hgal binds uniformly along the shaft of H-pili (126); this property of Hgal has been used to document the kinetics of H-pilus assembly (127). An Hgal plaque assay was utilized to determine which of the Tra1 transfer mutants were resistant or sensitive to Hgal lysis (Table 2-3). *E. coli* cells containing transfer mutants *trhR*, *trhY*, *trhF*, *trhH* and *trhG* were resistant to Hgal, suggesting that these transfer genes play a role in H-pili biosynthesis. This is consistent with the roles predicted for *trhF*, *trhH* and *trhG* using PSI-BLAST analysis of these genes. Cells containing plasmids with mutants of *traJ*, *traG*, *traI*, and *traH* remained sensitive to Hgal, suggesting that their role(s) in conjugation is not related to H-pili biosynthesis. These results would be expected for the relaxosome components and the coupling protein, as RP4 *traG* remained sensitive to phage (209).

2.3.5 Identification and Cloning of the R27 Origin of Transfer within Tra1

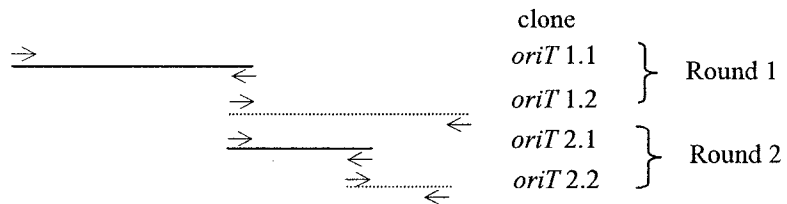
The *oriT* contains the *nic* site and is typically located next to the DNA processing genes within conjugative systems. It was therefore anticipated that the *oriT* of R27 would be present within the Tra1 region (Figure 2-3). A 757 bp intergenic region between *orf122* and *orf123* contains several hallmark features of *oriT* regions, including:

Figure 2-3. Origin of transfer. A) Genetic organization of the 1.3 kbp *KpnI-SnaBI* fragment containing *oriT* activity. Shown is the location of the 285 bp *oriT* between *traH* and *trhR*. B) Cloning strategy used to identify the 285 bp *oriT*. PCR primers were used to amplify regions and incorporate *KpnI* and *HindIII* restriction sites that were used to clone fragments into the same sites of pBAD30 (See materials and methods for details). Horizontal lines represent sub-clones of the 1.3 kbp *KpnI-SnaBI* fragment and are aligned with above schematic (A). Broken lines represent clones that were mobilized by R27, whereas solid lines represent clones that were not mobilized by R27. Round 1 identified a 977 bp region that was mobilized by R27 and was designated *oriT* 1.2. Round 2 identified a 285 bp region that was mobilized by R27 and was designated *oriT* 2.2. C) Nucleotide analysis of a 285 bp region with *oriT* activity. Three 8 bp and one 9 bp direct repeats were identified and are represented by arrows. No matches to any of the 5 nic site families were identified.

A)



B)



C)

```

GGTTATTGCTACTTAATGCCGATAACGACTCAGGCTTTGAGGTTTTTTTATACGGTTCACATTC
GTTAGCAAGGTCAGGGTTTTTTGATAAAAATTCTGGTTAGTTTGGTTAAAAAGTGTTACAAGTAA
GGGTAATGGCTGAAAGGTTAGTTTTAAGGTTCAAAGCGGCAGTATTA AAAATTCCAAAAGTTAC
TTTCATCCTTCAGAATCCAGACCTTAATTCATGTAGAAGATTCGTACAATTGTATTGGCGCA
AGGACAATCCGCACATGTCAGAATCAGAT

```

i) being located between diverging ORFs, ii) a high %A+T content (62.5% vs. 52% for R27) (not shown), and iii) a number of inverted and direct repeat sequences (not shown).

A 285 bp minimal *oriT* region was localized within the 757 bp intergenic region and was mobilized by R27 at a frequency of 10^{-3} transconjugants/donor (Figure 2-3). The *oriT* is located adjacent to *trhR* and contains three 8 bp direct repeats and one 9bp direct repeat. A comparison of the *oriT* nucleotide sequence to the five *nic* site families (218) revealed no matches. Additional studies are required to precisely identify the *nic* site within this region.

Transfer 2 Region

2.3.6 Nucleotide Sequence Analysis of Tra2 Region

The Tra2 region is 36 kb in length and contains 28 ORFs, four of which code for two separate partitioning modules (Chapter 3). All ORFs are transcribed in the same direction, with the exception of ORF004 and ORFs 015-018, which appear to constitute an operon. Previous analysis indicated that the Tra2 region encodes Mpf proteins that are related to Mpf proteins of IncF transfer systems, as determined by Basic Local Alignment Search Tool (BLAST) analysis (175). Prior to mutational and functional analysis of the Tra2 region, Position Specific Iterated-BLAST (PSI-BLAST) analysis, a more sensitive version of BLAST analysis, was performed and protein alignments with each of the predicted protein products of the Tra2 region and the findings are described quantitatively (Table 2-4). TrhL, E, B, V, C, P, W, U and N are homologous to Mpf proteins from the F factor (175), with levels of identity ranging from 20-32% (Table 2-4 and 2-5). The N-terminus of TrhW is similar to TrbC of the F factor, suggesting a gene fusion in R27 and that the functions of the latter two proteins are coupled in the F factor. TrhP (previously named TrhF) is homologous to the signal peptidase I protein family, which includes TraF, a transfer peptidase of IncP plasmids (187).

ORF031 is similar to TraK of the F factor and has been named TrhK (Figure 2-5 and Table 2-5). Interestingly, TrhK also shares a significant level of similarity to the HrcC/HrpH secretin family present in the Type III secretion system of organisms such as *Pseudomonas fluorescens* (167). The similarity shared between TrhK-like proteins and HrcC-like proteins is present in the C-terminus (Figure 2-5), the defining domain of

Figure 2-4. Open reading frame (ORF) map of the transfer region 2 of R27. Red ORFs indicate essential Mpf genes. Stippled ORFs indicate genes which regulate R27 transfer frequency. Light grey genes are not essential for conjugative transfer. Black ORFs are partitioning genes and the Inc region is a 3 kbp intergenic region involved in IncHI1 plasmid incompatibility (57). The mating pair formation genes have been designated *trh*. Black bent arrows represent the insertion location of mini-Tn10 and direction of CAT transcription. White bent arrows represent the insertion location of CAT cassette and direction of transcription. ORF map corresponds to coordinates 0 to 40 kbp and ORF003 to ORF034 on R27 (187).

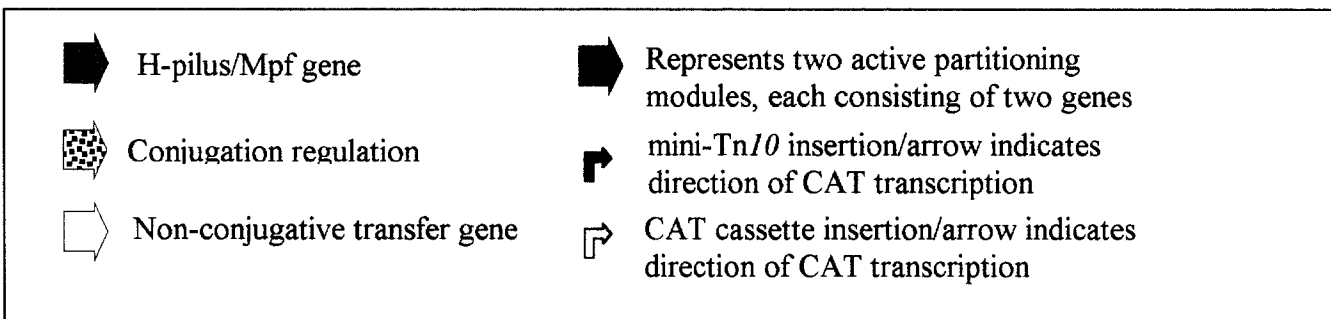
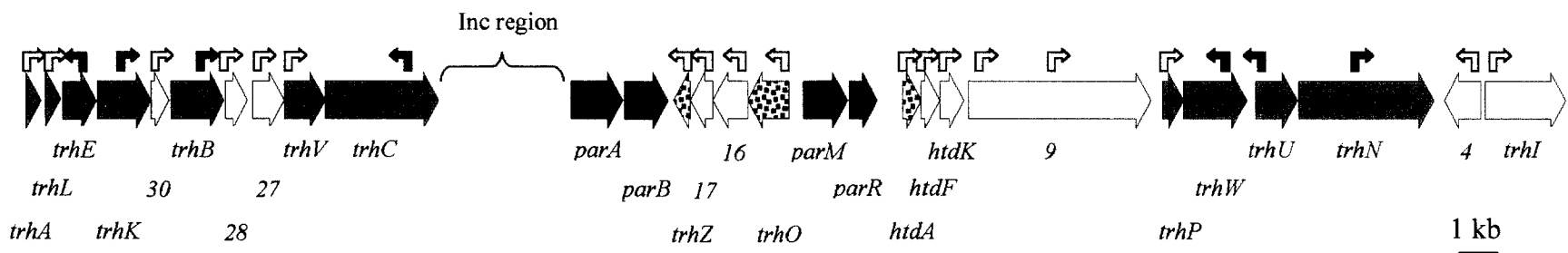


Table 2-4. Summary of computer analysis of nucleotide sequence of transfer region 2 from R27

Gene/ ORF ^a	Length (aa)	Mol Wt ^b	Motif ^c	PSI-BLAST results (protein/source/length of homolog)	Degree of relatedness (identical residues/range of identity=% identity)	Accession no. of homolog
<i>trhA</i>	117	12.4	none	HtdZ of R478 (126aa)	77/117=65%	AAL27017
<i>trhL</i>	105	12.4	none	HtdL of R478 (116aa) TraL of F (103aa)	76/105=72% 21/105=20%	AAL27018 BAA97945
<i>trhE</i>	261	29.2	none	HtdE of R478 (262aa) TraE of F (188aa)	194/261=74% 30/147=20%	AAL27019 BAA97946
<i>trhK</i>	410	44.4	none	HtdP of R478 (423aa) TraK of F (242aa)	337/423=79% 48/230=21%	AAL27020 BAA97947
<i>orf30</i>	146	16.4	none	HtdO of R478 (153aa)	60/138=43%	AAL27021
<i>trhB</i>	452	48.3	none	HtdB of R478 (451aa) TraB of F (475 aa)	319/452=86% 96/391=24%	AAD01913 BAA97948
<i>orf28</i>	170	19.0	none	HtdV of R478 (112aa)	39/75=52%	AAL27016
<i>orf27</i>	250	28.0	none	HtdT of R478 (326aa)	206/250=82%	AAD01914
<i>trhV</i>	316	33.8	Lipoprotein motif (21aa)	HtdD of R478 (316aa) TraV of F (171aa)	253/316=80% 24/96=24%	AAD01915 BAA97952
<i>trhC</i>	893	102.0	Walker A (463- 470aa) and Walker B (722-725)	HtdC of R478 (893aa) TraC of F (875aa)	748/893=83% 200/899=22%	AAD01916 BAA97954
<i>trhZ</i>	130	14.1	None	none		
<i>orf17</i>	173	19.0	Lipoprotein motif (15aa)	none		
<i>orf16</i>	279	30.8	none	none		
<i>trhO</i>	315	34.9	none	none		
<i>htdA</i>	150	16.7	none	HtdA of R478 (150aa)	126/149=84%	AAB05912
<i>htdF</i>	144	15.8	none	HtdF of R478 (141 aa)	71/142=50%	AAB37116
<i>htdK</i>	187	20.8	none	HtdK of R478 (177aa)	88/167=52%	AAB37117
<i>orf9</i>	1406	155.5	none	none		
<i>trhP</i>	170	19.4	Signal peptidase 1	TraF of RP4 (177aa)	28/124=22%	AAA98335

<i>trhW</i>	502	56.5	none	TraW of F (210aa) in C-terminus TrbC of F (212aa) in N-terminus	49/193=25% 34/146=23%	BAA97956 AAB61940
<i>trhU</i>	335	37.0	none	TraU of F (330aa)	104/320=32%	AAB61938
<i>trhN</i>	1058	116.7	none	TraN of F (602aa)	25/112=22% 27/132=20%	BAA97959
<i>orf4</i>	290	31.1	Lipoprotein motif (21aa)	none		
<i>trhI</i>	594	67.6	DNA Helicase motifs	DNA helicase II of <i>Serratia marcescens</i> (720aa)	167/640=26%	AAC46278

^a Gene designation and coordinates as in Sherburne et al. (187).

^b Molecular weight predicted with EditSeq program of Lasergene (DNASTar, Inc.)

^c Conserved Domain Database and ScanProsite (<http://ca.expasy.org/tools/scnpsite.html>)

Table 2-5. Effect of mutations in Tra2 on R27 conjugation.

R27 mutant ^a in the donor strain	Transfer ^b phenotype of mutant ^c	Relative conjugation frequency of dr R27 mutant (%) ^d	Relative conjugation frequency during complementation (%) ^e	Relative conjugation frequency of drR27 with over- expressed transfer protein ^f (%)	Plaque with Hgal ^g
<i>trhA</i>	-	0	0.2	93	-
<i>trhL</i>	-	0	0.7	208	-
<i>trhE</i>	-	0	2.2	150	-
<i>trhK</i>	-	0	15.9	130	-
<i>orf030</i>	+	55	N/D	N/D	+
<i>trhB</i>	-	0	14	79	-
<i>orf028</i>	+	10	N/D	N/D	+
<i>orf027</i>	+	100	N/D	N/D	+
<i>trhV</i>	-	0	0.2	72	-
<i>trhC</i>	-	0	90	95	-
<i>trhZ</i>	+	0.006	73	23	+
<i>orf017</i>	+	43	N/D	N/D	+
<i>orf016</i>	+	95	N/D	N/D	+
<i>trhO</i>	+	0.0002	77	83	+
<i>hidA^h</i>	+++	600 000	120	90	+++
<i>htdF</i>	+	7	N/D	N/D	+
<i>htdK</i>	+	7	N/D	N/D	+
<i>orf009</i>	+	0.6	N/D	N/D	+
<i>trhP</i>	-	0	131	54	-
<i>trhW</i>	-	0	144	88	-
<i>trhU</i>	-	0	1.2	90	+/-
<i>trhN</i>	-	0	133	82	+/-
<i>orf004</i>	-	34	N/D	N/D	+
<i>trhI</i>	-	76	N/D	N/D	+

^a Gene designation according to complete sequence of R27 (187) or this study. Donor strain was DY330R.

^b Ability of mutant to transfer via conjugation. Detectable matings scored as “+” and non-detectable (<10⁻⁸ transconjugants/donor) scored as “-“.

^c CAT cassette introduced into gene by either random transposon mutagenesis or homologous recombination as described in Materials and Methods.

^d Transfer frequency of drR27 mutant relative to drR27 [(drR27 mutant frequency / drR27 frequency) x 100%]. Due to the inherent variation of drR27 transfer frequency, relative frequency was determined using the drR27 transfer frequency for each experiment. drR27 transferred with an average frequency of 5×10^{-1} transconjugants/donor. Values represent the average values of two independent experiments.

^e Restoration of conjugation by complementation *in trans* using a cloned gene (see Table 1); N/D, not determined. Transconjugants/donor cell after 18 hr liquid mating with recipient DY330N, as described in Materials and Methods.

^f Designated transfer protein was over-expressed in donor containing drR27 during conjugation assay. Relative transfer frequency of drR27 with transfer protein / drR27 for each experiment. Values represent the average value of two independent experiments.

^g Ability of H-pilus specific RNA bacteriophage to form plaques with *E. coli* harboring designated mutant of drR27 (agar spot test). *E. coli* containing drR27 forms plaques when infected with H-gal.

^h Experiments and mutagenesis on *htdA* were performed on wild-type R27, which transfers at a frequency of 5×10^{-5} transconjugants/donor. All values in this row are relative to wild-type R27.

Figure 2-5. Alignment of Type IV secretion system secretin-like proteins of the TrhK family with the HrcC Type III secretion system secretins and the PulD Type II secretion system secretin. Represented below the alignment are the β -Domain and S-Domain from PulD. The β -Domain encompasses the transmembrane regions which are embedded into the outer membrane and the S-Domain interacts with the lipoprotein. Alignment was performed with ClustalW using the BLOSUM scoring matrix and shading was performed using GeneDoc in Conservative mode with shading to 4 levels. Proteins in order they are listed in alignment: TraK of F factor (GenBank Accession No. AAC44189), TraK of R391 (AAM08021), TraK of Rts1 (BAB93771), HtdP of R478 (AAL27020), TrhK of R27 (AAD54050), TraK of pED208 (AAM90706), TraK of pNL1 (AAD03962), TraK of SXT (AAL59718), HrcC of *Pantoea stewartii* (AAG01463), HrcC of *Erwinia amylovora* (AAB49179), HrcC of *Erwinia chrysanthemi* (AAC31975), HrcC of *Pectobacterium carotovorum* (AAK97280), HrcC of *Pseudomonas syringae* (AAC05014), RscC of *Pseudomonas fluorescens* (AAK81929) and PulD of *Klebsiella oxytoca* (P15644).

TraK F : ----ISNTSPNL---FTVP---GDRIIAVN---SDGAL--TNNEQTASG--VVVATVNNKPPFFLETER--G-LN : 100
 TraK R391 : ----TLITPGVNELPVALGHLNRIVTPFESP--QVRTS--DAQTOHKN-VVVVATDKESPVSYITPPGQ--EAPA : 132
 TraK Rts1 : IPSRQDIITPEPGVNTLPIISMGIINRIVTPFERP--TQRQLQ-LDDVKVNVNEN-AMVVYTPNSRPVALYIASEKGD--ESVS : 205
 HtdP R478 : YKEVQRVNIIPPGGNVIVPVSRLQNRISTSFKVA--SVSTSTPAEASIFVNGG-DWFISTNTDKPIGLMLSEDOV--PEST : 238
 TrhK R27 : YKEVQRVNIIPPGGNVIVPVSRLQNRISTSFKVA--SVSTSTPAEASIFVNGG-DWFISTNTDKPIGLMLSEDOV--PEST : 225
 TraK pED208 : ----ISNTDPNM-----IFIPGDKVT--ATAPGGMLADKRLTRAG--GLFTSVATRFTFVFETAR--GQT : 99
 TraK pNL1 : ----LTRISLAG-----DQFASVSKIS--TGNPAEDFKIVNEPREDIY--SVPDGFTKPNLSFGTTRK--G-YV : 126
 TraK SXT : ----TLITPGVNELPVALGHLNRIVTPFESP--QVRTS--DAQTOHKN-VVVVATDKESPVSYITPPGQ--EAPA : 132
 HrcC Pstew : ASIQLVIDEDGH---WETN---NDGQATGVKRG--TVSTQALISENRALVLGFFHWEESGERDRRIPILGDIPLW--G-RL : 499
 HrcC Eamyl : SSIQLMEDEDGH---WQTN---GDGQATGVKRG--TVSTQALISENRALVLGFFHWEESADRDRRIPILGDIPLW--G-QL : 498
 HrcC Echry : SSIQLVIDEDGQ---WETN---TEGTASGVKRG--TVSTQALIGENRALVLGFFHWEESGDRDKRVPILGDIPLW--G-KL : 515
 HrcC Pcaro : RSIQLVIDEDGQ---WETG---REGEASGVKRG--TVSTQALIGENRALVLGFFHWEESGDRDRRIPILGDIPLW--G-QL : 512
 HrcC Psyri : PQVQLVIDEDGQ---DIDIS--DINDTQPSVRKG--TVSTQAVIAEHGSLVIGFFHGLEANDKVKVPLILGDIPIY--GKLL : 516
 RscC Pfluo : HQIHLVIDEDGN---WDETNPDPNHLDVRRG--KYSTQAVMQEKRSLVIGFFHDTSSDQKKIPILGDIPLW--GKTL : 525
 PulD Koxy : IAGANQYNKDGTVSSSASALSSFNGLAAGFYQCNWALITATSSSTKNDLALTPSIVTLDNMEATFNVGQEVVLTGSGT : 469

β-Domain

TraK F : LSIQAVPREGAG-----RTIQVSD-----RGR-TGEEAGAWETSTP--YESLLEVTISQAVRGGKEEAGG : 157
 TraK R391 : LSVTLVPRRIP-----PREITLAIIDQQQWPKGVNVRKAATWETAQP--YVDSRDLRLRLALNELPEQY : 195
 TraK Rts1 : ISVSLVPQRIAPVQATEMLS-----RKLNNAVAVGGVSPIDYGGSEAKAKKWEQKDS--YVETVRNLLRTPVALGDIPEY : 279
 HtdP R478 : YNLTLVPLDVPGAMISVTTSLSPSMQAKRETSLDKQNYEEMARSQSEELAPDTPKQDD--HKQRIIDLLTPVALGEVPSGF : 318
 TrhK R27 : YNLTLVPLDVPGAMISVTTSLSPMMAKRETSLDKQNYEEMARSQSEELTPSDPRQDD--HKQRIIDLLTPVALGEVPSGF : 305
 TraK pED208 : FSVVATPVKGE-----RVYRLMSAE-----PPSRPETRKWETAQA--YEKLLISLNRAVLGDIPEY : 156
 TraK pNL1 : YKFLCQVRGND-----AEQVFTN-----TAIKTEAARDWEVRSS--PEDAAVRLAQAMYRSETIEGF : 182
 TraK SXT : LSVTLVPRRIP-----PREITLAIIDQQQWPKGVNVRKAATWETAQP--YVDSRDLRLRLALNELPEQY : 195
 HrcC Pstew : FTSRHEISQRERLFITPRLIG--DQTDPTRYVSADNRQQLSDAMARVERRHSSVN--LQDMVENALRDLAEGQSEAGF : 575
 HrcC Eamyl : FSSKRHEISQRERLFITPRLIG--DQTDPTRYVTADNRQQLSDAMGRVRRHSSVN--QHDVVENALRDLAEGQSEAGF : 574
 HrcC Echry : FTSRQHEVSRERLFITPHLIG--DQNDPTRYVSADNRQQLSDAMGRVAQRNSKT--LFGTVENALRDLAEGQSEAGF : 591
 HrcC Pcaro : FTSRHEVSRERLFITPHLIG--DQTDPTRYVSSANRQQLNGAMNRVAQRNSKT--LYSLTEGAFRDLAEGQSEAGF : 588
 HrcC Psyri : FQSRSELSQRERLFITPRLIG--DQVNPARYVQNGNPHDQDQMKRIKERRDGGG--LPTRGDIQKVFQVVDGAAPFEM : 594
 RscC Pfluo : VSSRERHNRERLFITPRLIG--DQDDPSRYLPQDDQAEQAALTPLARRYSHPQVPIKRSDFITTLARVVSCEVEKAF : 604
 PulD Koxy : TSGDNIPTNVERKTVGELKLVKPKINEGDSVLEIEQEVSSVADAASSTSSDLGATFN--TRTVNNAVLVGSGETVVVGSGL : 548

β-Domain

TraK F : Y----QVPVKETLQ-----APA--GLSSVADAVTIG--NHLKQVR--FAMENKTL-SALNIRE--SDFWQPGTRVVMFS : 219
 TraK R391 : DIR--LAGQTDTSFKC-----FQPG-LKFGFKQCQIVTG--HYFTYVY--GIVESPAD-EPIEASE--IACHAPDIVASAY : 261
 TraK Rts1 : ALG--NLTSSVSIPIPCNFNTGTVDYIRYFNFGQYING--SQFSVIV--GIACMTGP-TTVTVDE--SLGTHPQMARAL : 351
 HtdP R478 : SLQ--QDRLSRIPAPE-----QSPCNFNMYAKLQRLVG--SRELDVY--ILVKNDKP-YGQIVAD--QOCMAEGVIALSAL : 385
 TrhK R27 : SLQ--EDRLSRIPSE-----QSPCNFNMYAKLQRLVG--SRELDVY--VILVKNDKP-YGQVVAD--QOCITEGVVIALSAL : 372
 TraK pED208 : GEV--KPLSDGIRLPG-----GFSVTPLKAWAG--DQLRADR--YEBRNANT-WGVVANT--QDFWKKGVRAVVMFD : 218
 TraK pNL1 : EIR--QSVLEPVAVGK-----LEVQVQVEYRG--ADLKGLI--LKVNRNTGA-KPLTLDE--NLLAARGSVAFMT : 242
 TraK SXT : DIR--LAGQTDTSFKC-----FQPG-LKFGFKQCQIVTG--HYFTYVY--GIVESPAD-EPIEASE--IACHAPDIVASAY : 261
 HrcC Pstew : K-A--EASGERLNDIC-----QSTPGLFDNARGQWYSSDSGLRST--GAVRNITH-NLRFNE--ASCAGKRTLAVAV : 643
 HrcC Eamyl : Q-P--QTSGRLESEVC-----RSTPALLFESTRGQWYSSSTNGVQVLSV--GAVRNITSS-KPLRFDE--ANCASKRTLAVAV : 642
 HrcC Echry : T-I--DGSGPKLSEIC-----RTSPMSYQSNRYQWYSN--LSLSSTV--GAVRNITGT-QPLRFDE--ASCANSRTLAVAA : 657
 HrcC Pcaro : Q-A--DSKGARLGEVC-----RSQGLIYDSSRYQWYGN--GQVRSV--GAVRNITGGT-QPQRFDE--AACASSRTLAVAV : 654
 HrcC Psyri : HDG--ETLPEFETSLC-----DPGQGLSLDGQRSQWYAR--KDWGAVY--VAVRNITD-KPVRIDE--SRCGGRWVIGVAA : 661
 RscC Pfluo : N-A--ARMPLGLNTLC-----STRDLIALNTERSQWYAG--PPYNAVY--VAVRNITQFK-RNVRIDE--KEGSNSQTLAVTV : 670
 PulD Koxy : LDKSVSDTADKVPILG-----DIPVIGALFRSTSKKVK--RNLMFERTPTVIRDRDEYRQASSGNYTAFNDQAQSKQRGK : 621

β-Domain

TraK F : QPASQLLAGARMVYVIRDG---EGN----- : 242
 TraK R391 : WPSNILLFGEKTEYVVRNHRREEAVE--SORPSLLVGGEL--- : 300
 TraK Rts1 : WSRNTLAPGCKTEAFVFLRNGQQQVRVDDGARPKLAE----- : 388
 HtdP R478 : FDKAYLQGEHETELVVRDKLFKEREARVITRPSLIRK----- : 423
 TrhK R27 : FDKAYLQGEHETELVVRDKLFKEREQTRVITRPSLIRK----- : 410
 TraK pED208 : NNAQTLMGGRMTVTVIRNGEGEDGQR----- : 246
 TraK pNL1 : -FVSELAFGCAAAVYIQSN--GGQ----- : 264
 TraK SXT : WPRNILLFGEKTEYVVRNHRREEAVE--SORPSLLVGGEL--- : 299
 HrcC Pstew : WPHSSLAPGCSAEVYALQP---HRNIA-VTRESLNIH----- : 677
 HrcC Eamyl : WPHSALAPGCSAEVYAMDP---SRVLH-ASRESLNR----- : 676
 HrcC Echry : WPKTTLAPGCSAEVYALLP---AKNAQ-PSRASLEKPK----- : 691
 HrcC Pcaro : WPKTTLAPGCSAEVYALQP---ALTPQ-SARRNLLISR----- : 689
 HrcC Psyri : WPHAWLQGEHETELVAVRQPIKMAK--ESRPSLLRGAKP--- : 710
 RscC Pfluo : WPRAWLQGEHETELVAMRPVVKDEHLS--VPRPSLLTPTQKATP : 713
 PulD Koxy : ENNDAMLNQDLELTPRQDTAAFRQVS--AAIDAFNLGGNL--- : 660

S-Domain

Figure 2-6. Alignments of the processed pilin subunits from IncHI (R27 and R478) and IncP (R751 and RP4) transfer systems. The protein sequences of the pilin subunits have the leader sequences removed and the cleavage site shown (gray arrow). The protein sequences of the IncP pilin subunits are missing the 27 C-terminal residues, which are cleaved by an unknown peptidase (black arrow #1) and site of cleavage by the TraF peptidase is shown (black arrow #2). Alignments were performed in ClustalW and shaded in GeneDoc using conservative mode and three levels. Accessions numbers are TrhA (accession no. AAD54053), HtdZ (AAL27017), TrbC R751 (NP_044241) and TrbC RP4 (AAA26429).

secretin proteins (151). The alignment between TrhK-like proteins, HrpH-like proteins and PulD (prototypical secretin) suggests that TrhK-like proteins contain the β -domain, predicted to form the outer membrane ring, and the S-domain, which interacts with a lipoprotein (Figure 2-5) (72).

Besides sharing similarity to IncF plasmid Mpf proteins, the Tra2 Mpf proteins are similar to the Mpf proteins from the IncHI2 plasmid R478 from *Serratia marcescens* (Accession No. AF030442) (155), pNL1 from *Novosphingobium aromaticivorans* (NC_002033) (174), the IncJ element R391 from *Providencia rettgeri* (AY090559) (20), the IncT plasmid Rts1 from *Proteus vulgaris* (NC_003905) (144) and the SXT element from *Vibrio cholerae* (AY055428) (12) (data not shown).

The presence of nine Mpf proteins in the Tra2 and three Mpf proteins in the Tra1 region (108) which are homologous to Mpf proteins from the F factor means that R27 contains an equivalent to each of the essential Mpf proteins from the F factor (56), with the exception of the pilin subunit. Given the presence of *trhP*, whose gene product is homologous to the pilin processing protein TraF from IncP plasmids (47), the putative core regions of TrhA of R27 and HtdZ of R478 (IncHI2) was aligned with the core region of TrbC, the pilin of RP4 and R751, to identify conserved regions (Figure 2-6). The core region of TrbC is processed with the removal of the N-terminal 37 residues by the host-encoded LepB and the removal of the C-terminal 27 residues by an unknown host peptidase (47). This remaining 82 aa peptide, which contains the four residues to be removed by TraF, was aligned with the processed form of TrhA and HtdZ (leader peptide, predicted by SignalP, has been removed) using ClustalW. This alignment identified 15% identity and 34% similarity between all these proteins. Within the conserved regions are several residues which are highly conserved between TrbC and several of its homologs, including VirB2 from the Ti plasmid (48), particularly in the region which is cleaved by the transfer peptidase (Figure 2-6).

To identify conserved sequence motifs, the predicted protein sequence of each of the Tra2 ORFs was compared to both the Conserved Domain database and the Prosite database (Table 2-4). A lipoprotein motif was detected in TrhV, which is characteristic of the TraV protein family (81). Lipoprotein motifs were also found in ORF017 and 004. TrhC contains Walker A and Walker B motifs, suggesting that this protein binds ATP

and possibly energizes some aspect of conjugation. TrhP contains signal peptidase 1 motif, consistent with the PSI-BLAST analysis. TrhI contains DNA helicase II motifs, which is consistent with the PSI-BLAST analysis.

2.3.7 Tra2 Gene Disruptions and Identification of Transfer Mutants

Seven mini-Tn10 transfer mutants have been identified within the Tra2 region (*trhE*, *K*, *B*, *C*, *W*, *U* and *N*) (175). To identify a role in transfer for the remaining seventeen Tra2 genes (entire Tra2 excluding four partitioning genes), gene disruptions of each of these ORFs in R27 were systematically created, as previously described for the Tra1 region (108). Each mutant was then tested for its ability to transfer (Table 2-5). Gene disruptions of *trhA*, *L*, *V*, and *P* abolished conjugative transfer of R27. Disruptions of *trhO* and *trhZ* reduced transfer to 0.0002% and 0.006% of the transfer frequency of R27, respectively, whereas the disruption of most of the remaining genes had a minimal effect on transfer. Since mutations were made in drR27 (wild-type R27 with TnlacZ inserted into *htdA*), a CAT cassette was inserted into *htdA* within wild-type R27 to see if a different disruption of this gene (CAT 1 kb vs. TnlacZ 8.7 kb) had the same effect on transfer. An insertional disruption of *htdA* by CAT increased the transfer frequency of R27 by 6 000-fold, as did the insertion by TnlacZ (212). These data, combined with that from the random transposon mutagenesis experiments, indicate that 11 genes within the Tra2 region are essential for conjugative transfer. In addition, *trhO* and *trhZ* play a role in conjugative transfer by enhancing the transfer frequency of drR27, whereas *htdA* represses the transfer frequency of wild-type R27.

2.3.8 Genetic Complementation of Tra2 Transfer-Deficient Mutants

The wild-type gene corresponding to each of the transfer-deficient mutants was cloned into the expression vector pMS119EH (or HE) (Table 2-1). In addition, genes for *trhO*, *trhZ* and *htdA* were cloned in order to test for an effect on the corresponding mutants. Each clone was transformed into *E. coli* containing the appropriate drR27 transfer mutant. When the wild-type version of each transfer gene was expressed *in trans* with each of the transfer mutants, conjugative transfer was restored to varying degrees for each of the eleven transfer mutants (Table 2-5), demonstrating that each of these genes is

essential for conjugative transfer. When *trhZ* and *trhO* were expressed *in trans* within donors containing corresponding mutants, the transfer frequency was restored to R27 levels, indicating that these gene products have a positive effect on transfer. When *htdA* was expressed in donors with R27 (wild-type R27 within CAT inserted into *htdA*), the transfer frequency was reduced to wild-type R27 levels, indicating the *htdA* has a negative effect on the transfer frequency.

During the complementation experiments, the conjugation frequency varied between 144% (*trhW*) and 0.2% (*trhV*) of the transfer frequency of drR27. The variation could be due to polar transcriptional effects because of the CAT insertions and/or that the overexpressed transfer proteins reduce the conjugation frequencies. To address these possibilities, the complementation frequencies for each mutant were compared to the transfer frequency of drR27 when the corresponding transfer protein was over-expressed in donors during conjugation experiments (Table 2-5). Any difference in the conjugation frequency between the complementation and the over-expression experiments will reflect polar effects on downstream genes. Over-expression of transfer proteins had a minimal effect on transfer frequencies, especially for *trhL* and *trhV*, which had the lowest complementation frequencies. This suggests that both mini-Tn10 and CAT insertions resulted in partially polar transfer mutants of several genes. This observation has previously been noted for the Tra1 transfer genes (108). Nevertheless, this approach allows for the identification of essential transfer genes.

2.3.9 Hgal Plaque Assay of Tra2 Transfer-Deficient Mutants

Each Tra2 mutant was tested using an Hgal plaque assay to determine which mutants were resistant or sensitive to Hgal lysis (Table 2-5). *E. coli* cells containing transfer mutants *trhA*, *L*, *E*, *K*, *B*, *V*, *C*, *Z*, *P*, and *W* were resistant to Hgal. Hgal sensitivity was restored for each of these mutants when each mutant was complemented with the wild-type gene (data not shown). These observations suggest that these transfer genes are involved in H-pili biosynthesis. The ability of the *trhZ* mutant to resist Hgal is interesting since this mutant is capable of transferring at very low levels, suggesting that R27 is capable of transferring at a low frequency in the absence of H-pili. *E. coli* containing R27 containing mutations in transfer genes *trhU* and *trhN* were capable of

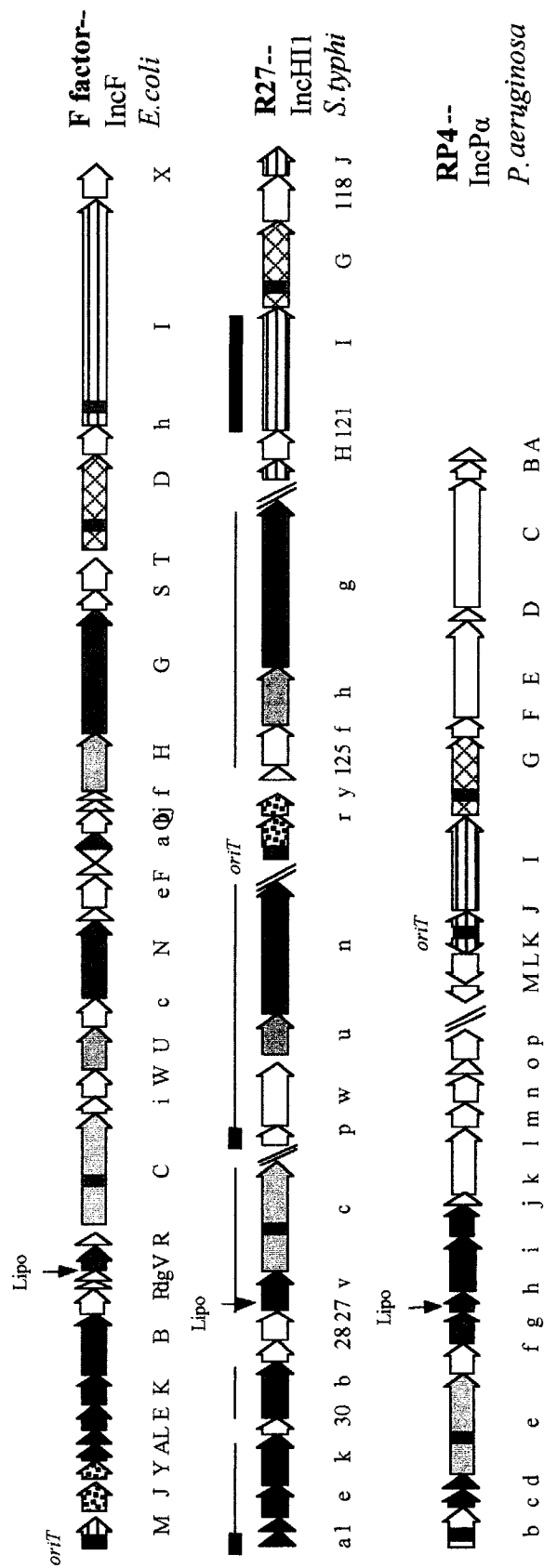
forming plaques, although they were notably smaller and not as clear as R27 plaques. Disruption of *htdA* in wild-type R27 resulted in plaques which were larger than those produced by wild-type R27; this is attributed to the increase in H-pilus production by donors (212). *E. coli* cells containing an insertional disruption of *orf030*, *028*, *027*, *trhO*, *orf017*, *016*, *htdF*, *htdK*, *orf009*, *004* and *trhI* were all capable of forming plaques, suggesting that these genes are not essential for H-pilus biosynthesis.

2.4 Discussion

The conjugative transfer genes of R27 are contained within two separate transfer regions, designated Tra1 and Tra2, which are separated by 63 kbp. Each region contributes to the conjugative transfer function of R27, since mutations in either region abolishes transfer. Tra1 contains the *oriT* and 9 essential transfer genes encoding a coupling protein, relaxosome proteins and Mpf proteins (108). Tra2 contains 11 Mpf genes that are essential for conjugative transfer. The 20 essential transfer genes identified within both the Tra1 and Tra2 likely represent the entire conjugative transfer apparatus encoded by R27, since our comparison to IncF and IncP conjugative transfer systems has identified an equivalent to each essential transfer component present in these systems (Figure 2-7).

The major component of the relaxosome is TraI. The relaxase motifs of TraI align best with relaxases from the IncP family, including the presence of only one catalytic tyrosine residue (187). Besides the three relaxase motifs, no homology exists between TraI and any of the known relaxases, including the IncP specified relaxases (Table 2-2). It therefore appears that TraI is distantly related to previously characterized relaxases. Relaxase families have been assigned based on the presence or absence of a helicase domain in their C-terminal region that is responsible for the DNA unwinding activity during conjugative transfer. Relaxases from the IncF/IncW plasmid groups contain a helicase motif, although these motifs and functions are absent in relaxases from the IncP plasmid group (24). TraI from R27 does not contain a helicase domain suggesting that TraI is from the IncP relaxase lineage; this is consistent with the alignment of the relaxase motifs. From our analysis, the best candidates for relaxosome

Figure 2-7. Comparison of the complete F, R27 and RP4 conjugative transfer regions (some regulatory genes excluded). Essential transfer genes are presented with color/pattern, with the same color/pattern representing homologous gene products, while non-essential transfer genes are white. The Mpf genes are solid in color and the coupling protein, relaxosome components and regulatory genes are patterned. Light gray genes represent gene products with no shared homology. Thin lines above the R27 map indicate homologs to the IncF system, while thick lines represent homologs to the IncP system. Lipo=lipoprotein motif; Red box=Walker A motif; Green box=origin of transfer; Upper case gene names=Tra; Lower case gene names=Trb (F and RP4) or Trh (R27). Double slash indicates non-contiguous regions. Arrow representing ORFs are proportional to the length of the ORFs.



accessory components are encoded by *traJ* and *traH*. Both are essential for transfer, but not for H-pilus synthesis, consistent with the characteristics of relaxosome accessory proteins.

The coupling protein of R27, TraG, shares only a low level of identity with characterized coupling proteins. The conserved regions are predominantly at or around the Walker A and Walker B motifs, indicating the functional importance of these motifs. It therefore appears that the coupling protein from IncHI1 plasmids is distantly related to known coupling proteins.

A 285bp region between *traH* and *trhR* was cloned and mobilized by R27. This region is present within a 757 bp intergenic region that contains hallmark features of *oriTs*. The nucleotide sequence of the 285bp *oriT* was compared to the five *nic* site families (218) and no matches were found. Precise identification of the *nic* site of R27 would allow one to determine if it is distantly related to one of the five *nic* site families, or defines its own family.

There are 5 Mpf genes within the Tra1 region and all are transcribed in the same direction and away from the *oriT*. The *trhR* and *trhY* genes code for proteins which share no homology to any component of known conjugative systems. These genes may represent T4SS components that are unique to IncHI1 plasmids. Alternatively, since genes that regulate conjugative transfer are generally present around the *oriT* and are the least well-conserved components of transfer systems (218), these ORFs may play a role in regulating conjugative transfer. Consistent with the latter idea, over-expression of TrhR and TrhY increased the transfer frequency of R27 (Table 2-3).

Three remaining Tra1 Mpf genes, *trhF*, *trhH* and *trhG*, (*trh* designates R27 Mpf genes) specify proteins that are homologous to the TraF, TraG, and TraH transfer proteins from IncF plasmids. In the IncF system, these proteins are required for Mpf/F-pilus synthesis, with TraG also being important for stabilizing mating pairs during conjugation (7, 54, 56).

Of the 11 Mpf proteins encoded within the Tra2 region, 9 are homologous to Mpf proteins of the IncF transfer system. Of these, TrhL, E, K, B, V, C and W are essential for conjugative pilus biosynthesis; the same function assigned to their F factor Mpf counterparts (56). TrhU and TrhN are not essential for H-pilus biosynthesis, but do

appear to play an auxiliary role in H-pilus assembly. Based on their homology and shared mutant phenotypes with *traU* (142) and *traN* (133) of the F factor, it is proposed that TrhU and TrhN also play a role in DNA transfer and mating pair stabilization, respectively. Including the 3 Mpf genes from Tra1, R27 contains an equivalent to 12 of the 13 essential F factor Mpf proteins, with the exception of the pilin subunit, illustrating that the IncH Mpf/T4SS secretion system shares a common ancestry with that of the IncF system. Although these proteins are responsible for conjugal piliation and subsequent DNA transfer, the exact roles of these proteins, collectively and individually, remain unknown. TrhC, a putative ATPase, was recently shown to form membrane-associated complexes and complex formation was dependent on the presence of TrhB, E and L (63). This suggests that these proteins form a multi-protein complex that may function in H-pilus synthesis or R27 transfer, or both.

A novel observation is that TrhK and TraK-like homologs share similarity with secretins. Secretins are outer membrane pores that are found in Type II and Type III secretion systems and allow passage of macromolecules across the outer membranes. Secretins form high molecular weight multimers (119) and preliminary results suggest that TrhK does as well (Lawley and Taylor, unpublished results). Secretins consist of two domains, a non-conserved N-terminal specificity domain and a conserved C-terminal domain, which defines the secretin family (72, 151). The C-terminal domain contains the β -domain, which inserts into the outer membrane, and a S-domain, which interacts with a stabilizing lipoprotein (72). Both the β and S-domains appear to be conserved in TrhK. TraK of the F factor was recently shown to be present in the outer membrane of donor cells and the C-terminal region interacts with TraV, a transfer lipoprotein (81). The presence of secretins in T4SS secretion systems would suggest a mechanism by which DNA and pili could transverse the outer membrane of donors.

The two remaining Tra2 encoded Mpf proteins, TrhA and TrhP, are homologous to the pilin (TrbC) and peptidase (TraF) of the IncP transfer system. Although the similarity between the pilin subunits is weak, the presence of the peptidase implies a maturation process for the H-pilin which is analogous to that observed for the P-pilus. This observation points to a common ancestry for IncH and IncP pilus subunit processing, but further work is required to demonstrate H-pilus subunit cyclization.

The presented analysis of the Tra1 and Tra2 regions indicates that the transfer components of R27 share a common ancestry with the IncP and IncF systems (Figure 2-7) (108). The relaxosome, pilin and transfer peptidase appear to share a common lineage with IncP plasmids, whereas the Mpf/T4SS is of the IncF lineage (Figure 2-7). There is no evidence of gene redundancy in any of these transfer systems. If the chimeric nature of these transfer systems did occur through DNA recombination between plasmids, the recombinant genomes subsequently underwent loss of redundant DNA resulting in the current transfer systems. The separation of the Tra1 and Tra2 by 63 kb and the mosaic organization of the transfer genes may be a remnant of such a recombination/DNA loss event. The transfer systems (*trb* and *vir*) of the Ti plasmid are also believed to have evolved by a similar method (3, 52). These observations imply a modular nature for the various transfer system components (Dtr, Mpf and coupling protein). Indeed, chimeric transfer systems consisting of Dtr (IncQ), coupling protein (IncP) and Mpf (Ti) functions constructed *in vivo* from different conjugative plasmid systems have been shown to be fully functional for conjugative transfer (77). Therefore, plasmids, especially larger plasmids, appear to evolve conjugative transfer systems by acquiring and combining transfer components from other conjugative transfer systems.

Chapter 3

Characterization of the Double Partitioning Modules of R27: Correlating Plasmid Stability with Plasmid Localization

A version of this work has been submitted for publication:

Lawley, T.D. and D.E. Taylor. 2003. Characterization of the double partitioning modules of R27: correlating plasmid stability with plasmid localization. *J. Bacteriol.* **185**(10): 3060-3067.

3 Characterization of the Double Partitioning Modules of R27: Correlating Plasmid Stability with Plasmid Localization

3.1 Introduction

Partitioning modules are found on many low-copy number plasmids and facilitate the faithful segregation of bacterial plasmids to daughter cells at cell division. Partitioning modules consist of a centromere region adjacent to two coregulated genes that encode for an ATPase and a centromere specific DNA binding protein (67). Gerdes *et al.* (60) have proposed the existence of two partitioning family modules based on the type of ATPase encoded. Type I modules encode for Walker-type ATPases and are exemplified by ParA/SopA systems encoded by P1 and F, respectively. Type II modules encode for actin-type ATPases and are exemplified by ParM of R1. Partitioning protein homologs are also involved in chromosome segregation in *B. subtilis* (91) and *Caulobacter crescentus* (139).

DNA binding partitioning proteins are typified by ParB/SopB of P1/F and ParR of R1, and bind to repeated DNA sequences within the centromere region. The ParB and ParR-centromere complex are referred to as the partitioning complex and mediate the pairing of plasmid molecules (46, 96). Binding of ParR to the centromere region also serves to regulate the expression of *parM-parR* as the promoter is within the centromere region (93). Binding of ParB to the centromere region of P1, found downstream of the *parA-parB* operon, results in ParB spreading into the surrounding sequences and promotes silencing of this DNA (173). The partitioning complex is localized to mid- (and quarter-) cell positions of *E. coli* and after duplication these complexes move rapidly to the quarter-cell positions, the mid-cell of the next generation (66, 148). It is not known what maintains the partitioning complex at the mid- and quarter-cell positions, however, it has been proposed that a host-encoded factor may be involved (67, 86).

The partitioning ATPases are cytoplasmic proteins whose ATPase activity is essential for partitioning (42, 94, 206). The ParA/SopA proteins are also involved in autoregulation of the partitioning operons (42). The ATPases interact with their cognate

DNA binding proteins (94, 169), suggesting that ATP hydrolysis may be linked to movement of the partitioning complex from the mid- to quarter-cell positions. Recently, it has been shown that ParM of R1 forms actin-like filaments with ATP-dependent polymerization properties. It has been proposed that polymerization of ParM into filaments begins at the partitioning complex and provides the necessary motive force to actively push the partitioning complexes from the mid- to quarter-cell positions (141).

IncHI1 plasmids frequently encode multiple antibiotic-resistance in *S. typhi* (92, 138, 165). R27, the prototypical IncHI1 plasmid, is a large conjugative plasmid which encodes resistance to tetracycline and possesses a mosaic genetic organization of backbone components (i.e. conjugation, replication and partitioning), suggesting a complex evolutionary history (107, 187). For example, the conjugative transfer system of R27 is a chimera of IncF and IncP-like systems (108, 109). Replication is determined by one of two replicons RepHI1A or RepHI1B (57, 58), maintaining a copy number of 1-2 copies per chromosomal origin (197). A third non-functional IncFIA replicon is also present on R27 and is responsible for one-way incompatibility with the F factor (58). Sequence analysis has identified two partitioning modules within the Transfer region 2 of R27 (187). The goal of this study was to determine, using genetic analysis and a GFP-LacI probe, how each partitioning module contributes to the stability of R27 and to study unstable partitioning mutants that have cellular localizations that are distinct from that of wild-type R27.

3.2 Experimental Procedures

3.2.1 Bacterial Strains and Plasmids

The following *E. coli* strains were used: DY330R^{ts} (W3110 Δ lacU169 gal490 λ cI857 Δ cro-bioA) (217), DY330R and DY330N (rifampicin and nalidixic-acid resistant temperature sensitive revertants of DY330^{ts}) (110) and DH5 α (*supE44 lacU169 (80lacZM15) hsdR17 recA1 endA1 gyrA96 thi-1 relA1*) (176). The following plasmids with relevant characteristics were used: R27 (IncHI1, tetracycline resistant) (187), pSG25 (cassette delivery vector, kanamycin^r, ampicillin^r) (66), pSG20 (GFP-LacI expression vector, arabinose inducible promoter, ampicillin^r) (66), pJP124 (Tn7 transposase vector,

chloramphenicol^r; gift from Dr. Nancy Craig), pOU82 (unstable test vector, ampicillin^r; gift from Dr. Michael Yarmolinsky) (59). The chloramphenicol acetyl transferase (CAT) and trimethoprim (Tp) resistance cassettes for insertional mutagenesis were amplified from pNK20 (101) and R751 (201), respectively.

3.2.2 Growth Conditions

All *E. coli* strains were grown in LB medium (Difco Laboratories) or MOPS minimal medium (MOPS buffer with 20 amino acids and 0.4% glucose or 0.4% glycerol)(66). During the construction of R27 *parR*::Tp when trimethoprim resistance was utilized, strains were grown with Mueller Hinton medium. When necessary the following antibiotics were added to the growth medium: ampicillin (Ap, 100µg/ml), kanamycin (Km, 50µg/ml), tetracycline (Tc, 10µg/ml), chloramphenicol (Cm, 16µg/ml) and trimethoprim (Tp, 50µg/ml). The growth temperature was 30°C for routine procedures. For microscopy, cells from overnight cultures were diluted 1/20 and grown at room-temperature to mid-log phase prior to induction of GFP-LacI. GFP-LacI was induced by adding 0.2% arabinose to the growth medium. Expression was then repressed after 30-40 minutes by adding 0.4% glucose to the medium and continuing growth for an additional 30 minutes.

3.2.3 Nucleotide Sequence and Statistical Analysis

Laser gene software (DNASTAR Inc., Madison, WI) was used for nucleotide sequence analysis. Repeated nucleotide sequences were identified with GeneQuest. The predicted protein sequence for each ORF was compared to the GenBank non-redundant database using PSI-BLAST. Statistical analysis was performed with the SigmaStat software package (Jandel Scientific).

3.2.4 Cloning of Par1 and Par2

The Par1 and Par2 regions were amplified from R27 DNA using Pfx high fidelity DNA polymerase (Gibco) using primers par1-f (5' ATATGGATCCCCGTTTAAAGTTACTGGT TACC), par1-r (5'ATATGGATCCCACCTTCTAGGCCCAATC), par2-f (5'ATATGGATCCTACT ACCGGATGAAAGTCATC) and par2-r (5'ATATGGATCCGTGATAACATTCAGTCAGCC).

Primers incorporated *Bam*HI sites into each end of the amplified DNA. Par1 and Par2 regions were digested with *Bam*HI and cloned into the *Bam*HI site of pOU82 (59), to create pPar1 and pPar2, respectively.

3.2.5 Construction of *parB* and *parR* Mutants

The *parB* and *parR* genes in Par1 and Par2 modules of R27, respectively, were mutated by inserting a CAT or Tp cassette using the *E. coli* recombination system (217). DNA substrates were generated through PCR with primers (~60nt) that produced a linear CAT or Tp cassette with 40 bp terminal arms homologous to the desired target site. Primers to create DNA templates to disrupt *parB* with CAT were trev204 (5'ACTGAAGTAATCCATCGCTCCGGGCTTCAAGGCCTGAAAGCTGTGACGGAAGATC ACTTC) and trev205 (5'GCCTCAAGCTTCCGCCATTGTGTAATGTAAAAATTTCTTTATTTCAG GCGTAGCACCAG), to disrupt *parR* with CAT were trev206 (5'ACATCGTGGCGAGCAGATT TCTCTAATAAGATCTGCAATCCTGTGACGGAAGATCACTTC) and trev207 (5'CATTAATAAA ACTAGATAACTCGGGGAAGAGATTATTTAGTTATTTCAGGCGT AGCACCAG), to disrupt *parR* with Tp were trev535 (5'ACATCGTGGCGAGCAGATTTCTCTAATAAGATCTGCAATCTTCGCT GCTGCCCAAGGTG) and trev536 (5'CATTAATAAAACTAGATAACTCGGGGAAGAGATTATTT AGGTGCACTCAACCGTGAATTC). DNA substrates were introduced by electroporation into DY330R^{ts} harboring R27 that was grown according to Yu et al. (217). Cells were plated on agar plates containing both tetracycline, to select for R27, and chloramphenicol or trimethoprim, to select for the desired insertions. To screen presumptive colonies, the target gene was PCR amplified and analyzed with 1% agarose gel electrophoresis. An increase in the size of the ORF by 700 bp (Tp) or 900 bp (CAT) demonstrated that the resistance cassette had been inserted into the target gene of R27.

3.2.6 Pulsed-Field Gel Electrophoresis

Preparation of agarose-embedded *E. coli* and restriction endonuclease digestion as well as electrophoresis and image processing are described elsewhere (200), except that *Not*I was used to digest the DNA.

3.2.7 Stability Assay

DH5 α containing the test plasmid (each of which contained either the entire β -galactosidase gene or a fragment encoding for the β -galactosidase α fragment) was grown overnight in LB broth with selection at 37°C and shaken at 200 rpm. Overnight cells were diluted 1/100 000 into fresh LB broth without antibiotics and grown as described above. Aliquots were removed at the times indicated on the graphs (Figure 3-2), serially diluted and plated on nutrient plates containing X-Gal (5-bromo-4-chloro-3-indolyl- β -D-galactopyranoside) at 50 μ g/ml. Blue plasmid containing colonies and white plasmid-less colonies were counted and the percentage of plasmid-containing cells was plotted against time. Each experiment was done twice and the average values plotted.

3.2.8 R27::*lacO* Construction

To produce a R27::*lacO* construct that was stable and mating proficient, pSG25 was first transformed into *E. coli* strain Stbl-2 and then R27 was mated into these cells using the methods previously described (199). Once the presence of both plasmids was confirmed using plasmid isolation procedures, electroporation was used to introduce pJP124 into the strain. pJP124 contains the Tn7 transposase genes cloned into pACYC and promotes random transposition of Tn7 into conjugating plasmids (216). Cells containing all three plasmids were collected from agar plates in 1 ml of PBS and 0.1 ml of this cell suspension was used to inoculate 10 ml of fresh LB + Ap, Tp, and Cm. Cells were grown to mid-exponential phase and were used as donors for mating. Transposition of the cassette into R27 was achieved by mating R27 to DY330R and selecting with tetracycline, for R27, and kanamycin, for the cassette. To ensure the cassette did not transpose into transfer genes, transconjugants were pooled and mated into DY330N [pSG20] (cells containing pSG20 express GFP-LacI). Several colonies were then individually screened to ensure stability and mating efficiency, one of which was used for further analysis. Within this construct, the cassette was found to be inserted into an intergenic region between genes *orf183* and 184, as determined by sequencing the region flanking Tn7 with primer NLC95 (5'ATAATCCTTAAAACTCCATTCCACCCCT) (216).

3.2.9 Microscopy and Photography

For microscopy experiments, cells were grown as indicated and for time-lapse experiments cells were grown in LB broth. A 1 ml aliquot of the sample was collected, pelleted and resuspended in 20-50 μ l of MOPS medium. A 1 μ l sample was added to a MOPS medium/1.5% agarose slab on a microscope slide. A cover slip was added and the edges sealed with vacuum grease. For mating experiments the samples contained a 5:1 donor to recipient ratio. Fluorescence microscopy was performed using a Leica DMRE microscope equipped with a CDD camera (Cooke SensiCam) and a standard FITC filter set (Chroma). Samples were illuminated with a UV (Leica HB100) source and images collected and processed using SensiControl 4.0 and PhotoPaint (Corel). Quantitative measurements (i.e. number of foci, foci location and cell size) were performed as described (66).

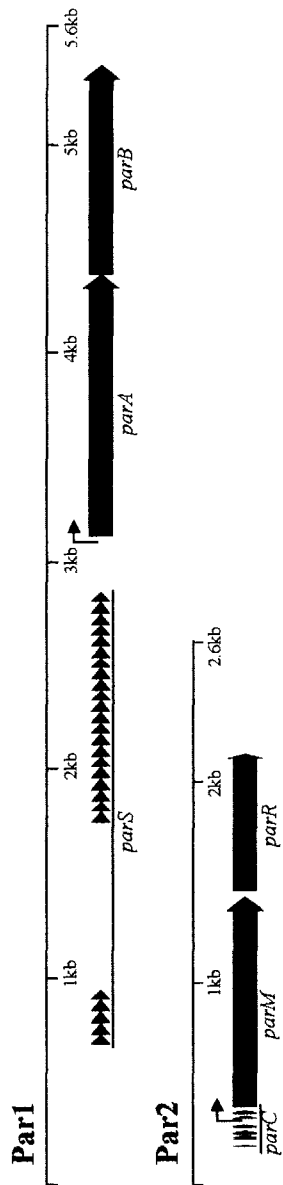
3.3 Results

3.3.1 Nucleotide Sequence Analysis of Par1 and Par2

Two partitioning modules were identified within the conjugative transfer region 2 (Tra2) of R27 which are separated by 2.7 kb and transcribed in the same direction (Figure 3-1) (109, 187). Partitioning module 1 (Par1) contains two genes, arranged in a putative operon, whose gene products are similar to ParA/SopA and ParB/SopB protein families exemplified by P1 and the F factor (60). ParA_{R27} (417aa) shares 20% identity with SopA_F and contains a WalkerA ATPase motif (GTGGKS). ParB_{R27} (335aa) shares 27% identity with ParB_{P1}. Upstream of *parA* are putative -10 (tagaat) and -35 (aataca) sequences; 240bp upstream of the *parA* translation start codon are 26 direct repeats of 34 bp (cccCctTAaTcGcCAg--ccATGG-gg-a--c-g; upper case conserved, lower case majority, dash non-conserved). These repeats likely serve as the centromere region and have been designated *parS*.

The partitioning module 2 (Par2) contains two genes, arranged in a putative operon, whose gene products are homologous to ParM and ParR of R1 (60). ParM_{R27} (344aa) is 33% identical to ParM_{R1} and contains the actin-like ATPase motifs characteristic of these proteins (60). ParR_{R27} contains no detectable similarity to ParR_{R1}.

Figure 3-1. Genetic organization of Par1 and Par2 modules of R27. Blue ORFs are *parA* and *parM* which encode ATPases belonging to the Walker and actin-type ATPase families, respectively. Green ORFs encode centromere-binding proteins. The region shown indicates the region cloned for stability assay. Black arrows indicate positions of direct repeats and raised arrows indicate putative promoters. GenBank Accession number is AF250878.



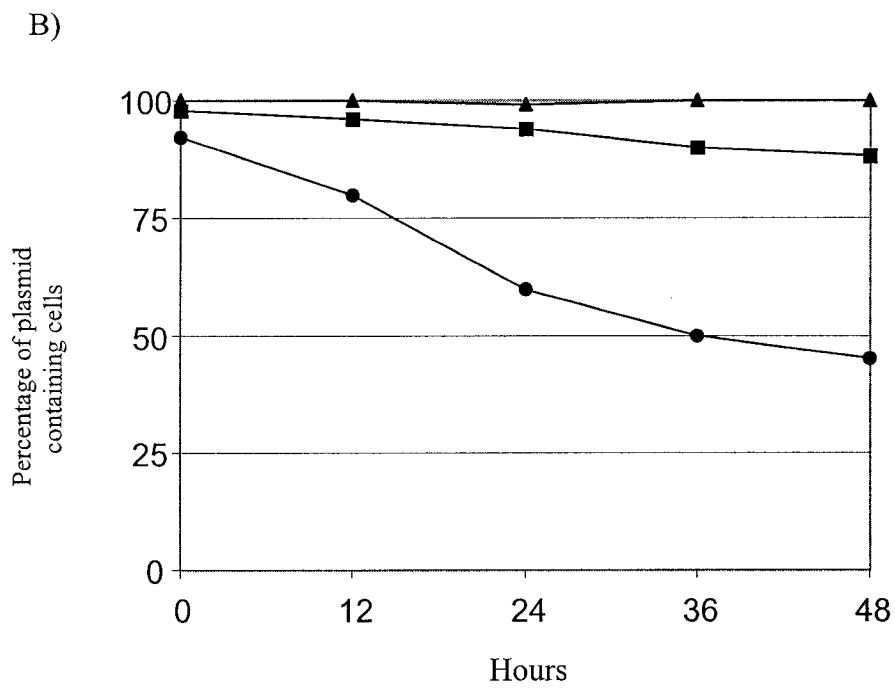
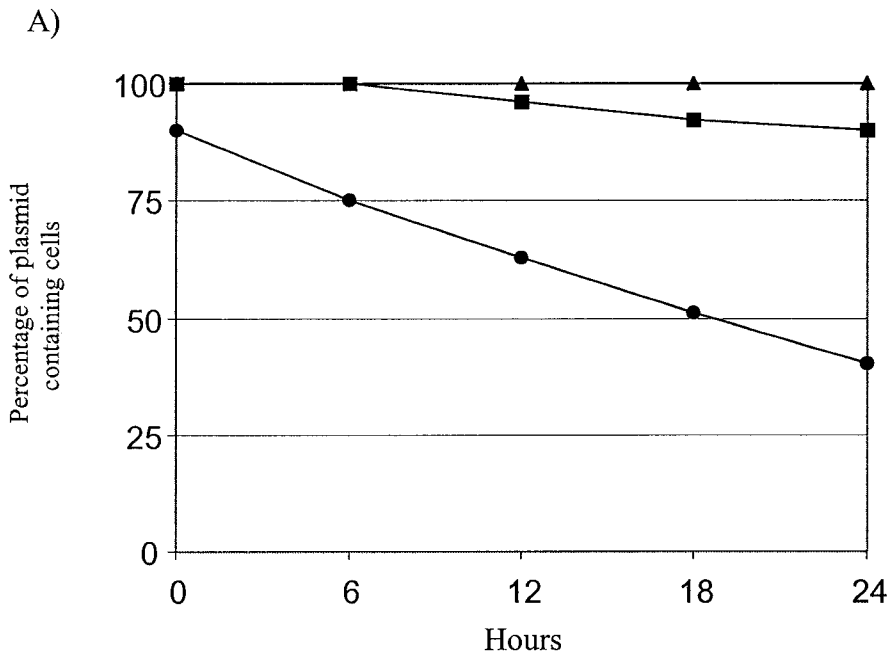
ParR-like proteins maintain few conserved residues and vary in size and were proposed to be functionally analogous based on genetic localization (60). Upstream of *parM* are putative -10 (tataaa) and -35 (ttgacc) sequences. The promoter region is flanked by two sets of 6 bp direct repeats (dr_1 :GtTtaa and dr_2 :AaAaCA), such that dr_1 is present 7 times upstream of the promoter and dr_2 is present 5 times downstream. These repeats likely represent the centromere region and have been designated *parC*.

3.3.2 Stability of Par1 and Par2 Clones and R27 *parB* and *parR* Mutants

To determine if both partitioning modules are functional Par1 and Par2 were cloned into pOU82, creating pPar1 and pPar2. pOU82 is an unstable R1 derivative used for stability assays and is *lac*⁺ so the frequency of plasmid loss can be monitored using X-Gal, where plasmid containing colonies are blue and plasmidless colonies are white (59). Stabilization of pOU82 by either Par1 or Par2 would therefore demonstrate that the partitioning module is functional. Clones pPar1 and pPar2 and pOU82 alone were grown overnight in DH5 α with selection then diluted 1/100 000 in fresh LB broth without selection and grown for 24 hours. Samples were taken every 6 hours, serially diluted and then plated on X-Gal containing LB plates. The frequency of plasmid stability was then plotted versus time (generation time was 40 minutes) (Figure 3-2A). After 24 hours, pPar1 was present in 100% of the cells and pPar2 was present in 90% of the cells, whereas pOU82 was present in 40% of the cells. These results suggest that both Par1 and Par2 are functional partitioning modules. In addition, Par1 stabilized pOU82 more efficiently than Par2.

To test the ability of Par1 and Par2 in stabilizing R27, insertional mutations of *parB* (*par1*-) and *parR* (*par2*-) were created in $drR27$, a derepressed derivative of R27 containing *TnlacZ* inserted into *htdA* (212). Stability assays were performed as described above except that stability was tested over 48 hours (Figure 3-2B). After 48 hours without selection, R27 was present in 100% of the cells. In the same period of time, the *parB*::CAT mutants were present in 45% of the cells and the *parR*::CAT mutants were present in 88% of the cells. These results suggest that both Par1 (*parB*::CAT) and Par2 (*parR*::CAT) are involved in stabilizing R27 and that the contribution of Par1 towards R27 stability is greater than that of Par2.

Figure 3-2. Verification that Par1 and Par2 from plasmid R27 are functional partitioning modules. Partitioning stability assay for: A) Par1 and Par2 cloned into the unstable test vector pOU82. Symbol for pPar1 is ▲, pPar2 is ■, and pOU82 is ●. B) Stability assay for drR27 (▲), drR27 *parB*-(*par1*-) (●) and drR27 *parR*-(*par2*-) (■). Strains were grown in *E. coli* at 37°C in LB without selection. See Text for details.

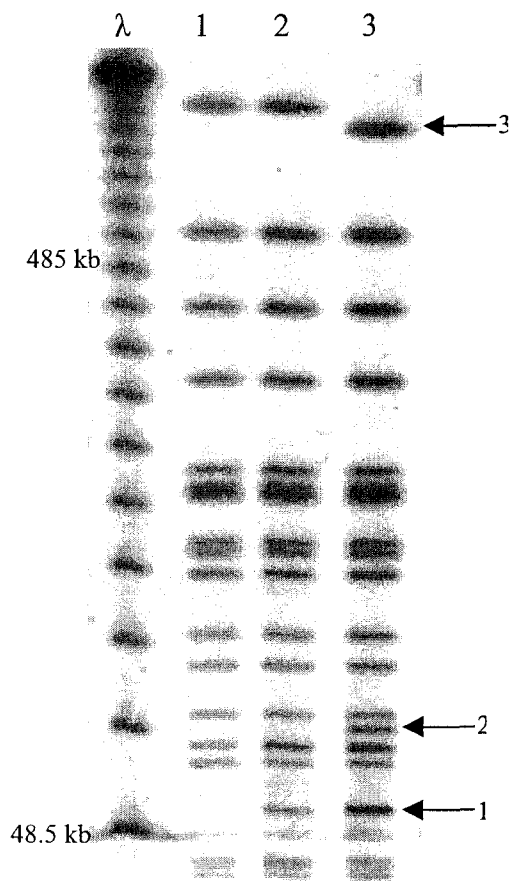


3.3.3 Double Partitioning Mutant of R27

A double-partitioning mutant of R27 was created by inserting a trimethoprim-resistance cassette into *parR* of the R27 *parB::CAT* mutant. Several mutants were isolated but were unable to be transferred by conjugation from DY330R^{ts} into DH5 α in order to perform the stability assay. Using resistance markers to monitor the presence of R27 in DY330 cells, it was found that the double-partitioning mutants were 100% stable after 24 hours (data not shown). *E. coli* cells containing the double-partitioning mutants formed plaques when infected with Hgal, an H pili specific phage (108) and mobilized a cloned *oriT* (108), suggesting that the conjugation apparatus of R27 *parB::CAT parR::Tp* was functional. Since mutations in either *parB* or *parR* did not affect plasmid transfer ability, neither of these gene products is essential for conjugation (data not shown). Given the above observations, it was hypothesized that the double-partitioning mutant of R27 may have integrated into the chromosome.

To determine if R27 *parB::CAT parR::Tp* was present in the extra-chromosomal form or was inserted into the chromosome, pulsed-field gel electrophoresis was performed on the DNA of the *E. coli* strains in which the double Par- mutation had been created. Figure 3-3 shows a pulsed-field gel banding pattern of DNA from DY330R (lane 1), the host strain, DY330R[R27 *parB::CAT*] (lane 2) and DY330R[R27 *parB::CAT parR::Tp*] (lane 3) digested with the restriction endonuclease *NotI*. Both lane 2 and 3, representing R27-containing strains, contain a common band that is not present in lane 1, the host strain, and is therefore specific to R27 (arrow 1). Lane 3, representing the double mutant, contains a band not present in either of the other lanes (arrow 2) and a decrease in a band size (arrow 3). These two differences in the banding patterns would be expected if R27 *parB::CAT parR::Tp* did insert into the chromosome thereby creating a banding pattern different from DY330R (lane 1) and DY330R[R27 *parB::CAT*](lane 2). These results suggest that creating a double-partitioning mutant of R27 resulted in R27 inserting into the chromosome, preventing conjugation of R27 DNA out of the donor. Since DY330R is *recA*⁺ and both *E. coli* and R27 are known to contain several insertion sequences (i.e. IS1, IS2, IS30) (187) it is possible that R27 *parB::CAT parR::Tp* integrated into the chromosome via homologous recombination, where it would be stably maintained.

Figure 3-3. Pulsed-field gel electrophoresis to illustrate the banding patterns of *NotI* digested DNA from DY330R (lane 1), DY330R[R27 *parB*::CAT] (lane 2) and DY330R[R27 *parB*::CAT *parR*::Tp]. The left lane is a λ ladder of 48.5 kb increments. Arrow to right indicate 1) R27 specific band, 2) R27-chromosome specific band and 3) decrease in chromosomal band size due to R27 insertion into chromosome.



3.3.4 Localization of R27::*lacO* in *E. coli*

The *lacO*/GFP-LacI system was used to visualize the cellular location of R27::*lacO* and R27::*lacO* Par- in live *E. coli* expressing GFP-LacI. Expression of GFP-LacI (encoded by pSG20) resulted in GFP-LacI binding to the tandem operators and caused the hybrid repressor molecules to cluster as a fluorescent focus that was visualized by fluorescence microscopy and represents the location of the plasmid molecule (66). Fluorescence images were collected of asynchronous cells and the cell length, number of foci per cell and position of focus were determined for each cell. To compare plasmid localization under different growth rates each of the three *lacO*-containing, R27 plasmids were visualized when cells were grown in LB (fast growth) and MOPS (slow growth) minimal media. These results are summarized in Figures 3-4 and 3-5. When *E. coli* expressing GFP-LacI and containing R27::*lacO* was grown in LB and MOPS >99% of the cells contained GFP foci. Cells grown in LB cells containing R27::*lacO* had 1 focus (1.2%), 2 foci (26.3%), 3 foci (42.4%), 4 foci (25.3%) or 5 foci (3.9%) (Figure 3-5). When grown in MOPS cells containing R27::*lacO* had 1 focus (44.4%), 2 foci (43.6%) or 3 foci (12%). These results demonstrate that R27 localization is remarkably symmetric within live *E. coli*. Localization results of R27::*lacO* Par- are given below.

3.3.5 Time-Lapse Observations of R27::*lacO* Foci Duplication

Figure 3-6 shows representative experiments that demonstrate the kinetics of R27 focus duplication in *E. coli* growing on a nutrient agarose surface. In the cells with one focus, the focus duplicated at the mid-cell and the two foci moved apart rapidly, within 5 minutes, to the quarter-cell positions. In cells containing two foci, one focus duplicated at the quarter-cell position and subsequently one focus remained at the quarter-cell region while the second focus moved to the mid cell region. In three foci cells, the mid cell focus duplicated and the resulting foci then moved to either side of the division plane. Since the focus patterns before and after focus duplication and movement resemble the localization patterns of asynchronous *E. coli* populations, these observations likely represent the progression of the plasmid vegetative-cycle, where plasmid foci can duplicate at either the mid or quarter-cell positions.

Figure 3-4. Representative micrographs of the localization of R27 (a-d) and R27 partitioning mutants (*parB* and *parR*) (e-h) in live *E. coli*. a) 1 focus at mid cell, b) 2 foci at quarter cells, c) 3 foci at mid and quarter cells, d) 4 foci at mid and quarter cells, e) 1 focus at pole, f) 2 asymmetric foci at mid and quarter cell, g) and h) scattered GFP signal. Images e-h are representative of both partitioning mutants.

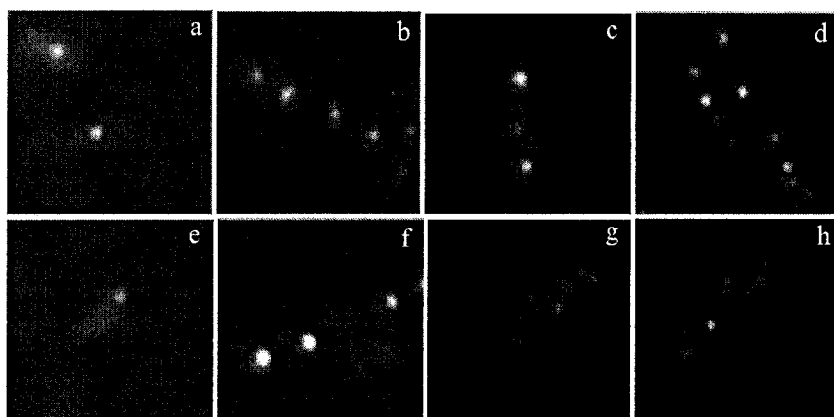
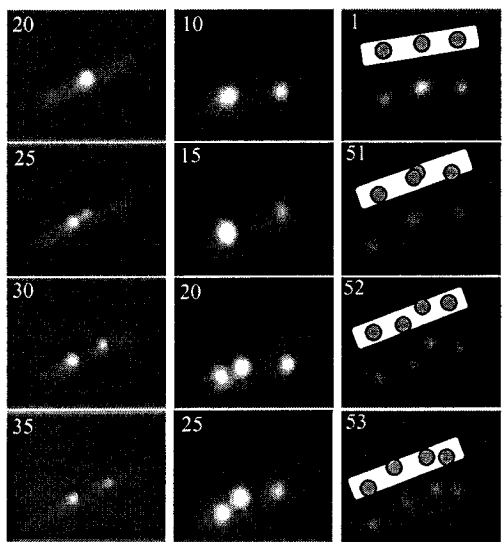


Figure 3-5. Summary of R27 and R27 partitioning mutants *parB-/par1-* and *parR-/par2-* localization in *E. coli* grown in MOPS (slow growth) and LB (fast growth) media. Cells types represent number and location of GFP foci. Values are given as a percentage of the total number of cells analysed for each plasmid type under each growth condition. Sample sizes are included. Boxed values highlight 1) the localization patterns for cells containing 1 and 2 foci from partitioning mutants whose foci positions are statistically different than wtR27, 2) the diffuse patterns seen in cells containing partitioning mutants but not wtR27 and 3) the high percentage of cells without a GFP signal, indicating plasmidless cells.

Number of Foci	Cell Types	Percentage of Cells (%)					
		LB			MOPS		
		wt (n=335)	<i>parB</i> ⁻ (n=408)	<i>parR</i> ⁻ (n=319)	wt (n=117)	<i>parB</i> ⁻ (n=267)	<i>parR</i> ⁻ (n=230)
1	1/2	1.2	2.0	1.6	44.4	6.7	23.8
1	1/4	0	2.2	1.0	0	19.5	0
2	symmetric	26.3	4.2	24.5	43.6	28.8	47.0
		0	10.5	0.3	0	11.2	0
2	asymmetric	42.4	21.8	33.6	12.0	19.1	23.8
		25.3	9.6	19.1	0	6.0	3.5
3		3.9	3.7	1.0	0	0	0
4		0	2.4	0	0	0	0
5		0	37.5	14.5	0	0	0
6		0.9	6.1	5.0	0	8.6	2.6
scattered							
no foci							
		100	100	100	100	100	100

Figure 3-6. Time-lapse fluorescence microscopy of R27 plasmid foci duplicating at either the mid or quarter cell positions of *E. coli*. Time image was collected is indicated in the top left hand corner. Left (vertical) time-lapse series depicts one focus duplicating at the mid-cell region, center time-lapse series depicts a focus duplicating at the quarter-cell region and the right time-lapse series depicts a focus duplicating at the mid-cell region.



3.3.6 Localization of R27 Partitioning Mutants in *E. coli*

When *E. coli* expressing GFP-LacI containing the R27::*lacO parB*::CAT mutant was grown in LB and MOPS, 93.9 and 91.4% of the cells contained GFP signals (discrete foci or scattered pattern), respectively. Of the LB grown cells 37.5% contained a scattered GFP pattern that was clearly distinguishable from discrete foci and not seen in cells containing wild-type R27 (Figure 3-4 and 3-5). Scattered patterns occupied the entire cell and were dynamic when viewed in real time, resulting in images that gave a smeared appearance. None of the MOPS grown cells contained scattered patterns. Cells containing *parB*::CAT and grown in LB which displayed discrete foci contained 1 focus (4.2%), 2 foci (14.7%), 3 foci (21.8%), 4 foci (9.6%), 5 foci (3.7%) or 6 foci (2.4%). Cells containing *parB*::CAT and grown in MOPS contained 1 focus (26.2%), 2 foci (40%), 3 foci (19.1%) or 4 foci (6%).

When *E. coli* expressing GFP-LacI containing the R27::*lacO parR*::CAT mutant (*parR*::CAT) was grown in LB and MOPS, 95 and 97.4% of the cells contained GFP signals (discrete foci or scattered pattern). Of the LB grown cells 14.5% contained a scattered GFP pattern that was clearly distinguishable from discrete foci (Figure 3-5). None of the MOPS grown cells contained scattered patterns. Cells containing *parR*::CAT and grown in LB contained 1 focus (2.6%), 2 foci (24.8%), 3 foci (33.6%), 4 foci (19.1%) or 5 foci (1.0%). Cells containing *parR*::CAT and grown in MOPS contained 1 focus (23.8%), 2 foci (47.0%), 3 foci (23.8%) or 4 foci (3.5%).

3.3.7 Statistical Analysis of R27 Localization

The localization patterns of the R27 partitioning mutants contained both scattered patterns, which were not seen with R27, and discrete foci. To determine if there is a significant difference in discrete focus localization patterns between R27 and either of the partitioning mutants, statistical analysis of the localization data of the one focus and two foci cells grown in MOPS and LB was performed. For the 2 foci data the focus positions were averaged to create a data set that represents the midpoint between the foci. Initially a t-test was used to compare the median values, but some of the data sets either did not fit a normal distribution (*parB*::CAT 1 focus MOPS and LB and 2 foci MOPS and LB) or contained standard deviations (*parR*::CAT 2 foci LB) which were not equal to the wild-

type data set. Therefore the non-parametric Mann-Whitney test (critical value set at $\alpha = 0.05$) was performed to compare the mutant data sets to those of the wild-type R27 locations. Figure 3-5 summarizes the statistical analysis.

The Mann-Whitney test indicated that there is a statistically significant difference between the localization patterns of cells containing R27 *parB*::CAT with 1 focus grown in MOPS ($P < 0.001$), the averaged 2 foci cells grown in MOPS ($P = 0.015$), the one focus cells grown in LB ($P = 0.006$) and the average of 2 foci cells grown in LB ($P < 0.001$) and the R27 grown under the corresponding conditions. Significant differences between the localization pattern of the R27 *parR*::CAT mutant 1 focus cells grown in LB ($P = 0.004$) and the average of 2 foci cells grown in LB ($P = 0.006$) and the R27 grown under the corresponding conditions. There is no significant difference between the localization patterns of the R27 *parR*::CAT mutant 1 focus cells grown in MOPS ($P = 0.817$) and 2 focus cells grown in LB ($P = 0.417$) and R27 grown under the corresponding conditions.

3.4 Discussion

In this work it was demonstrated that R27 contains two independent, functional partitioning modules, Par1 and Par2, which belong to the type I and type II partitioning families, respectively (60). In both the cloning stability test and the mutational stability tests Par1 was shown to be the major stability determinant whereas Par2 contributes to stability in a minor, yet significant, manner. Each of the R27 Par- mutants is therefore referred to as being partitioning impaired, as they each maintain some stabilizing abilities. The inability of a double Par- of R27 to exist in the extra-chromosomal form illustrates the extreme instability of such a mutant and attests to the importance of the partitioning modules to the maintenance and backbone of IncHI1 plasmids. The redundant partitioning modules provide extra stability to R27, as both partitioning modules contribute to the stability of R27, and likely play a key role in the persistence of IncHI1 plasmids within *S. typhi* (92, 138, 165). The only other plasmid known to contain a double-partitioning module is pB171, a 90 kb virulence plasmid from enteropathogenic *E. coli* (45).

The cellular location of R27::*lacO* was visualized with a GFP-LacI probe within live *E. coli*. R27 foci were located at the mid- and quarter-cell locations. Cells grown in MOPS (slow growth) predominantly contained 1, 2, or 3 foci whereas cells grown in LB (fast growth) predominantly contained 2, 3 or 4 foci, suggesting that the number of foci per cell is related to the growth rate and the cell-cycle. Several larger plasmids, including F, P1, R1, RP4 and R751 are also known to be localized to the mid- and quarter-cell positions (66, 95, 110, 148, 166) and each focus consists of multiple plasmid molecules (67, 166). Time-lapse experiments demonstrated that plasmid foci duplicate at either the mid- or quarter-cell positions. These observations imply that the progression of the R27 plasmid vegetative cycle starts with one focus duplicating at the mid cell and the resulting 2 foci moving to the quarter-cell positions. Subsequently, a focus at the quarter-cell position duplicates and one focus moves to the mid-cell while the other remains at the quarter-cell position, creating a cell with a mid-cell focus and two quarter-cell foci. In three foci cells, it appears as though the mid-cell focus duplicated and then both foci were positioned on either side of the division plane. These movements and localizations result in complete stability of R27, as R27 was not lost from any cells in a long-term stability assay.

Based on the work on other model partitioning systems (F, P1 and R1), it is presumed that the positioning of R27 foci at the mid- and quarter-cell regions is determined by both ParB and ParR, bound to the centromere, interacting with an unknown host factor. Likewise, the motive force which moves R27 foci between mid- and quarter-cell positions might be determined by the polymerization of ParM (141) and possibly ParA into actin-like filaments, with the partitioning complex serving as the nucleation point. Such a model would imply that the actions of both partitioning modules are coordinated such that the timing of partitioning and the interacting host factor would be similar. This is interesting as Type I and II partitioning families are believed to have different evolution histories (60), yet appear to stabilize plasmids using a similar mechanism.

The presence of two partitioning modules with different stability contributions gave a unique opportunity to correlate plasmid localization with plasmid stability, where R27 is completely stable, R27 *par2-/parR-* is moderately stable and R27 *par1-/parB-* is

unstable. From these analyses two types of partitioning-impaired localization patterns were recognized that are distinct from R27 localization and are therefore indicative of plasmid instability: i) mis-localized discrete plasmid foci and ii) scattered plasmid patterns. When partitioning mutants formed discrete foci, the localization patterns of the both Par- plasmids in one or two foci cells grown in LB differed significantly with those of R27, whereas only the localization pattern of the *parB*-/Par1 plasmid in one and two foci cells grown in MOPS differed significantly with the R27. Due to the nature of the partitioning mutants, it is expected that one cause of plasmid instability resulted from a reduced ability of the R27 partitioning complex to become tethered to the mid- and quarter-cell positions. The tethering deficiency of Par1 and Par2 mutants could explain both the instability and the mislocalized focal patterns observed for Par1 and Par2 mutants. It is interesting that the localization patterns of the *parR*-/Par2 mutant grown in MOPS did not differ significantly from that of R27. This suggests that the Par1 module alone is sufficient to stabilize R27 at slower growth rates, but not at faster growth rates.

A large percentage of the Par- cells grown in LB, but not R27 cells, contained scattered GFP signals suggesting that the plasmids were randomly dispersed throughout the cytoplasm. The partitioning mutants were expected to be impaired in plasmid pairing which could reduce the formation of plasmid clusters (discrete foci), resulting in instability. Therefore the scattered patterns may represent individual plasmid molecules. The fact that the scattered pattern was absent from partitioning mutants grown in MOPS suggests that the pairing impairment would be suppressed at a slower growth rate. The pronounced instability of the partitioning-impaired plasmids at faster growth rates, that is mis-localized plasmid foci and scattered patterns, is likely a direct result of the increased replication as reflected by multi fork replication. As a result the number of plasmids per cell would increase and the carrying capacity of only one of the R27 partitioning modules would have surpassed, resulting in randomly dispersed individual and clustered plasmid molecules.

Chapter 4

Bacterial Conjugative Transfer: Visualization of Successful Mating Pairs and Plasmid Establishment in live *Escherichia coli*

A version of this work have been published in the following manuscript:

Lawley, T.D., G.S. Gordon, A. Wright, and D.E. Taylor. 2002. Bacterial Conjugative Transfer: Visualization of Successful Mating Pairs and Plasmid Establishment in live *Escherichia coli*. *Mol. Microbiol.* 44:947-956.

4 Bacterial Conjugative Transfer: Visualization of Successful Mating Pairs and Plasmid Establishment in live *Escherichia coli*

4.1 Introduction

The life cycle of a conjugative plasmid contains three phases – replication, partitioning, and conjugation. In the past these processes have been compartmentalized into distinct stages, however, it is becoming apparent that these functions are continuous processes that overlap throughout the cell cycle (17). Fluorescence microscopy methods have made it possible to demonstrate that plasmid molecules reside at defined positions within the bacterial cell, located at the mid-cell and quarter-cell regions (66, 95, 148, 166). The fact that the host replisome and plasmid-encoded partitioning proteins are located at similar positions (114) suggests a physical association between plasmid replication and partitioning. These processes and the associated plasmid movements are referred to as the vegetative cycle, as discussed in Chapter 3. A component of the IncP plasmid group partitioning apparatus, KorB (centromere binding protein), also serves as a regulator of plasmid replication and conjugation, highlighting the presence of molecular control circuits that coordinate the plasmid backbone functions and thereby link the plasmid vegetative cycle to the conjugative cycle (16, 17).

Plasmid replication occurs every generation and ensures that the plasmid copy number is maintained within each bacterial cell. Vegetative replication is initiated at the origin of replication (*oriV*) usually by the plasmid-encoded replication initiator protein and is carried out by the host-encoded replisome (43). Active partitioning ensures that each daughter cell receives plasmid molecules during cell division. Partitioning is performed by the plasmid-encoded partitioning system, which generally consists of two proteins and a centromere region (60, 140). Conjugation is a special type of DNA replication in which one strand of the replicated plasmid molecule is retained in the donor cell while the second strand is transferred to the recipient cell in the 5' to 3' direction (218). Bacterial conjugation allows plasmid molecules to transfer horizontally throughout a bacterial community. Horizontal transfer is mediated by a specialized

plasmid-encoded protein complex called the conjugative apparatus and relies on several host-encoded factors, including the replisome (100).

Recently, Grahn and colleagues (69) identified the cellular locations for each of the 11 Mpf/T4SS proteins from the IncP α alpha plasmid RP4. All but one of these proteins was found to be localized to the outer membrane. The Mpf proteins were also found in an intermediate membrane fraction between the inner and outer membrane and it has been proposed that this fraction is responsible for the formation of conjugative junctions observed between stable mating pair aggregates (177). Conjugative junctions are the most likely regions where the proposed conjugative pore would mediate T-strand transfer through the donor and recipient membranes, although this has yet to be demonstrated equivocally. Despite much work, the precise roles and interactions between the Mpf proteins remain poorly understood.

A working model of conjugation has been proposed, which is based primarily on the characterization of individual transfer proteins (218). Such a model is speculative concerning the localizations and movements of the transferring DNA and does not take into account the other key aspects of the plasmid lifecycle — vegetative replication and active partitioning. The objective of this present work was to document the localization and movements of the IncP β plasmid R751 during conjugation using the *lacO*/GFP-LacI system. Comparisons of R751 during conjugation to R751 under non-conjugative conditions has identified key localizations and movements associated with plasmid establishment in the transconjugant. An analysis of successful mating pairs has identified regions of direct contact where plasmid DNA is transferred from donor to recipient cells. These experiments were initially performed with R27 but analysis was hampered due to the low frequency of transfer under the conditions used. R751 was found to be the ideal model system for this approach and has provided an unprecedented visualization of conjugation.

4.2 Experimental Procedures

4.2.1 Bacterial Strains and Plasmids

The following *E. coli* strains were used: Stb12 (F- *mrcA recA1 endA1 lon gyrA96 thi supE44 relA1* λ -; Life Technologies), DY330 (W3110 Δ *lacU169 gal490* λ *cl857* Δ *cro-bioA*) (217), DY330R (temperature resistant revertant of DY330, rifampicin^r) and DY330N (temperature resistant revertant of DY330, nalidixic acid^r). The following plasmids with relevant characteristics were used: R751 (IncP β , trimethoprim^r) (201), pSG25 (*lacO* cassette delivery vector, kanamycin^r, ampicillin^r) (66), pSG20 (GFP-LacI expression vector, arabinose inducible promoter, ampicillin^r) (66) and pJP124 (Tn7 transposase vector, chloramphenicol^r; gift from Dr. Nancy Craig).

4.2.2 Growth Conditions

All *E. coli* strains were grown in LB (Difco Laboratories) medium or MOPS minimal medium (MOPS buffer with 20 amino acids and 0.4% glucose or 0.4% glycerol) (66). During the construction of R751::*lacO* when trimethoprim resistance was utilized, strains were grown with Mueller Hinton medium. When necessary the following antibiotics were added to the growth medium: ampicillin (Ap) (100 μ g/ml), kanamycin (Km) (50 μ g/ml), tetracycline (Tc) (10 μ g/ml), chloramphenicol (Cm) (16 μ g/ml) and trimethoprim (Tp) (10 μ g/ml). The growth temperature was 30°C for routine procedures. For microscopy, cells from overnight cultures were diluted 1/20 and grown at room-temperature to mid-log phase prior to induction of GFP-LacI. GFP-LacI was induced by adding 0.2% arabinose to the growth medium. Expression was then repressed after 30-40 minutes by adding 0.4% glucose to the medium and continuing growth for an additional 30 minutes. For membrane labeling FM 4-64 (Molecular Probes) was added to the medium at the same time as induction at a final concentration of 2 μ g/ml. Control experiments illustrated that FM 4-64 stained cells could not cross-contaminate non-labeled cells during mating experiments on nutrient agarose slabs. Mating on microscope slides is described in Microscopy and Photography section (4.2.5).

4.2.3 R751::*lacO* Construction

To produce a R751::*lacO* construct that was stable and mating proficient, pSG25 was first transformed into *E. coli* strain Stbl-2 and then R751 was mated into these cells using the methods previously described (76). Once the presence of both plasmids was confirmed using plasmid isolation procedures, electroporation was used to introduce pJP124 into the strain. pJP124 contains the Tn7 transposase genes cloned into pACYC that promotes random transposition of Tn7 into conjugating plasmids (216). Cells containing all three plasmids were collected from agar plates in 1 ml of PBS and 0.1 ml of this cell suspension was used to inoculate 10 ml of fresh LB + Ap, Tp, and Cm. Cells were grown to mid-exponential phase and were used as donors for mating. Transposition of the *lacO* cassette into R751 was achieved by mating R751 to DY330R and selecting with trimethoprim, for R751, and kanamycin, for the *lacO* cassette. To ensure the *lacO* cassette did not transpose into transfer genes, transconjugants were pooled and mated into DY330N [pSG20] (cells containing pSG20 express GFP-LacI). Several colonies were then individually screened to ensure wild-type mating efficiency, one of which was used for further analysis. Within this construct, the *lacO* cassette was found to be inserted into an intergenic region between genes *qacE* and *tniC*, as determined by sequencing the region flanking Tn7 with primer NLC95 (5'ATAATCCTTAAAACTCCATTTCCACCCCT) (216).

4.2.4 Construction of R751::*lacO* Transfer Mutants

To construct a R751::*lacO* transfer mutant, the method of Yu et al. (217) was used to insert a CAT cassette (chloramphenicol resistance gene from mini-Tn10; 25) into the *traI*, the relaxase gene which is essential for transfer. The primers Trev5004 (5'AACTACATCACCGACGCCCAAAGCAAAGACCACCGGCTCTGTGACGGAAGATC ACTTC) and Trev5005 (5'ACCTCCGTGATGGGTCTGGATGGAACCGGCTTCGCATTATTTCAG GCGTAGCACCAG) were used to amplify the CAT cassette and add 40 bp to each end that are homologous to 75 bp from the start codon of *traI*. This product was introduced by electroporation into DY330 harboring R751::*lacO* and cells were selected on LB containing Cm and Kan. Potential mutant plasmids were isolated and the primers Trev5000 (5'TATAGAATTCAATGATCGCCAAGCACGTGC) and Trev5001 (5'TATAGGATCCT

CAGTGATGGTGATGGTGATGTCTACTCCTTCCTTCGACG) were used to amplify the *traI* gene. An increase in size of 900 bp indicated that the CAT cassette was inserted into the *traI* gene.

4.2.5 Microscopy and Photography

For microscopy experiments, cells were grown as indicated. One ml aliquots of samples were collected, pelleted and resuspended in 20-50 μ l of MOPS medium. A 1 μ l sample was added to a MOPS medium/1.5% agarose slab on a microscope slide. A cover slip was added and the edges sealed with vacuum grease. For mating experiments the samples contained a 5:1 donor to recipient ratio.

Fluorescence microscopy was performed using a Leica DMRE microscope equipped with a CCD camera (Cooke SensiCam) and a standard FITC filter set (Chroma). Samples were illuminated with a UV (Leica HB100) source and images collected and processed using SensiControl 4.0 and PhotoPaint (Corel). Time-lapse microscopy was performed on a Zeiss LSM510 laser scanning microscope equipped with a CDD camera. For dual labeling experiments, samples were excited with an Argon laser (488nm; GFP) and HeNe1 (543nm; FM 4-64) and visualized with a LP505nm (GFP) and LP650nm (FM 4-64) filters. Images were collected with Zeiss Software (Version 2.5) and processed with PhotoPaint (Corel). Quantitative measurements (i.e. number of foci, foci location and cell size) were performed as described (66).

4.3 Results

4.3.1 Localization of R751 in *E. coli*

The intracellular localization of R751 in *E. coli* was investigated using the *lacO* /GFP-LacI system. A *lacO* cassette, consisting of 256 tandem repeats of the lactose operator and the kanamycin resistance gene flanked by Tn7 inverted repeats, was introduced into R751 by random transposition (See Experimental Procedures). Expression of GFP-LacI (encoded by pSG20) resulted in GFP-LacI binding to the tandem operators and caused the hybrid repressor molecules to cluster as a fluorescent focus that

was visualized by fluorescence microscopy and represented the location of the plasmid molecule (66).

Fluorescence images were collected of asynchronous cell populations that were grown either in LB media or MOPS minimal medium, resulting in different growth rates. The cell length, the number of foci per cell and the position of each focus was determined for each cell. Under either growth condition >99% of the cells contained discrete GFP foci when viewed by fluorescence microscopy, whereas controls of *E. coli* (R751,pSG20) and *E. coli* (pSG20), which expresses GFP-LacI, displayed a uniform green fluorescence (Figure 4-1 A[i]). When *E. coli* containing R751::lacO was grown in LB medium, ~97% of the cells contained either 2 (35.5%), 3 (37%), or 4 (24.3%) foci (Figure 4-1 A [iii-v], 4-2 d-f). To test the effect of decreased growth rate on R751:: lacO foci localization and distribution, cells were grown in MOPS minimal medium. Under these conditions 98.5% of the cells contained either 1 (30%), 2 (53.4%), or 3 (15.1%) foci (Figure 4-1 A[ii-iv], 4-2A a-c).

To identify the intracellular localization of R751, the positions of the foci were plotted against cell length (Figure 4-2 a-f). When cells contained one or two foci, these foci were located at the mid-cell position or quarter-cell positions, respectively. When cells contained three foci, these were located at the 1/4, 1/2 and 3/4 positions. In cells with four foci, foci were located at the 1/5, 2/5, 3/5, and 4/5 cellular positions. Therefore R751 plasmid molecules reside at or close to the mid- and quarter-cell regions of *E. coli*. Figure 4-2 a-f also illustrates that the number of foci increases with cell length. Cells grown in MOPS minimal medium preferentially contained 1, 2, or 3 foci, with average cell lengths of 0.9, 1.2, and 1.4 microns, respectively (Figure 4-2 a-c). Cells grown in LB medium preferentially contained 2, 3, or 4 foci, with average cell lengths of 1.2, 1.4 and 1.8 microns, respectively (Figure 4-2 d-f). Regardless of whether the cells were grown in MOPS or LB, cells with two or three foci averaged the same cell length, illustrating the strong correlation between cell length and number of foci.

Since the localizations and movements of R751 during conjugation are of interest, the subcellular location of R751:: lacO in *E. coli* was determined when in the presence of recipient cells. This was to test if the localization patterns of R751 changed while the host cells were mating. DY330R (R751:: lacO, pSG20) [donor] expressing GFP-LacI

Figure 4-1. Intracellular localization of R751::*lacO* in *E. coli* donor (A) and transconjugant (B) cells expressing GFP-LacI. GFP-LacI was expressed from cells containing pSG20 with 0.2% arabinose induction for 30-45 minutes. Donors (A) and transconjugants (B) were grown in 2 μ g/ml of FM 4-64, which stains the membranes red (see Experimental Procedures). (A) Fluorescence micrographs show representative donor cell types; control cells *E. coli* DY330R (R751, pSG20) (i); (A, ii-v) donor cells containing: one focus located at the mid-cell (ii); two foci located at the quarter cell positions (iii); three foci located at the mid and quarter-cell (iv); four foci located at the 1/5, 2/5, 3/5 and 4/5 cellular positions (v). In B, donors cells (DY330N+R751::*lacO*) were mated with recipient cells (DY330N+pSG20) expressing GFP-LacI and stained with 2 μ g/ml FM 4-64. (B) Combined fluorescence/DIC micrographs show representative transconjugant cells within mating aggregates containing one focus located at the quarter-cell and one focus located at the mid-cell (i); two foci symmetrically located (ii); two foci asymmetrically located (iii); three foci located at the cell-quarters and mid-cell (iv); and four foci located at the 1/5, 2/5, 3/5 and 4/5 cellular locations (v).

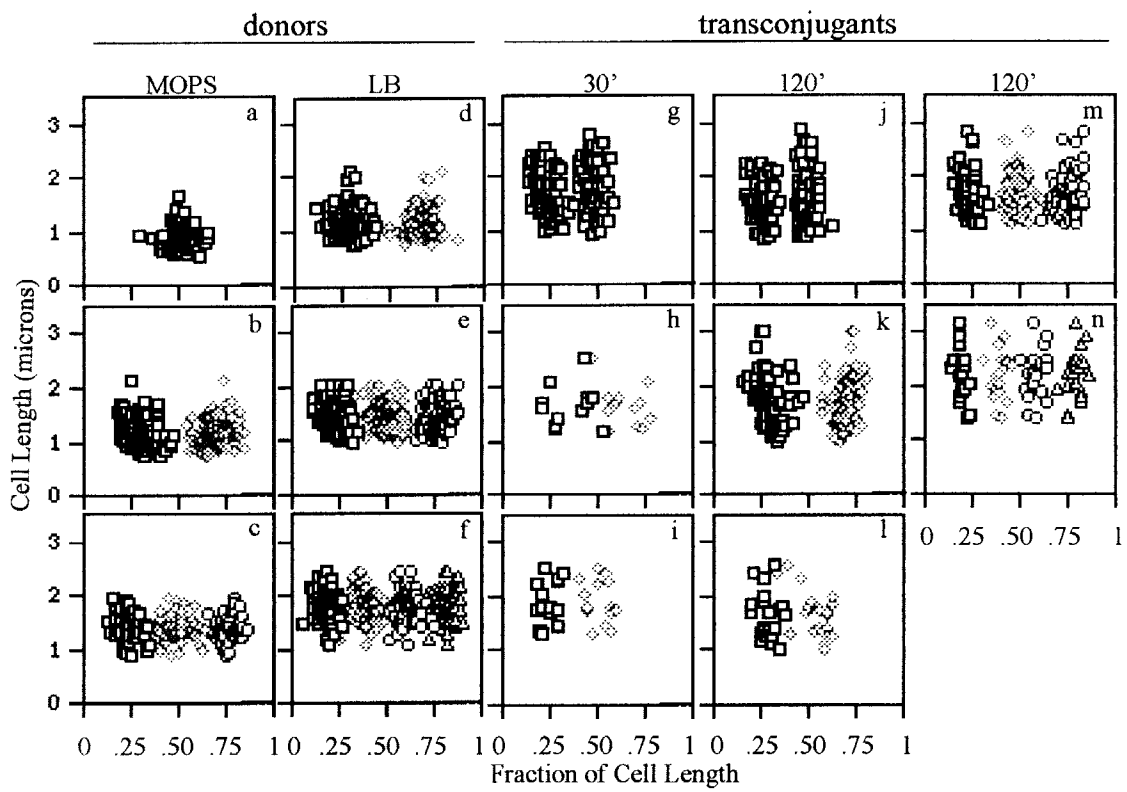
A) Donors



B) Transconjugants



Figure 4-2. Localization of *R751::lacO* as a function of cell length in donor cells (a-f), 30 minute (g-i) and 120 minute (j-n) transconjugant cells. The distance of GFP foci was measured from one cell pole. (a-f) *R751::lacO* localization in donor cells expressing GFP-LacI grown in MOPS medium (a-c; n=410) with one, two and three foci per cell, respectively, and in donor cells expressing GFP-LacI grown in LB (d-f; n=349) with two, three and four foci per cell, respectively. In 2g-i and 2j-n, donor cells containing *R751::lacO* were mated with recipients expressing GFP-LacI. (g-i; n=215) The localization patterns of *R751::lacO* in transconjugants at 30 minutes after the start of mating illustrating (g) one focus located at either the mid or quarter cell regions, (h) two foci patterned symmetrically about the mid cell, (i) two foci patterned asymmetrically. (j-n; n=376) The localization patterns of *R751::lacO* in transconjugants at 120 minutes after the start of mating illustrating (j) one focus located at either the mid or quarter cell regions, (k) two foci patterned symmetrically about the mid cell, (l) two foci patterned asymmetrically, (m) three foci located at the mid and quarter cell positions, and (n) four foci located at the 1/5, 2/5, 3/5, and 4/5 positions.



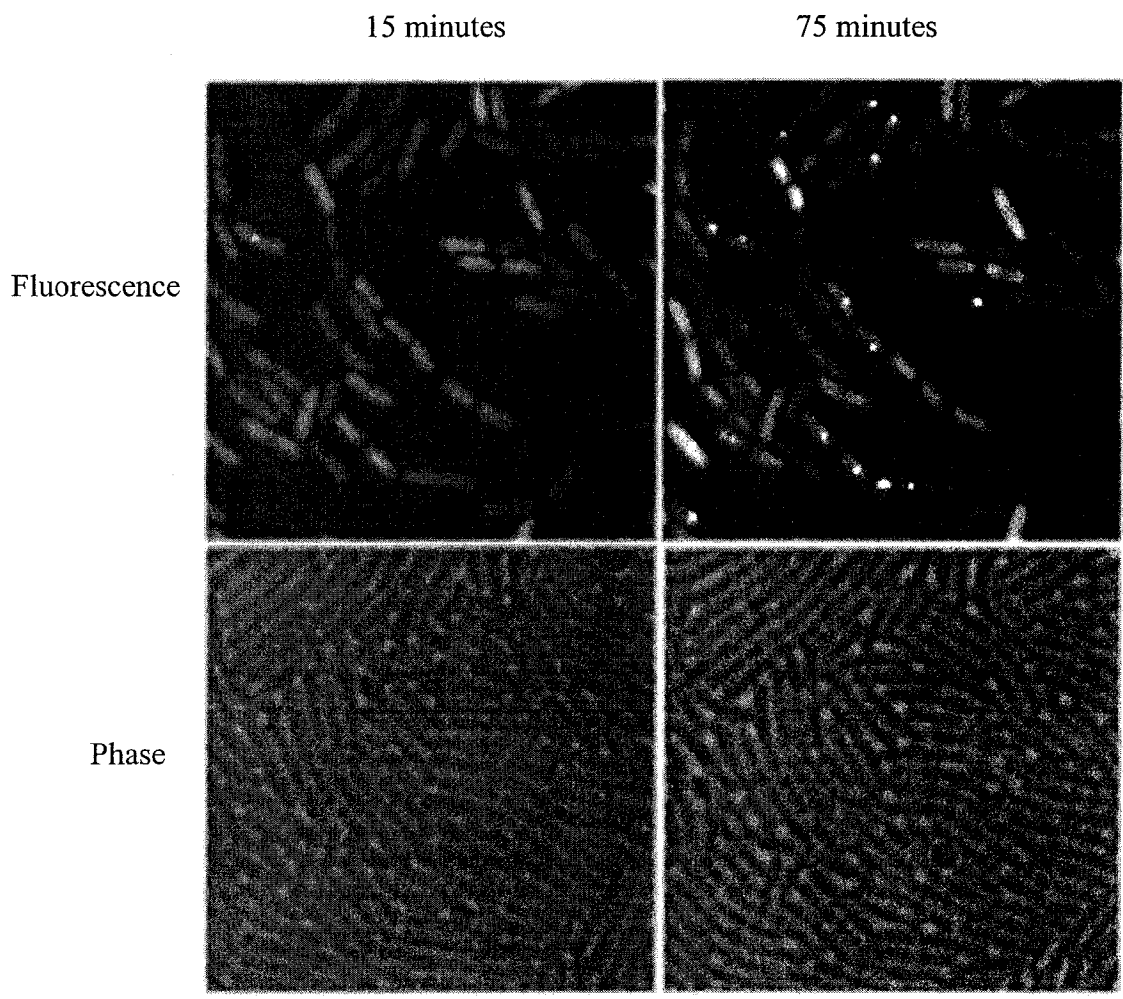
and DY330N [recipient] were grown as described above, mixed together in equal proportions, and placed on a nutrient agarose slab at room temperature. Under these conditions, ~20% of the donor cells transfer R751:: *lacO* to recipients after 60 minutes of mating, as determined by conjugation experiments. When viewed with fluorescence microscopy R751:: *lacO* was visualized only in donor cells. Fluorescent images were collected of mating aggregates (filling the entire field of view with phase contrast) after 30 and 60 minutes and the positions of plasmid foci in donor cells were plotted against cell length. R751:: *lacO* was found to localize to the quarter- and mid-cell positions in donors (data not shown). These GFP foci patterns are indistinguishable from those in Figure 4-2 d-f.

4.3.2 Establishment of R751:: *lacO* in Recipient (Transconjugant) After Conjugative Transfer

It was reasoned that the *lacO*/GFP-LacI system could be used to detect the localization of R751:: *lacO* as it enters the recipient, forming the transconjugant, and then afterwards during the subsequent events which enable the plasmid to become established in the new host. This is based on the observations that: 1) GFP-LacI expression in the absence of the *lacO* cassette resulted in uniform fluorescence of the bacterial cytoplasm and 2) GFP-LacI expression in the presence of the *lacO* cassette results in discrete GFP foci representing the plasmid molecule. Therefore, by expressing GFP-LacI in the recipient and mating with a donor containing R751:: *lacO*, the progression of conjugation can be monitored by differentiating between recipients and transconjugants. It should be noted that the conjugative plasmid enters the recipient as a single strand, and since LacI binds to double stranded *lacO*, it was expected that R751::*lacO* would be observed shortly after complementary strand synthesis in the transconjugant cell. Complementary strand synthesis has been proposed to occur concurrently with DNA entry (218).

Donor [DY330R (R751:: *lacO*)] and recipient [DY330N (pSG20)] expressing GFP-LacI were mixed together and placed on a nutrient slab and fluorescence microscopy was used to collect images of mating aggregates every 15 minutes. Discrete GFP foci appeared in recipients in a time-dependent manner (Figure 4-3), whereas no GFP foci appeared when wild-type R751 was used in donors or in recipients expressing

Figure 4-3. Fluorescence and phase-contrast micrographs of mating aggregates demonstrate the utility of *lacO*/GFP-LacI system in differentiating between donors, recipients and transconjugants. Donors (DY330R+R751::*lacO*) were mated with recipients (DY330N+pSG20) expressing GFP-LacI on agarose nutrient slabs and images collected every 15 minutes. Time-lapse microscopy illustrates the appearance of GFP foci in recipients, representing transfer of R751::*lacO* from donor to recipients and converting them to transconjugants, within a one-hour time interval. Recipients are uniformly fluorescent cells and transconjugants contain GFP foci on fluorescent micrographs. The corresponding phase-contrast micrographs illustrate that recipients and transconjugants are surrounded by non-fluorescent donor cells. Within a one-hour period approximately 25% of the recipients are converted to transconjugants.



GFP-LacI alone (data not shown). The first GFP foci were observed approximately 15 minutes after donors and recipients were mixed together. After 90 minutes, approximately 25% of the recipients contained at least one GFP focus. Transconjugants appeared predominantly in mating aggregates, rarely in regions where cell concentrations were low and never when donors and recipients were not in direct contact with each other. To confirm that the appearance of GFP foci represents a conjugation event, a *traI::CAT* transfer-deficient mutant of R751:: *lacO* was used in matings. The R751 *traI::CAT* mutant failed to transfer during routine conjugation assays and no GFP foci appeared in recipients during the microscopic conjugation assay (data not shown).

To investigate the later stages of conjugation and establishment of R751 in transconjugant cells, the localization and distribution of R751:: *lacO* in transconjugants was determined at 30 and 120 minutes after the start of conjugation. At 30 minutes and 120 minutes after mating was initiated 7% and 23% of the recipient cells in mating aggregates respectively contained GFP foci.

Fluorescent images were collected of mating aggregates and the cell length, the number of foci and position of foci were determined for each transconjugant. After 30 minutes of *lacO* mating, transconjugants (30 minute transconjugants) contained either one (88%) or two (12%) foci (Figure 4-1 B[i-iii], 2g-i). At 120 minutes after mating was initiated, transconjugants (120 minute transconjugants) contained one (46.8%), two (32.4%), three (15.2%), or four (5.6%) foci (Figure 4-1 B[i-v], 2j-n). To determine the localization of R751 in transconjugants, the position of the foci was plotted against cell length (Figure 4-2 g-n). When transconjugants contained one focus it was located at either the mid-cell or quarter-cell position, independent of cell length (Figure 4-2 g and j). When two foci were present in the transconjugants they were located either symmetrically about the middle of the cell (Figure 4-2 h and k) or asymmetrically with one at mid-cell and the other at the quarter-cell position (Figure 4-2 i and l). At 120 minutes, the pattern seen in transconjugants containing 3 or 4 foci was similar to that seen in donor cells (Figure 4-2 m and n).

In order to better define the localization pattern of the two asymmetric foci in transconjugants, a comparison was made to both donors and transconjugants with two symmetrically positioned foci. When donors contained two foci, the positions were

located at an average of 29% and 68% (LB) or 30% and 70% (MOPS) of the cell length as measured from one pole. The average midpoint between foci was therefore 48% (LB) and 50%, resulting in the symmetrically positioned foci (Figure 4-2 b and d). When 30 minute and 120 minute transconjugants contained two symmetric foci, the positions were located at an average of 34% and 66% (30') or 30% and 70% (120') of the cell length from one cell pole. The average midpoint between foci was therefore 50% (30') and 50% (120') (Figure 4-2 h and k). When 30 minute and 120 minute transconjugants contained two asymmetrically positioned foci, their positions were located at an average of 24% and 50% (30') or 28% and 54% (120') of the cell length from one cell pole. The average midpoint between foci is 37% (30') and 41% (120'), resulting in the asymmetric localization patterns observed in Figure 4-2 i and l.

4.3.3 Time-lapse Observations of Plasmid Appearance and Duplication in Recipient Cells.

Figure 4-4 shows the kinetics of appearance of fluorescent foci in recipient cells following mixing of donor (R751:: *lacO*) and recipient (GFP-LacI) on an agarose surface. In the two examples shown, single fluorescent foci had formed just 18 minutes (left panels) and 22 minutes (right panels) after mixing donor and recipient. Foci were consistently seen to appear either at the mid-cell (left panels) or the quarter-cell positions (right panels). The resulting patterns resemble the quarter- or mid-cell localization patterns seen in transconjugants with one focus (Figure 4-2 g and j).

Following the appearance of single foci in recipient cells, these were seen to duplicate yielding two foci one of which migrated slowly away from the other as shown in Figure 4-5. In the examples shown, duplication occurred either at the cell quarter position (upper panels) or the cell center (lower panels). In the former case one of the two foci moved from the quarter position to the cell center while in the latter it moved from the cell center to the quarter position. The resulting asymmetric patterns resemble those shown in Figures 4-2 (i and l).

Figure 4-4. Time-lapse fluorescence microscopy of mating aggregates where donors are transferring R751::*lacO* to recipients expressing GFP-LacI. Mating aggregates were placed on a nutrient agarose slab and images were taken every two minutes. The time shown started at the beginning of mating. Conjugative transfer of R751::*lacO* to recipients results in a rapid clustering of GFP-LacI to the *lacO* cassette within a matter of minutes. The left (vertical) time-lapse series shows R751::*lacO* targeted to mid-cell region of recipients after transfer and the right time-lapse series shows R751::*lacO* targeted to quarter-cell region of recipients after transfer

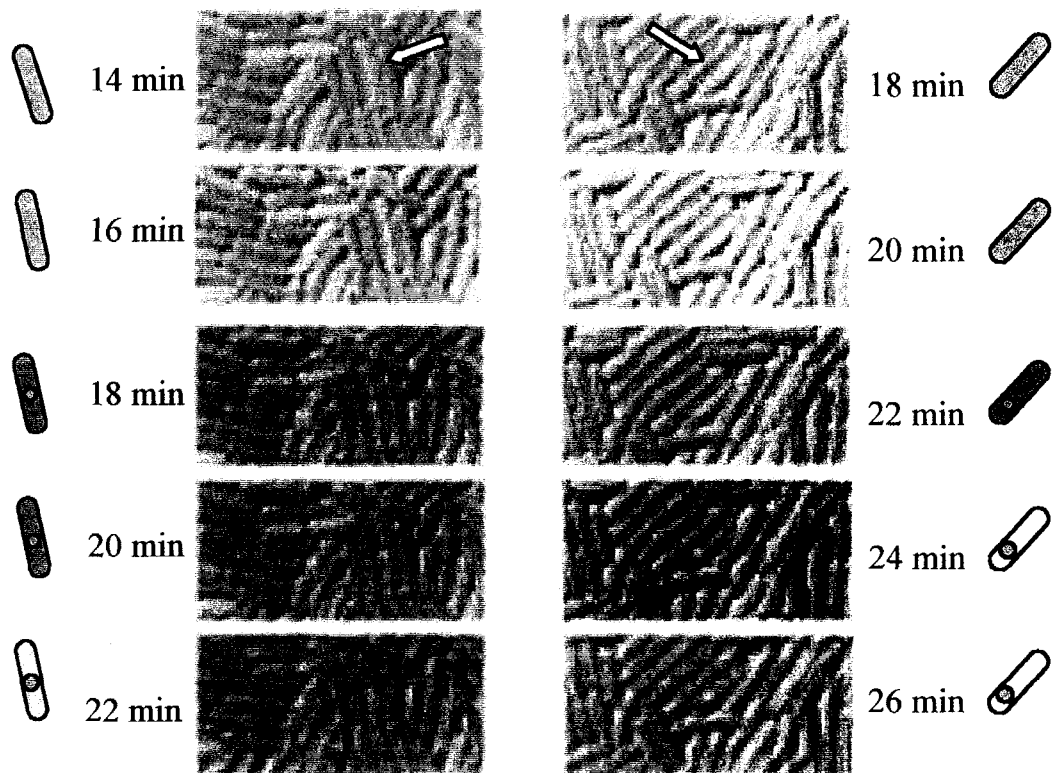
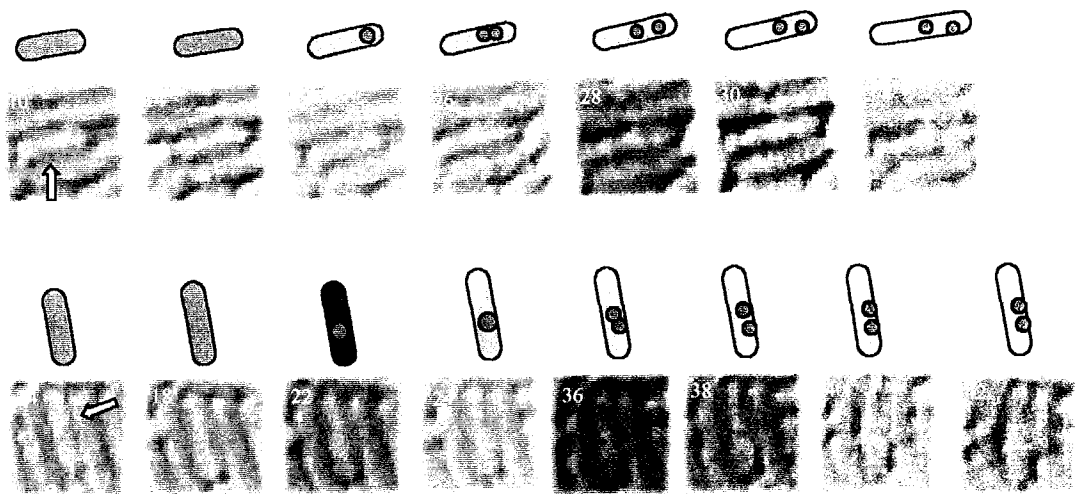


Figure 4-5. Time-lapse fluorescence microscopy of duplicating, but not actively partitioning, foci in transconjugants. Mating aggregates were placed on a nutrient agarose slab and images were taken every two to four minutes. Time was started at the beginning of mating and is indicated by minutes in the top left corner.



4.3.4 Spatial Relationship between Donor and Transconjugant during Conjugative Transfer.

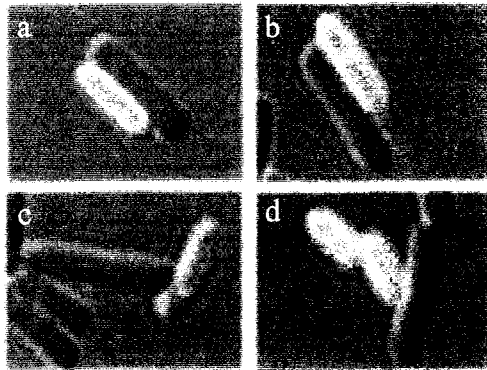
In order to investigate the locations of conjugative junctions between donor and recipient cells and therefore the route by which DNA is transferred, images were collected of successful mating pairs that consisted of only one donor (R751:: *lacO*) that was in direct contact with a transconjugant cell(s) (expressing GFP-LacI) shortly after conjugative transfer. This approach is particularly attractive since donor and recipients are easily distinguishable, and new transconjugants are easily identified. Preliminary time-lapse experiments demonstrated that *E. coli* remained stationary on the nutrient agarose slab for periods of time exceeding the 20 minute window used to observe successful mating pairs. In addition, the slight elongation of cells during the 20 minute period did not appear to alter the spatial relationship between cells (estimated generation time of 120 minutes by direct observation and cell counts).

Donor (R751:: *lacO*) and recipient (GFP-LacI) were placed on an agarose slab. Samples were scanned for isolated successful mating pairs and images were collected for up to 35 minutes after the start of conjugation. Since under these conditions no transconjugants were observed within the first 15 minutes of mating, such transconjugants would have contained R751 for no more than 20 minutes. In addition, only transconjugants with one focus were chosen for analysis. These criteria ensured that transconjugants were young and therefore the region of contact between donor and transconjugant cells contained the conjugative junction and therefore the mating pore.

Images of 35 successful mating pairs were collected and categorized according to the spatial relationship between the donor and transconjugant cells (Figure 4-6). Twenty-seven mating pairs were found to be aligned parallel to each other with the lateral walls in direct contact, four mating pairs were aligned perpendicular to each other with the cell pole of the transconjugant in direct contact with the lateral wall of the donor, and three mating pairs were aligned perpendicular so that the cell pole of the donor was in direct contact with the lateral wall of the transconjugant. No successful mating pairs were visualized that were aligned with pole against pole.

Within the regions of contact no obvious gaps were identified. The lengths of the contact regions were measured for each of the three categories. The average length for

Figure 4-6. Combined fluorescence/DIC micrographs of mating pairs. Regions of direct contact between donors and transconjugants represent locations of mating pore through which DNA is transferred. Recipients were expressing GFP-LacI and grown in 2 μ g/ml FM 4-64 prior to mating with donors on nutrient agarose slab. Representative mating pairs of an unsuccessful mating pair (a) and successful mating pairs that are aligned with the lateral wall of donor and transconjugants in direct contact (b) with pole of donor in direct contact with the lateral wall of transconjugants (c) and with lateral wall of donor in direct contact with pole of transconjugants (d).



the contact regions were $1.19 \mu\text{m} \pm 0.37$ when cells were aligned lateral wall to lateral wall, $0.43 \mu\text{m} \pm 0.03$ when the lateral wall of the donor was aligned to the pole of transconjugants and $0.44 \mu\text{m} \pm 0.03$ when the pole of the donor was aligned to the lateral wall of the transconjugant.

4.4 Discussion

In this work a GFP-LacI fluorescent probe was used to examine conjugal DNA transfer in *E. coli*, mediated by the IncP β plasmid R751. Using this approach it was found that R751 is localized as discrete foci either at mid-cell or quarter-cell positions in *E. coli* donors, reinforcing the notion that plasmids reside at specific subcellular sites (66, 95, 148, 166). The increase in plasmid foci likely represents a progression through the cell-cycle, as the number of foci is strongly correlated with cell length. Recently, Pogliano *et al.* used the GFP-LacI system to determine that the IncP α plasmid, RK2, was localized in *E. coli* in the same manner as R751. Using time-lapse microscopy it was demonstrated that RK2 foci duplicate at the cell center and migrate rapidly to the quarter-cell positions, illustrating the relationship between the foci locations (166).

R751 is maintained at the mid- and quarter-cell positions by the partitioning proteins IncC and KorB (125); KorB localizes to the mid- and quarter-cell regions of *E. coli* (16). KorB is also known to bind to 11 sites on the R751 genome and regulates several operons, including those controlling replication and conjugation functions (201). The bacterial replication machinery is a stationary multi-protein complex that also resides at the mid- and quarter-cell positions (114). The placement of R751 at the same locations as the replication machinery would allow plasmid molecules access to the vegetative replication process. Therefore, the key components that control both vertical and horizontal transmission of R751 are located at the same intracellular regions.

It is also known that the relaxosome is maintained at a nicked/un nicked equilibrium *in vivo* -- even in the absence of conjugation (32). Taken together, these observations imply that the relaxosome is maintained at the mid-cell or quarter-cell positions in *E. coli* until a proposed “mating signal” (100) is targeted to these regions. This would result in unwinding of the plasmid molecule, with subsequent production of the transfer intermediate, which would then be targeted to the Mpf apparatus, via

interaction between the relaxase and the coupling protein, for transfer to the recipient cell. Whether or not the transferring plasmid molecule is maintained at these positions remains to be determined.

The appearance of R751 DNA in recipient cells during mating was visualized using donor cells containing R751:: *lacO* and recipient cells expressing the GFP-LacI fusion. Distinct, single fluorescent foci, indicative of DNA transfer, appeared in the recipient cells in as little as 18 minutes after mixing donor and recipient (Figure 4-4). The transferred DNA was not randomly distributed throughout the recipient cells but rather was localized either at the cell center or the quarter position in the cell.

It should be noted that the plasmid is transferred from the donor as a single-stranded DNA molecule that is converted to double-stranded DNA as it enters the recipient (218). Since GFP-LacI recognizes only double-stranded DNA, no conclusions can be made about the site of DNA entry or where it is initially duplicated in the recipient cell. However, it is probable that the GFP foci first observed represent transferred plasmid DNA immediately after complementary strand synthesis. Thus, it is likely that the positioning of newly synthesized double-stranded plasmids at the mid-cell or quarter-cell positions reflects their rapid entry into vegetative replication. One possibility is that sites of entry are random and that replication complexes form at these sites and then move to specific sites in the cell. Alternatively, the incoming DNA may be rapidly targeted to established replication factories, which have been demonstrated to occupy positions located at the cell mid- or quarter-cell positions (114).

An important question raised by these observations is how the single-stranded plasmid molecule is targeted to either the mid- or quarter-cell positions prior to becoming double stranded? Although there is little data to explain how this happens, two possibilities could be envisioned. First, the incoming DNA could diffuse rapidly to either the mid- or quarter-cell positions. An alternative and more attractive model would be that the single-stranded DNA may be guided to these locations as a nucleoprotein complex. An obvious candidate would be the relaxosome complex. The relaxosome is known to exist in the donor, however, it has yet to be demonstrated to exist in the recipient. Another candidate would be a nucleoprotein complex comprised of the IncP encoded primase, TraC, and the T-strand. TraC is transferred to the recipient via the

conjugative apparatus and is believed to instigate complementary strand synthesis by generating primers that initiate lagging strand synthesis (172).

Shortly (10 to 12 minutes) after their appearance in recipient cells, individual foci were seen to duplicate, producing two foci, which migrated slowly apart resulting in an asymmetric localization pattern that is characteristic of partitioning deficient plasmids (95, 148). This is most likely due to the initial absence of the plasmid-encoded partition machinery in the recipient cell. The observation that the majority of foci in transconjugants are symmetrically positioned, 120 minutes after Mpf, suggests that the partition machinery is fully established by this time.

A central premise of conjugative transfer is that donor and recipient are in close physical contact, although there is evidence that direct contact is not essential (80). In order to address this issue with living cells, the unique ability of the GFP-LacI technique to identify individual mating pairs was exploited, allowing for the distance between donor and recipient cells to be monitored. In these studies transconjugants were only observed when in direct contact with donor cells, thus supporting the notion that intimate contact between mating pairs is a prerequisite for DNA transfer. The regions of intimate contact between donors and recipients most likely contain the same type of conjugative junctions that were observed between *E. coli* donors and recipients with electron microscopy (44, 177).

It was also noted that the connections between mating cells occur at various positions along the pole or lateral walls of both donor and recipient cells. RP4-encoded conjugative junctions were also located at any membrane surface between fixed donor and recipient cells (177). This implies that mating pores can be formed at virtually any point in the cell membrane of donors and DNA can be transferred into any available location along the recipient membrane. Such a view is consistent with recent observations that proteins involved in DNA transfer, encoded by plasmids RP4 (IncP α) and R27 (IncHI1), are localized non-specifically throughout the length of the cell membrane (63, 69). A likely model is that each donor cell contains several mating pores, all of which are potentially viable, but only one becomes active when it successfully docks with a recipient cell, an essentially random event.

Chapter 5

General Discussion

5 General Discussion

This thesis has focused on two aspects of conjugation in gram-negative bacteria: 1) the conjugative apparatus of the IncHI1 plasmid R27 and 2) the movements and localizations of R27 and R751 (IncP β) during both the vegetative cycle and conjugative cycle.

In Chapter 2, the essential components of the complete conjugative transfer system of the IncHI1 plasmid R27 were identified. Functional and computer analysis categorized the transfer system into T4SS/Mpf components, relaxosome components, the coupling protein or putative regulatory components. As only the F ((IncF) (56) and references within), RP4 (IncP α) (76) and R64 (IncI1) (105) transfer systems have been characterized in this manner, this work establishes R27 as a model conjugative system and provides a foundation for more in depth studies on the R27 transfer system.

In Chapters 3 and 4, a method to label plasmid molecules with GFP was used to visualize plasmid molecules. Conjugative plasmids reside in clusters at specific regions of the donor cell due to the active partitioning apparatus. During conjugative transfer single-stranded DNA (ssDNA) appears to be able to exit any membrane region of the donor cell and enter the recipient at any membrane region through regions of intimate contact between donor and recipient cells. The transferred ssDNA is targeted to the host replisome for replication. These experiments mark the first time both mating pairs and plasmid DNA have been visualized during conjugative transfer.

This discussion will initially cover each of these aspects of conjugation separately in the sections: 5.1) **T4SS** which will discuss the T4SS components, evolution, ecology and mechanism of the H/F-like Mpf/T4SS and 5.2) **Plasmid Behaviour** which discusses the DNA processing reactions in the context of the route(s) by which the transferring DNA strand takes during transfer from donor to recipient during conjugation. Both of these topics will be combined to refine the model of conjugative transfer, which will be used to define key steps in the conjugative cycle in gram-negative bacteria using cell biology.

5.1 T4SS

5.1.1 Mpf System of R27 and F Define a T4SS Subfamily

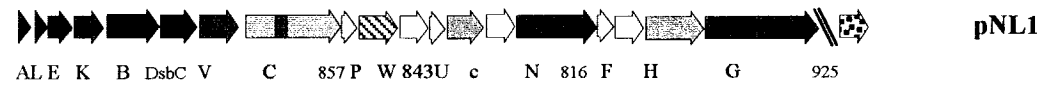
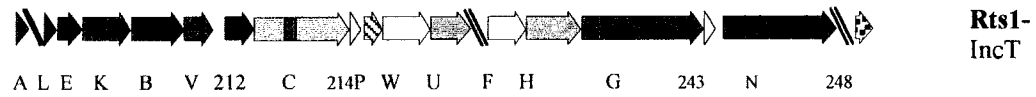
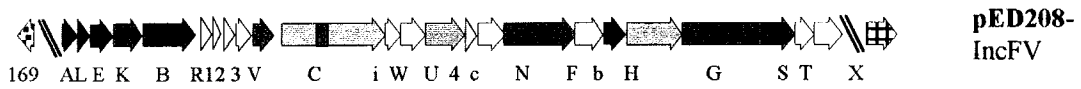
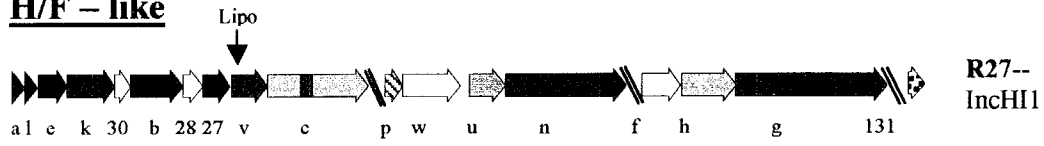
T4SS were once viewed as highly conserved molecular machines. However, with the accumulation of genome sequences and the careful analysis of several model T4SS, it has become apparent that there exist at least three different T4SS subfamilies: F-like, P-like and I-like (31, 109, 111)(Figure 5-1). The comparison of the complete transfer system of R27 to other systems illustrates that the T4SS of R27 and F each contain the same essential components, therefore defining the H/F-T4SS subfamily, which also includes the T4SS from IncT (Rts1), IncJ (R391), IncHI2 (R478) and pNL1 plasmids and the SXT element (Figure 5-1) (111). The essential components of the H/F-T4SS differs in significant ways from P-like systems such as those encoded by IncP, IncW and IncN plasmids and the VirB T4SS of the Ti plasmid (Figure 5-1) (111). These differences translate into different pilus structures which correlate with differences in mating efficiencies of these transfer systems in liquid and on solid media. The differences between H/F- and P-like T4SS suggest a specialization which may be related to the ecological nature of these transfer systems. In addition, the comparison of the T4SS also allowed for the identification of the conserved components of both H/F-like and P-like T4SS, which will be used to define the core components of the conjugative pore. A discussion of each of these observations will follow the overview of the essential H/F-like T4SS components presented below.

5.1.2 H/F-Like T4SS Components

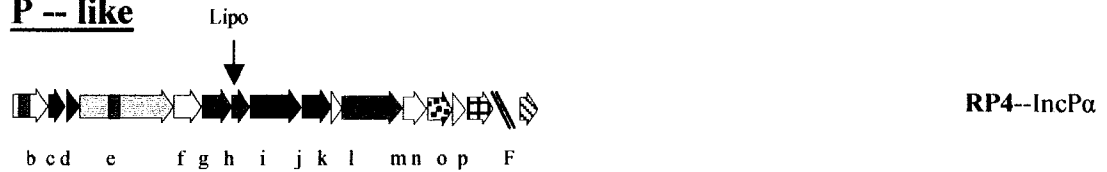
The essential components of the H/F-like T4SS are defined as those Mpf proteins that are essential for conjugation, as determined by mutagenesis and complementation experiments of both R27 and the F factor (56, 108, 109, 111). Results obtained from investigations into individual transfer proteins from both the R27 and the F factor T4SS are combined to create transfer protein families in this overview, as it is likely that homologs are functionally equivalent and contribute to the T4SS in a similar manner. Figure 5-2 is a representative model of the H/F conjugative pore based on the available information from investigations into the R27 and the F factor transfer proteins. Based on work on the F factor, these proteins are organized according to three proposed functions:

Figure 5-1. Comparison of H/F-like T4SS with each other and with P- and I-like T4SS. Transfer genes are presented with color/pattern, with the same color/pattern representing homologous gene products (See Table 5-1), while non-essential transfer genes are white. Light gray genes represent transfer gene products with no shared homology to other T4SS subfamilies. Lipo=lipoprotein motif; Red box=Walker A motif; Upper case gene names=Tra; Lower case gene names=Trb (F, pNL1 and RP4) or Trh (R27). Double slash indicates non-contiguous regions. The gene sizes are relative to each other. Maps were produced using the indicated GenBank accession number: F-NC002483; pED208-AY046069; R27-NC002305; Rts1-NC_003905; pNL1-NC_002033; R391- AY090559; SXT-AY055428; RP4-NC001621; R64-AB027308. See text for details and references.

H/F -- like



P -- like



I -- like

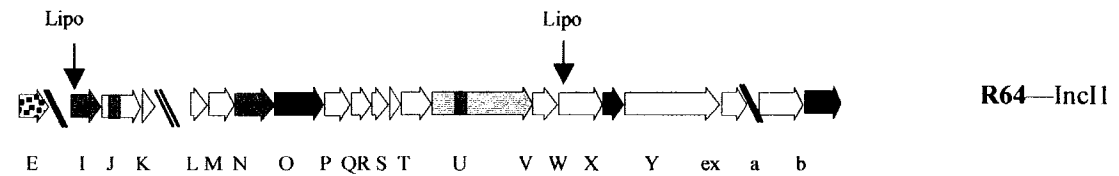


Figure 5-2. A representation of the H/F-like T4SS transfer apparatus. The pilus is shown as assembled with TraA (pilin) subunits extending from the inner membrane through a putative secretin-like outer membrane pore formed by TraK. TraK is anchored by TraV and interacts with TraB in the inner membrane. TraB interacts with the coupling protein creating a continuous pore from the cytoplasm thru the cell envelope to the extra-cellular environment. Inner membrane proteins TraL and TraE are shown interacting with TraC at the pilus base, where it may drive pilus assembly in an energy-dependent manner. TraC also interacts with TraB. The mating pair formation (Mpf) proteins include TraG and TraN which aid in mating pair stabilization (Mps). TraF,H,U,W and TrbC, which together with TraN are specific to H/F-like systems and might have a role in pilus retraction, pore formation and mating pair stabilization.

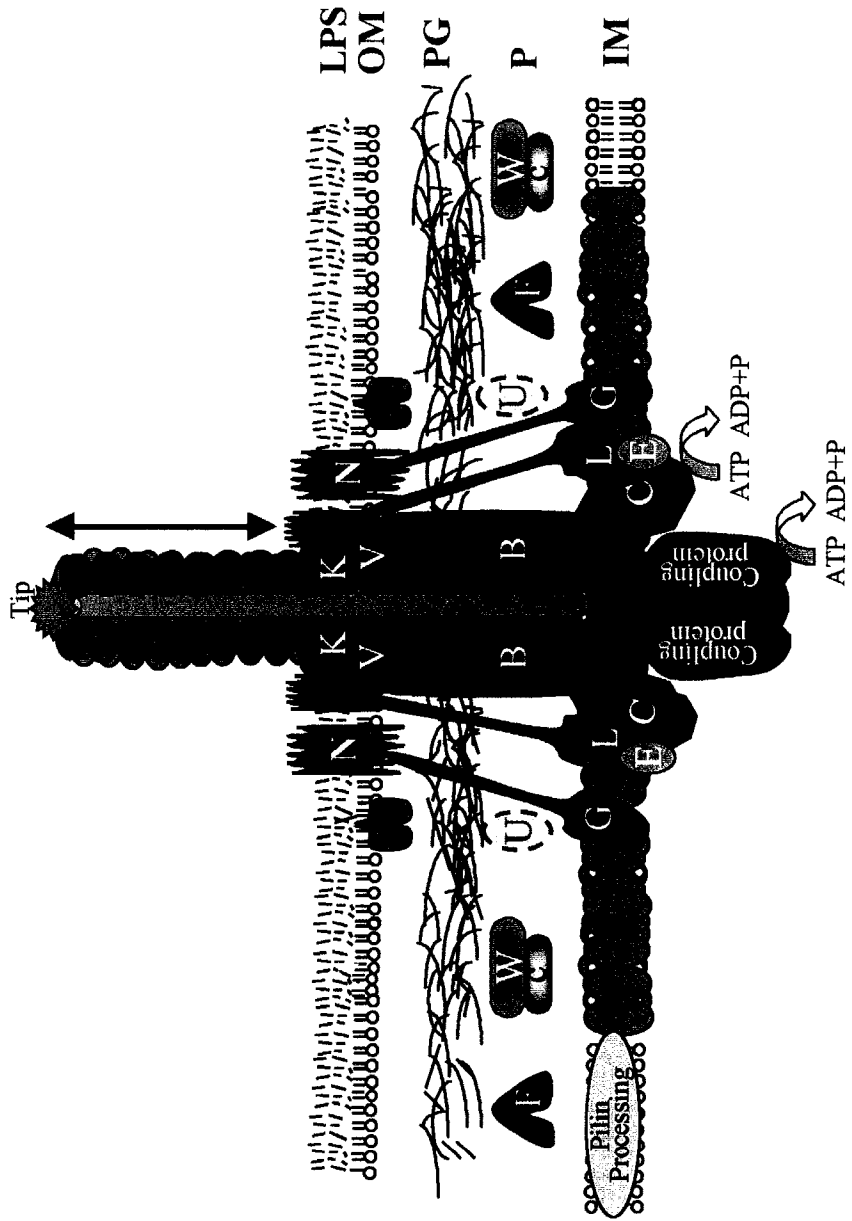


Table 5-1. Summary of conserved H/F-like T4SS components. Shaded components indicate homology to P-like T4SS.

R27 ^a T4SS Protein	IncF Homolog	IncP Homolog ^d	IncI homolog ^d	Size Range ^e (aa)	Cellular Location(s) ^f	Motifs ^g	Proposed Function	Interacting partners in F and P-like T4SS ^h	Interaction reference
TrhA	TraA	TrbC/VirB2	TraX	112-128	IM, E		Pilin	TraX _F , TraQ _F	81
TrhL	TraL	TrbD/VirB3		93-105	IM			TrhC _H	62
TrhE	TraE	TrbJ/VirB5		130-261	IM/P			TrhC _H	62
TrhK	TraK	TrbG/VirB9	TraN	299-410	P/OM	Secretin	Pore	TraB _F , TraV _F	80
TrhB	TraB	TrbI/VirB10	TraO	429-475	IM/P	Coiled-coil	Pore	TraK _F , TrhC _H , coupling protein _H	61, 80
TrhV	TraV	TrbH/VirB7	TraI	171-316	OM	Lipoprotein	Pore	TraK _F	80
TrhC	TraC	TrbE/VirB4	TraU	799-893	IM	ATPase	Secretion	TrhB _H , TrhE _H , TrhL _H	62
TrhG	TraG	TrbL/VirB6		912-1329	IM/P		Mating pair stabilization	TraS _F	7
TrhP ^b		TraF		150-368	IM	peptidase	Transfer peptidase		
TrhW ^c	TraW ^c			210-502	P			TrbC	
	TrbC		TrbB	203-254	P			TraW	
TrhU	TraU			330-358	P		DNA transfer		
TrhN	TraN			602-1230	OM	cysteine rich	Mating pair stabilization Adhesin		
TrhF	TraF			257-363	P	Disulfide Isomerase	Disulfide bond formation		
TrhH	TraH			453-501	OM	Coiled-coil			
Orf130	Orf169			169-265	IM	Lysozyme	transglycosalase		
Orf027	TrbB			230-298	P	Disulfide Isomerase	Disulfide bond formation		

^a Nomenclature according to the that designated in Chapter 2.

^b R27, Rts1, R391, SXT and pNL1 systems each contain a peptidase with the peptidase of pNL1 containing an N-terminal fusion to TrbI, suggesting a coupled function. F and pED208 do not contain peptidases.

^c R27, Rts1, R391, SXT systems TrbC is fused to the N-terminus of TraW, suggesting a coupled function, whereas they are separate proteins in F and pED208.

^d Homology deduced based on similarity identified with PSI-BLAST analysis or functional analogy.

^e Range is determined by comparing homologs in R27, F, pED208, Rts1, R391, SXT and pNL1.

^f Inner membrane (IM), periplasm (P), outer membrane (OM) and extracellular (E).

^g Motifs identified with ScanProsite (<http://ca.expasy.org/tools/scanprosite/>), CDD (<http://www.ncbi.nlm.nih.gov/BLAST/>) or Coils (http://www.ch.embnet.org/software/COILS_form.html).

^h Transfer system in which interaction identified is indicated with subscript.

1) pilin and pilin processing, 2) pilus tip formation and pilus extension and 3) mating pair stabilization (56). Other conserved but non-essential components of H/F-like T4SS are TrbB, a putative thioredoxin homologue, and Orf169, a lytic transglycosylase (Figure 5-1 and 5-2 and Table 5-1). It should be noted that each of the R27 T4SS genes has been named after the F counterpart except that R27 genes were named *trh* instead of *tra*. For historical reasons each protein family described below has been named Tra, reflecting the F factor as the progenitor system. Where needed the plasmid origin of the transfer protein will be indicated with a subscript (i.e. Trh_{C_H} would indicate TrhC from IncH plasmids).

5.1.2.1 H/F-Like T4SS Propilin Processing

The propilin subunits from H/F-like T4SS range in size from 112-128 aa (Table 5-1). The pilin subunit is poorly conserved among T4SS, for example the pilin subunit of the R27 shares more similarity with the IncP pilin than with the IncF pilin (109). All propilin subunits contain a long leader sequence that is either known or predicted to be cleaved by the host leader peptidase, LepB, to produce a peptide of 68-78aa (129, 130). After removal of the signal sequence, the F pilin subunit is oriented such that both the N- and C-terminus are positioned into the periplasm (82, 131). Indeed, all pilin subunits of the H/F-T4SS, characterized and uncharacterized, contain two hydrophobic regions that could serve as transmembrane regions. Pilin subunits typically undergo an additional processing reaction, which, so far, have been identified as acetylation in F-like pilins (F, R1, R100-1, pED208) (132) or cyclization in P-like pilins (RP4 and Ti) (47).

Each system within the H/F-like T4SS contains a known or putative pilin-processing protein that is either an acetylase (F, pED208) or peptidase (R27, Rts1, R391, SXT and pNL1). F pilin acetylase, TraX, acetylates the N-terminus of F pilin after it is inserted into the inner membrane (132). By analogy to P-like propilin processing (48), the propilin subunits of R27, Rts1, R391, SXT and pNL1 are likely cleaved at the C-terminus and possibly cyclized by the transfer peptidase, although this has yet to be demonstrated. Pilin insertion into the membrane and the subsequent maturation are the first steps in pilus production. Assembly of conjugative pili on the bacterial surface is

determined by the remainder of the T4SS (except the C-terminal region of TraG and TraN and TraU proteins). F pilin subunits are stored as a pool in the inner membrane prior to assembly on the cell surface (143). Pili are assembled by addition of pilin subunits to the base of the pilus, as demonstrated for H-pili of R27 (127). In response to contacting a suitable recipient, it is likely that pilus retraction proceeds in reverse to extension, in an energy independent manner, so that the pilin subunits would be returned to the inner membrane pool and possibly serve as part of the conjugative pore.

The lack of sequence conservation in pilin sequence could be due to: i) rapid evolution of the pilin subunits in response to strong selective forces of extra-cellular factors such as phage and receptors on recipients and/or ii) lateral gene transfer of F-like (acetylase) and P-like (peptidase) propilin and processing genes between T4SS subfamilies.

5.1.2.2 H/F-Like T4SS Pilus Assembly

R27 and F mutants in *traL*, *E*, *K*, *B*, *V*, *C*, *W*, *F*, *H*, and the N-terminus of *traG* (only performed in F) generate broadly similar phenotypes, which include the inability to assemble pili and transfer DNA (56, 108, 109). Using a sensitive M13K07 phage (binds to the pilus tip) transducing assay, Anthony *et al.* (7) identified two F factor mutant subgroups: a) those mutations which prevent pilus tip formation on the cell surface (*traL*, *E*, *K*, *C*, *G*) and b) those that allow tip formation but block pilus extension (*traB*, *V*, *W*, *F*, *H*). These observations imply that pilus production follows two steps: the formation of the pilus tip on the cell surface followed by extension of the tip to form an extended pilus. This provided the first example in any T4SS of a differentiation of roles for Mpf proteins and serves as a basis of identifying the roles, individually and collectively, of the T4SS components. The H/F-like T4SS components will be organized according to these results (Table 5-1).

5.1.2.2.1 Pilus Tip Formation

The M13 F-pilus bacteriophage binds specifically to the pilus tip and not to the pilus sides (7, 179). Based on these observations, it has been proposed that the long

flexible conjugative pili encoded by the F factor contain a tip receptor or an epitope that is distinct from the shaft or sides of the pilus (131). The tip may be composed of a protein other than the pilin subunit. Alternatively, the distinctive epitope at the tip of the may be due to a differently exposed surface of the pilin subunit at the curvature of the tip. Regardless, the differential binding of the M13 phage to the tip was exploited in determining which transfer proteins were required to progress pilus assembly so that only the pilus tip is exposed on the donor's surface (7, 179) (Table 5-1).

TraL Members of the TraL family range in size from 93-105 amino acids (aa) and are homologous to TrbD_P (103 aa) and VirB3_{Ti} (108 aa) (188). TraL is predicted to localize to the inner membrane, as is TrbD_P (69). TrhL_H of the R27 was shown to be essential for the formation of TrhC_H complexes, indicating either a direct or indirect interaction between TrhL_H and TrhC_H (63).

TraE TraE family members range in size from 130-261 aa and are homologous to TrbJ_P (258 aa) and VirB5_{Ti} (220 aa) (56). They are predicted to be located in the inner membrane, as has been shown for TrbJ_P (RP4)(69). TrhE_H of R27 was shown to be essential for the formation of TrhC_H complexes (63).

TraK The TraK family of proteins range in size from 299-410 aa and are homologous to TrbG_P (297 aa), VirB9_{Ti} (293 aa) and TraN_I (327 aa). TraK-like proteins are predicted to be located in the periplasm and outer membrane (56, 81). This protein family shares similarity to secretin proteins (Figure 2-5), specifically the HrcC subgroup as exemplified by *Pseudomonas syringae*. TraK proteins are conserved in both the β -domain and S-domain of the prototypical secretin PulD of *Klebsiella oxytoca*. The β -domain is present in all secretins and is proposed to be embedded within the outer membrane to form the typical ring structure of secretins. The S-domain is a region of 60 aa that binds to a lipoprotein which serves as a periplasmic chaperone (72). The presence of a secretin within T4SS suggests a mechanism by which both pilus and DNA could transverse the outer membrane. The C-terminus of TraK_F has been shown to interact with TraV_F, a

lipoprotein, and the N-terminus of TraK_F interacts with TraB_F, an inner membrane protein (81). The TraB-TraK-TraV_F complex likely forms an envelope spanning structure similar to that of VirB10-VirB9-VirB7 from the Ti plasmid T4SS (10).

TraC Members of the TraC family of proteins range in size from 799-893 aa and are homologous to TrbE_P (852 aa), VirB4_{Ti} (788 aa) and TraU_I (1014 aa). TraC proteins are predicted to have a peripheral inner membrane localization (63, 180). All members of this protein family contain both Walker A and Walker B motifs, suggesting they energize conjugation, possibly pilus assembly (27), although the importance of these motifs has yet to be demonstrated. Using TrhC-GFP fusions, TrhC_H of R27 was shown to form complexes, possibly containing other transfer proteins in the inner membrane. The formation of TrhC-GFP complexes was dependent on the presence of TrhB_H, E_H and L_H, suggesting either a direct or indirect interaction between these proteins (63).

TraG TraG proteins range in size from 913-1329 aa. The N-terminus is homologous with TrbL_P (528 aa) and VirB6_{Ti} (295 aa), both of which are also predicted to contain multiple transmembrane regions and are essential for pilus biosynthesis (W. Klimke and L.S. Frost, unpublished observations), whereas the C-terminus appears to be specific to the H/F T4SS (see below). TraG proteins have two roles in conjugation — the N-terminus is involved in pilus tip formation and pilus assembly and the C-terminus is involved in mating pair stabilization (55) (see below). The N-terminal 500-600 aa is proposed to be localized in the inner membrane and contains 6-8 transmembrane regions, whereas the remaining C-terminal region is predicted to be located within the periplasmic space.

5.1.2.2.2 *Pilus Extension*

IncH and F plasmids (as well as IncJ and T plasmids) specify long flexible conjugative pili ranging in size between 2 and 20 μm (23), about 1 to 10 times longer than a typical laboratory grown *E. coli* cell. Listed below are 5 transfer proteins which

are required to extend the pilus from the cell surface, the stage preceding tip formation (7) (Table 5-1).

TraB Members of the TraB protein family range in size from 429-475 aa and are homologous to TrbI_P (463 aa), VirB10_{Ti} (377 aa) and TraO_I (429 aa) within their C-terminal regions. The N-terminal regions contain coiled-coiled domains, which are probably involved in multimerization, and a proline rich domain, which suggests an extended structure (7, 62). TraB proteins are predicted to contain an N-terminal anchor with the bulk of the protein located within the periplasm. TrhB_H of R27 was recently shown to interact with itself and the coupling protein TraG_H (62). Therefore the coupling protein “couples” TraB of the T4SS to the relaxosome.

TraF The TraF protein family ranges in size from 257-363 aa and are unique to the H/F-T4SS. These proteins share similarity to the thioredoxin superfamily, characterized by the C-X-X-C motif and a thioredoxin fold (B. Hazes, unpublished data). Since TraF is localized to the periplasmic space these proteins likely play a role in thiol redox chemistry within the periplasm, possibly involving disulfide bond formation or isomerization. It is interesting to note that several T4SS components localized to the periplasm contain multiple cysteine residues (102). In addition, it has been proposed that members of this protein superfamily act as chaperones (33). In light of these observations, perhaps TraF proteins are key to the disulfide bond chemistry of H/F-like T4SS.

TraH TraH proteins range in size from 453-501 aa and are unique to the H/F-like T4SS subfamily. Members of the TraH protein family are localized to the periplasm/outer membrane (134) and contain C-terminal coiled-coil domains, suggesting the formation of higher order structures, either with other TraH molecules or other components of the T4SS.

TraW-TrbC Members of the TraW protein family range in size from 210-502 aa and are unique to the H/F-like T4SS subfamily. TraW and TrbC are two separate proteins in F, pED208 and pNL1, whereas TrbC is fused to the N-terminus of TraW proteins from R27, Rts1, R391 and SXT. The fusion of TrbC to TraW may suggest that the functions of these proteins are coupled. Both proteins are proposed to be located in the periplasmic space.

TraV TraV-like proteins range in size from 171-316 aa. Although TraV proteins share no similarity to TrbH_P (160 aa), VirB7_{Ti} (55 aa) or TraI_I (272 aa) they are functional analogs based on their lipoprotein nature. In addition, TraV_F has been shown to interact with TraK_F, the putative secretin, and VirB7_{Ti} is known to interact with VirB9_{Ti} (11). TraV proteins likely stabilize the secretin structure within the outer membrane.

5.1.2.3 H/F-Like T4SS Mating Pair Stabilization

Mating pair stabilization (Mps) is a unique feature of H/F-like T4SS and is believed to be at least partially responsible for facilitating DNA transfer in liquid environments (55, 103). Mps occurs after both initial contact between donor and recipient and conjugal DNA synthesis and before DNA transfer, for which Mps is required (100). The gene products responsible for Mps will be discussed individually.

TraG The C-terminus of TraG is involved in mating pair stabilization. This region is predicted to be located within the periplasmic space and has been proposed to interact with TraN to stabilize mating pairs. A second C-terminal product TraG_F, which is believed to be a cleavage product of the full-length protein, has been detected in the periplasm (55). TraG_F is involved in entry exclusion, a process by which DNA synthesis and transport from the donor cell is blocked by TraS_F in the inner membrane of the recipient cell. TraG_F function in this regard is plasmid specific for TraS_F and this specificity maps to the C-terminal domain of TraG_F (L.S. Frost, unpublished observation).

TraN TraN-like proteins are 602-1230 aa long and are unique to H/F-like T4SS. This family of proteins is referred to as “adhesins” as they are present in the outer membranes of donors and interact directly with recipient cells to stabilize the mating pairs prior to DNA transfer (103). The N- and C-termini of TraN proteins are highly conserved whereas the central region displays extensive divergence. The central variable region of TraN_F has been shown to interact with LPS and OmpA of recipients (103). This interaction, however, is not universal since the closely related TraN_{R100} does not interact with the same targets. It has been proposed that TraN proteins interact with other yet unidentified T4SS components (103).

TraU Members of the TraU protein family range in size from 330-358 aa and are unique to the H/F-like T4SS subfamily. TraU is a periplasmic protein which is essential for DNA transfer but not for formation of conjugative pili (109), as 20% of donors containing F *traU* mutations produced F-pili. TraU is therefore proposed to be involved in DNA transfer and may play a secondary role in pilus assembly (109, 142). The latter observation implies that TraU might have a role in mating pair stabilization since mutations in *traU*, *G* and *N* have the same phenotype, that ability to produce pili but not transfer DNA.

5.1.3 Relationships between H/F and P T4SS

The T4SS subfamilies share a common core of components, reflecting their common evolutionary origin, yet each subfamily contains distinct components that indicate divergent evolution. Based on protein similarity, the common core components shared between H/F-like and P-like, the best understood T4SS subfamilies, include (F/P): TraC/TrbE (ATPase), TraB/TrbI, TraE/TrbJ, TraL/TrbD, TraK/TrbG (secretin) and TraG(N-term.)/TrbL. Additional core components can be assigned based on functional analogies: TraV/TrbH (lipoprotein) and TraA/TrbC (pilin subunits and the associated processing proteins) (Figure 5-1 and Table 5-1). The non-conserved, and therefore defining components, are a subset of Mpf proteins which are unique to each subfamily.

H/F-like T4SS contain TraW, U, N, TraG (C-term.), F, H and TrbC, which are not present in P-like T4SS, whereas the P-like T4SS contain TrbB (ATPase) and TrbF, which are not present in H/F-like T4SS (Figure 5-1 and Table 5-1). It is likely that the differences in the essential components represent the specialization of conjugation abilities, likely mediated by the differences in conjugative pilus structure and the mating pair stabilization proteins TraG and TraN.

It has been long been recognized that there are two types of conjugative pili, long flexible pili and short rigid pili (22). It is now evident that long flexible pili are encoded by plasmids with H/F-like T4SS (IncH, F, T, J), whereas short rigid pili are encoded by plasmids with P-like T4SS (IncP, N, W, I). It is noteworthy that in addition to the short rigid conjugative pili, IncI plasmids code for non-conjugative Type IV pili (104). The long flexible pili produced by H/F-like T4SS measure 2-20 μm and have a diameter of 8 nm with a central lumen measuring 2 nm. H and F-pili are frequently seen attached to cells and appear flexible in electron micrographs. In contrast, short rigid pili specified by P-like T4SS are seldom seen attached to donors. P-like pili measure 8-12 nm in diameter (47). The differences in pilus structure are unlikely to be dictated by differences in pilin processing, such as acetylation or cyclization, since acetylases and transfer peptidases can be present in both H/F-like and P-like T4SS.

Long flexible pili facilitate mating in liquid and on solid media with approximately equal efficiencies, whereas short rigid pili result in a surface-preferred mating phenotype (21, 22). Long flexible pili likely allow mating pairs to stabilize within the liquid milieu, therefore facilitating mating in a liquid medium. F-pili are capable of retraction (153, 154, 163), possibly in a manner reminiscent of Type IV pili encoded by Type II secretion systems (137, 190). Retraction is proposed to occur in response to a “mating signal” received from the pilus tip once it contacts a suitable recipient. In addition, the non-conserved Mpf proteins are likely responsible for the differences in mating capabilities. For example, TraN and TraG proteins of the H/F-like T4SS have been implicated in mating pair stabilization, perhaps enhancing mating in liquid by stabilizing the mating pair(s) against the shearing forces of the fluid environment.

The above observations are consistent with those made from ecologically-based studies on conjugative plasmid transfer. H/F-like T4SS are usually present on mobile

elements in enteric bacteria, which are likely to encounter both the mammalian digestive tract and raw sewage. These environments are generally nutrient rich and comprise both solids and liquids (205). Plasmids containing H/F-like T4SS have been shown to transfer in the human digestive tract (6), and are found to transfer more efficiently in aquatic environments than those containing P-like T4SS (112). In contrast, P-like T4SS are generally associated with soil organisms, such as *Pseudomonas* spp. and *Agrobacterium* spp., and have been shown to transfer efficiently in nutrient-limiting soil environments, whereas plasmids containing H/F-like T4SS were unable to transfer under identical conditions (168). It is therefore possible that the differences in the Mpf systems (H/F vs P T4SS) could reflect the difference in the ecological niche of the transfer systems.

Other conjugative elements which contain H/F-like T4SS include, besides R27 and the F factor (*E. coli*) (56), pED208 (IncFV; *S. typhi*) (124), Rts1 (IncT; *Proteus vulgaris*) (144), R391 (IncJ; *Providencia rettgeri*) (20) SXT (*Vibrio cholerae*)(12) and pNL1 (*Novosphingomonas aromaticivorans*) (174) (Figure 5-1). *Neisseria gonorrhoeae* contains an H/F-like T4SS which is not used for conjugation, but rather for the secretion of DNA (78). Notably, no H/F-like T4SS have been reported that secrete virulence factors and no H/F-like T4SS, to date, have been shown to secrete proteins (172), although it would be extremely difficult to detect transfer of a small number of proteins.

Conjugative elements which contain P-like T4SS include RP4 (IncP α ; *Pseudomonas aeruginosa*) (158), R751 (IncP β ; *Klebsiella*) (201), pKM101 (IncN; *S. typhimurium*) (215) and R388 (IncW; Accession No. X81123) (see (31)). In many respects, P-like T4SS appear to be capable of transferring/secretion/taking up a broader repertoire of molecules. For example, IncP and IncI plasmids are also known to transfer TraC and Sog, DNA primases respectively, from donor to recipient (172). As noted above, *H. pylori* utilizes a subset of the P-like T4SS for DNA uptake (88). Many pathogens use P-like T4SS to secrete virulence factors into hosts as proteins or nucleoprotein complexes, such as the T-DNA of the Ti plasmid (220), CagA of *H. pylori* (9, 183, 193) and pertussis toxin of *Bordetella pertussis* (36, 211). It is noteworthy that conjugative plasmids containing the P-like T4SS are broad host-range (IncP, W and N)(73). In addition to the differences in pilus structure between H/F and P-like T4SS, the

ability of P-like T4SS to secrete both DNA and protein to a broader range of cells may also suggest another fundamental difference between these T4SS families.

5.1.4 The Core of the Conjugative Pore

The nature of the conjugative pore is a question central to conjugation, as well as to the biology of T4SS, and we have only recently begun to understand how single-stranded DNA can transverse the membrane of donor cells. At the inner face of the pore are coupling proteins, which are present in all conjugative transfer systems (122). This information is reviewed here. Coupling proteins are inner membrane proteins that are known to couple, or recruit, the cytoplasmic relaxosome to the membrane-associated T4SS/Mpf (26, 77). More recently, direct interactions between relaxase and coupling proteins has been demonstrated (182, 195). The crystal structure of TrwB, the coupling protein of the IncW plasmid R388, has been determined (65). TrwB contains a large hexahomomeric spherical cytoplasmic domain, resembling DNA ring helicases and F1-ATPases in structure (64). The protein forms a central channel that crosses the inner membrane and measures 2 nm in width, which could easily accommodate a single strand of DNA (1 nm). Llosa *et al.* (122) have recently proposed that the coupling protein uses ATP hydrolysis to energize the “pumping” of DNA through the coupling protein channel.

Recently, the coupling protein of R27, TraG_H, has been shown to interact with the N-terminus of TrhB_H, a member of the TraB family (62). TrhB_H was also shown to form multimers, possibly forming a ring structure which could extend the pore of the coupling protein into the periplasmic space (62). TraB_F of the F factor was recently shown to interact with TraK_F, which in turn interacts with TraV_F, a stabilizing lipoprotein (81). Using PSI-BLAST it was found that the TraK family of proteins share homology to secretins (Figure 2-5), which are known to form outer membrane rings that allow the passage of macromolecules (150, 151). A TraK secretin structure could extend the conjugative pore from TraB through the outer membrane, although this needs to be demonstrated experimentally.

Consistent with the idea that TraB, K and V form the core of the pore which transfers DNA, expression of VirB3, 4, 7, 8, 9 and 10 in *A. tumefaciens* recipients increased the efficiency of RSF1010 transfer (18). This suggests that the presence of

these proteins within recipients aids the transferring DNA in reaching the cytoplasm. Since all of these VirB proteins, except VirB8, have a homolog/analog in H/F-like T4SS, including the core of the putative pore (TraB, K and V; Table 5-1), it is likely that the pore extends from the donor outer membrane to the recipient cytoplasm. Consistent with this proposal, homologs of VirB7-10 have been shown to be responsible for DNA uptake by *Helicobacter pylori* (88), illustrating that these proteins likely represent the minimal membrane-spanning pore for DNA transfer.

Although these observations suggest a mechanism by which DNA can transverse the donor envelope (Figure 5-2), the mechanism by which the DNA transverses the recipient envelope to gain access to the cytoplasm remains a key question. It is possible that TraB, K, V (or VirB7-10) proteins are transferred into the recipient and form a conjugative pore in the recipient that interacts directly with the donor pore, such that the putative secretins of donor and recipient form a complex. This would create a continuous conduit from the donor to recipient cytoplasm. Alternatively, DNA could transfer through the pilus, which is situated within the conjugative pore, and the pilus could penetrate the recipient envelope and deposit the DNA directly within the recipient cytoplasm. The later idea is conceivable in light of the finding by Jin and He (97, 98), who visualized protein secretion from the tip of Type III secretion system pili. This observation implies that the pilus can serve as a conduit for macromolecular trafficking. It is therefore conceivable that DNA, possibly as a nucleoprotein complex, could also be transferred through the conjugative pilus.

5.2 Plasmid Behaviour

5.2.1 Vegetative Cycle vs. Conjugative Cycle

In the past few years prokaryotic biologists have utilized cell biology techniques in addressing key questions concerning fundamental processes in bacteria, such as cell division and DNA segregation. The results have transformed our view of the bacterial cell to a highly organized and dynamic organism. Bacterial low-copy number (1-2 copies per *oriC*), narrow host-range plasmids (F, P1, R1, R27) and moderate-copy number (6-8 copies per *oriC*), broad-host range plasmids (RK2, R751) reside at well-defined positions

located at the mid and quarter-cell positions of *E. coli* throughout the cell-cycle (Chapter 3 and 4) (66, 95, 148, 166). The partitioning apparatus pairs plasmid molecules, forming plasmid clusters, and maintains plasmid clusters at the mid- and quarter-cell positions (67). An increase in plasmid clusters results from cluster duplication at the mid- and quarter-cell regions and subsequent movement of clusters towards opposite directions in the cell, reflecting a progression of the cell cycle. Plasmids likely replicate within the clusters, as the host replication machinery is present as a fixed assembly at these same intracellular regions (114), and plasmid cluster movement is directed by the partitioning apparatus (148). Paired plasmids are aligned by the centromere binding protein which determines the orientation for partitioning by ATPase polymerization, ensuring faithful division of the cluster molecules (96). These localizations and movements are determined by the replication and partitioning functions and are sufficient to stabilize plasmids and are therefore central to the vegetative cycle.

The localization patterns of high copy number plasmids without partitioning functions has also been investigated. The IncQ plasmid R1162 (T.D. Lawley and D.E. Taylor, unpublished observations) (copy number 10-16) and a pUC-derived plasmid (166) (copy number ~70) were both visualized with the GFP-LacI/*lacO* system. Both plasmids gave diffuse and discrete focus patterns, similar to that seen with R27 partitioning impaired plasmids (Chapter 3). The diffuse patterns likely represent individual plasmids randomly dispersed throughout the cytoplasm, whereas the discrete foci likely represent plasmid clusters. As neither of these plasmids contains partitioning functions, the clustering of plasmids may be a replication related phenomenon similar to the “handcuffing” mechanism proposed for P1 (29).

The linkage of the plasmid vegetative cycle to the bacterial cell cycle is not yet clearly understood, however, both cycles are related because the number of plasmids and plasmid foci per cell are linked to the cell growth rate. In contrast to the initiation of chromosome replication and segregation, which is highly coordinated with the cell cycle, the initiation of plasmid replication and segregation occurs randomly throughout the cell cycle (67, 87, 149). Plasmid replication and partitioning are essential for plasmid survival, whereas conjugation provides bacteria with tremendous adaptability by driving gene flow not only between prokaryotes, but also between prokaryotes and eukaryotes

(84, 207, 220). Although plasmid replication, partitioning and conjugation are each functionally independent of each other, these functions must be coordinated, such that each contributes to the successful maintenance and spread of a plasmid within a bacterial community. This is best understood in IncP plasmids, where the partitioning protein KorB (ParB/SopB partitioning homolog) also serves as a transcriptional regulator of replication and conjugation and therefore links the backbone functions to create a complex molecular circuitry (17). Since the partitioning protein equivalent, ParB, of R27 (Chapter 3) and F (Andrew Wright, personal communication) are not involved in plasmid conjugation and replication, it is not likely that such a complex molecular circuitry exists in IncHI1 and IncF plasmids, as seen in IncP plasmids.

The conjugative cycle, which is a deviation of plasmid molecules from the vegetative cycle, is when plasmid molecules undergo DNA transfer replication resulting in single-stranded plasmid DNA, or T-strand. The T-strand leaves the cytoplasm of the donor and passes through the cell envelopes of both donor and recipient bacteria, via the conjugative pore, prior to becoming established within the recipient, where the plasmid molecule re-enters the vegetative cycle. The application of cell biology techniques to plasmid biology has allowed for visualization of the localizations and movements of plasmids in *E. coli* during the cell cycle and during conjugation. These observations will be correlated with conjugal DNA processing, the conjugative pore and the host replication machinery during conjugation, in order to present an overview of the conjugative cycle from the perspective of the transferring plasmid molecule.

5.2.2 Relaxosomes and the Initiation of Transfer

DNA relaxases are responsible for both the initiation and termination (see below) of conjugation. Well characterized relaxases from gram-negative bacteria are those encoded by F (TraI), RP4 (TraI), R1162 (MobA) and R388 (TrwC) (106). These enzymes contain three conserved domains within the N-terminal region (106, 159). Domain I of IncP, IncQ and IncHI1 relaxases contains conserved tyrosine residues, which serves as the catalytic center for the DNA cleavage-rejoining reaction, whereas Domain I of the relaxase molecules encoded by R388 and F contains two conserved tyrosine residues. Domain II is involved in binding DNA in the *oriT* and domain III is proposed

to form part of the catalytic center along with domain I (159). Relaxases together with accessory proteins, which can be plasmid or host encoded, form stable nucleoprotein complexes at the *oriT*, which are referred to as relaxosomes (162).

Relaxosomes catalyze a site- and strand- specific DNA cleavage at the nick site (*nic*) within the *oriT*. Cleavage results in a covalent link between the 5' end of the DNA molecule and the conserved tyrosine residue within domain I on the relaxase. For TrwC of R388 only one of the conserved tyrosine residues can serve this function. The 3' end of the *nic* site is sequestered by the relaxosome, in an unknown manner, to maintain the superhelical nature of the plasmid molecule. In response to an unknown "mating signal" nicking and subsequent unwinding of the relaxosome complex creates the transfer intermediate, the T-strand, and results in a free 3' OH upstream of the *nic* site. Continuous extension of the 3' OH by the host replisome (162) by a rolling circle replication mechanism replaces the T-strand (49). Although it has only been shown that IncF and IncI1 plasmids transfer with 5' to 3' polarity, this is likely a general feature of bacterial conjugation in gram-negative bacteria (106).

For gram-negative relaxases three families have been described: 1) P-like relaxases (IncP, IncHI, IncT, IncJ), 2) Q-like relaxases (IncQ) and 3) F-like relaxases (IncF, IncW, IncN). Q- and F-like relaxases contain C-terminal domains that have a DNA replication-associated function that is essential for conjugation, whereas such domains are missing from P-like relaxases. The C-terminus of MobA of R1162 (IncQ) contains primase functions that are required for mobilization (85). The primase is proposed to initiate complementary strand synthesis of the T-strand in the recipient and likely facilitates the broad-host range of IncQ plasmids (85). F-like relaxases, TraI of F (IncFI) (25, 135) and TrwC of R388 (IncW) (71, 123), contain DNA helicase functions in their C-terminal region. These DNA helicases possess 5' to 3' DNA unwinding activity that produces the single-stranded T-strand for transfer (25, 71, 123, 135). Presumably, for plasmids which encode for relaxases without the DNA primases and DNA helicase, priming and unwinding are performed by a host-encoded factor.

The number of relaxase molecules per donor for F TraI (1) and R388 TrwC (F. de la Cruz, personal communication), F-like relaxases, is estimated at 800 and 1 000, respectively. RP4 TraI, a P-like relaxase, is estimated to be present at 5-10 molecules per

donor cell (E. Lanka, personal communication) but there are no numerical estimates available for the Q-like relaxase MobA (R. Meyer, personal communication). These estimates indicate that there are enough relaxase molecules for every plasmid to contain a relaxosome. For donors containing F and R388 there would be a large pool of free relaxase molecules. As plasmids containing relaxosomes are maintained in the supercoiled form, the presence of relaxosomes apparently does not affect replication and partitioning. Interestingly, GFP fusions to the C-terminus of the F-like relaxase TrwC of R388 and the P-like relaxase TraI of R27 resulted in little to no detectable signal, although both were functional for transfer (T.D. Lawley, unpublished observation). Relaxosomes exist in a nicked/un-nicked equilibrium within donor cells, such that plasmid isolation and subsequent release of the relaxosome with detergents results in a subpopulation of the plasmid molecules in the open circular form, whereas the remainder are supercoiled (32). Therefore, as plasmid molecules are undergoing vegetative replication and partitioning (i.e. the vegetative cycle), each plasmid molecule exists as a relaxosome in anticipation of a proposed “mating signal” which would trigger a transfer event, initiating the conjugative cycle.

When R751::*lacO* localization in donor cells was visualized with a GFP-LacI probe during conjugation, no deviation of plasmid foci from the characteristic mid- and quarter-cell positions was observed. This would suggest that entire plasmid foci do not move to the conjugative pore, but I was not convinced that this method was sensitive enough to detect subtle movements of a focus to the pore or to detect individual molecules migrating to the pore. Interestingly, R27 partitioning mutants and R1162, each of which were randomly located throughout the donor cytoplasm, were each transferred, implying that the transferring plasmid DNA is not confined to mid- and quarter-cell positions. These observations suggest that if the “mating signal” targets the relaxosome, then the signal must be such that it can reach throughout the cytoplasm. In addition, this observation would suggest that the transferring plasmid may migrate to the pore for transfer. Since *traD_F* (F factor coupling protein) mutants were impaired in conjugal DNA synthesis (replacement strand synthesis in the donor), this may suggest that the coupling protein is important in DNA unwinding and rolling circle replication (100). Perhaps conjugal DNA synthesis occurs in the vicinity of the coupling protein and the conjugative

pore. This would be consistent with the transferring plasmid, or region of the transferring plasmid, moving to the conjugative pore during transfer.

5.2.3 Relaxosomes and the Termination of Transfer

Termination of conjugative transfer occurs when the relaxase bound 5' end of the T-strand is rejoined to the 3' end to create a covalently-closed DNA molecule. Therefore the reconstituted *oriT* needs to be cleaved to release the T-strand from the replacement strand in the donor. Rejoining/termination is likely performed by the 5' bound relaxase, as relaxases can catalyze the rejoining reaction. Two important and related questions remain to be answered: 1) Does the relaxase pilot the T-strand into the recipient during transfer? and 2) Does the 5' linked relaxase cleave the reconstituted *oriT* or is cleavage performed by a second relaxase? Figures 5-3, 5-4 and 5-5 represent three potential models for DNA transfer and termination at the conjugative pore. The three models differ in the localization and number of relaxosomes needed for a complete transfer event and will be used to discuss these two questions. These models are based on my interpretation of previously proposed transfer and termination mechanisms, which have been considered in the context of the bacterial cell.

Model 1, which is consistent with the model proposed by Richard Meyer (164), predicts that the relaxase transfers through the conjugative pore (Figure 5-3). After rolling circle replication replaces the T-strand, a second round of replication begins and the reconstituted *oriT* is also passed through the pore. The relaxase in the recipient cleaves the reconstitutes *oriT* and rejoins the 5' and 3' ends of the T-strand. The 5' end of the replacement strand is then withdrawn into the donor. This model has two major flaws. First, although TrwC, which contains two active tyrosine residues, is capable of a second cleavage reaction while covalently bound to the 5' end of the T-strand, the RP4 relaxase, TraI, and the R1162 relaxase, MobA, which each only contain one tyrosine residue, are not capable of cleaving while covalently bound to the 5' end of the T-strand. Therefore, the cleavage of the reconstituted *oriT* cannot be performed by the transferred relaxase and a second transferred relaxase would be required for cleavage. Second, the free 5' end of the replacement strand, which would be at least partially replaced by RCR would need to be rejoined to the 3' end of the replacement strand, which would also need

Figure 5-3. Model 1 for DNA transfer and termination of conjugation in gram-negative bacteria. The model illustrates a transferring plasmid containing a relaxosome located in the vicinity of the conjugative pore in the donor cell. The conjugative pore is within the conjugative junction between donor and recipient cells, represented by tightly appressed outer membranes between the donor and recipient inner membranes. Initial captions represent the relaxosome cleaving the *nic* site and subsequent initiation of T-strand unwinding. Unwinding of the T-strand in the 5' to 3' direction is coupled to RCR to replace the T-strand. **Model 1**, which is consistent with the model proposed by Richard Meyer (164), shows the relaxase transferring through the conjugative pore. After RCR replaces the T-strand, a second round of replication begins and the reconstituted *oriT* also passes through the pore. The relaxase would cleave the reconstituted *oriT* and rejoin the 5' and 3' ends of the T-strand. The 5' end of the replacement strand is then withdrawn into the donor.

Model 1 Transferred-One Relaxosome Model

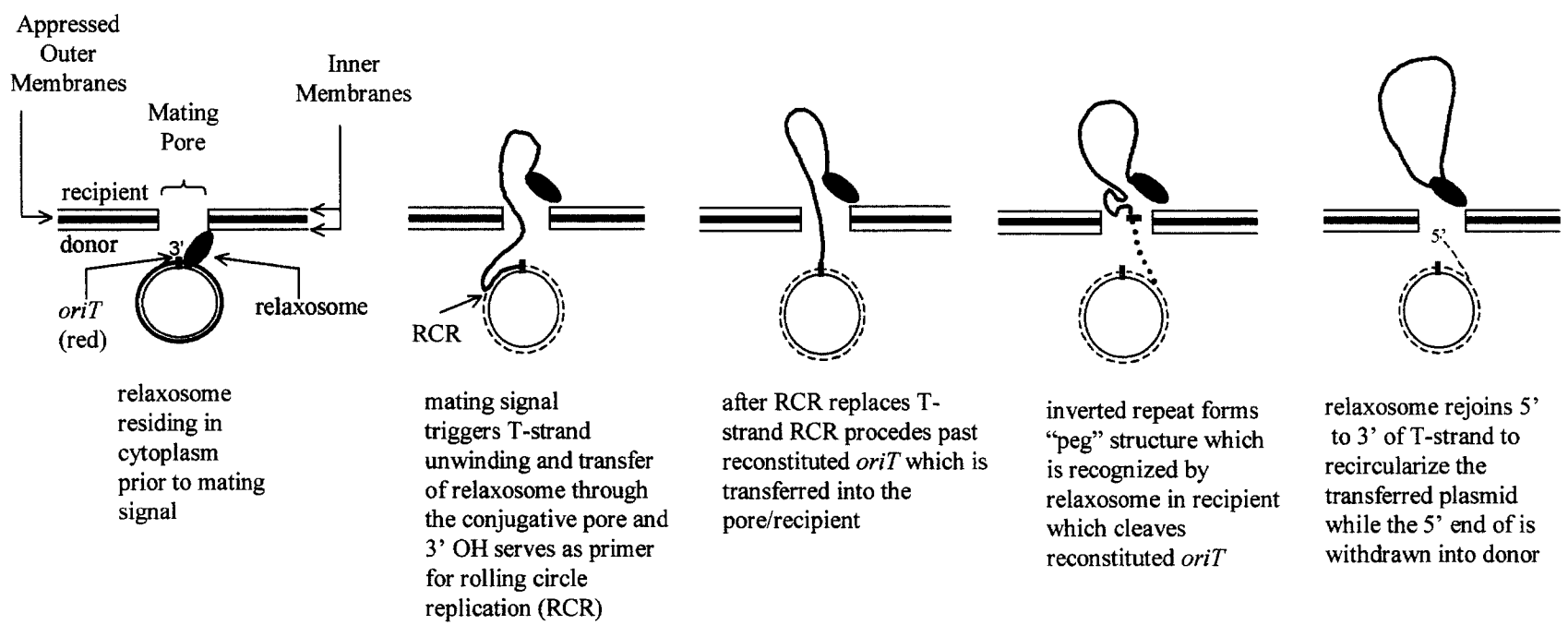


Figure 5-4. Model 2 for DNA transfer and termination of conjugation in gram-negative bacteria. The model illustrates a transferring plasmid containing a relaxosome located in the vicinity of the conjugative pore in the donor cell. The conjugative pore is within the conjugative junction between donor and recipient cells, represented by tightly appressed outer membranes between the donor and recipient inner membranes. Initial captions represent the relaxosome cleaving the *nic* site and subsequent initiation of T-strand unwinding. Unwinding of the T-strand in the 5' to 3' direction is coupled to RCR to replace the T-strand. **Model 2**, which is consistent with the model proposed by Willetts and Wilkins (214), shows the T-strand looping through the conjugative pore while the relaxosome remains in the donor. The reconstituted *oriT* is cleaved by the relaxase and the plasmid is recircularized prior to transfer into the recipient.

Model 2

Non-Transferred-One Relaxosome Model

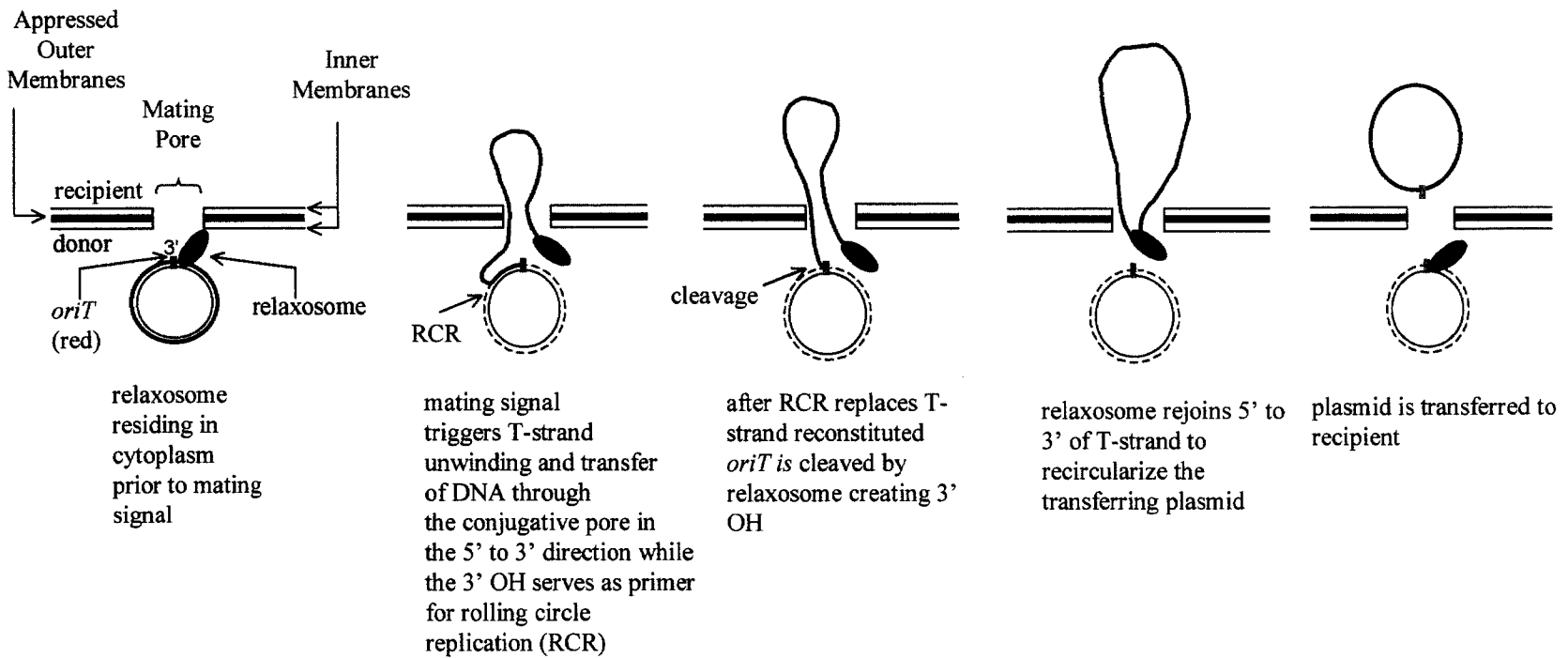
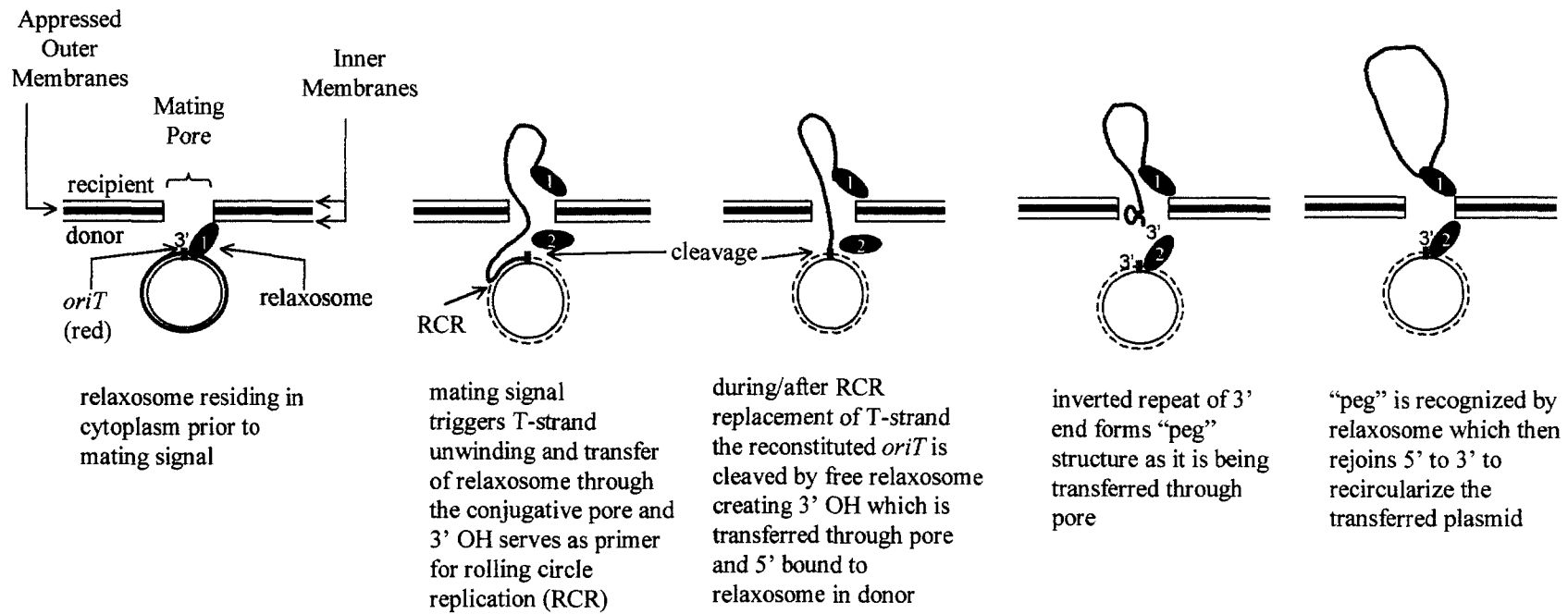


Figure 5-5. Model 3 for DNA transfer and termination of conjugation in gram-negative bacteria. The model illustrates a transferring plasmid containing a relaxosome located in the vicinity of the conjugative pore in the donor cell. The conjugative pore is within the conjugative junction between donor and recipient cells, represented by tightly appressed outer membranes between the donor and recipient inner membranes. Initial captions represent the relaxosome cleaving the *nic* site and subsequent initiation of T-strand unwinding. Unwinding of the T-strand in the 5' to 3' direction is coupled to RCR to replace the T-strand. **Model 3**, which is consistent with the two-step model proposed by Fernando de la Cruz (122), shows the relaxase transferring through the conjugative pore. A second relaxosome would cleave the reconstituted *oriT* within the donor, releasing the T-strand 3' end. The T-strand 3' end then transfers into the recipient and is rejoined to the T-strand 5' end by the relaxase, terminating transfer.

Model 3

Transferred-Two Relaxosome Model



to be cleaved. A second relaxosome in the donor would be required to fulfill these reactions. Therefore, model 1 does not account for the second cleavage in the donor or the rejoining of the replacement strand, which would be especially critical for the maintenance of low-copy number plasmids in the donor.

Model 2, which is consistent with the model proposed by Willetts and Wilkins (214), predicts that the T-strand would loop through the conjugative pore, while the relaxosome remains in the donor (Figure 5-4). The reconstituted *oriT* is cleaved by the relaxase and the plasmid is recircularized prior to transfer into the recipient. Although not predicted by this model, a second relaxosome would be required to cleave the reconstituted *oriT* prior to rejoining the ends of the T-strand, for reasons discussed in Model 1. A concern with this model is that the looping of the single-stranded DNA would promote interactions between different regions of the T-strand within the pore. Given that the conduit of the coupling protein TrwB measures only 2 nm in diameter, two strands of DNA may fit into the pore (ssDNA ~ 1 nm in width), however they would be extremely close to each other. In addition, as no single-stranded DNA binding proteins are thought to be essential for transfer, these regions are predicted to be naked single-stranded DNA. The distance between donor and recipient inner membranes, and therefore the distance that the T-strand transfers between cytoplasm, is approximately 25 nm. This means that two ~75 bp of regions of the T-strand would be in close proximity or in contact within the conjugative pore. Therefore there are topological concerns to this model, as the combination of inverted repeats and interactions between regions of homology on the T-strand would likely result in clogging of the pore.

Model 3, which is consistent with the two-step model proposed by Fernando de la Cruz (122), predicts that the relaxase is transferred through the conjugative pore (Figure 5-5). A second relaxosome, possibly from the free relaxosome pool in the donor, cleaves the reconstituted *oriT* within the donor, releasing the T-strand 3' end. The T-strand 3' end is then transferred into the recipient and is rejoined to the T-strand 5' end by the transferred relaxase, terminating transfer. All aspects of this model are consistent with what is known of T-strand transfer and relaxosomes, except that there is no evidence for relaxase transfer in conjugative systems. Demonstrating relaxase transfer will be especially difficult, as only one relaxase would be transferred per conjugation event.

Supporting the notion of relaxase transport into the recipient, VirD2, a relaxase homolog of the VirB transport system, pilots oncogenic DNA from *A. tumefaciens* into plant cells (89).

Due to the above considerations, Model 3 is the most appropriate one at this time for predicting the transfer of DNA and termination of conjugation. To verify this model, relaxase transfer into the recipient must be demonstrated, as well as the identification of the use of two relaxase molecules per conjugation event.

5.2.4 Conjugative Junctions and the Site of Transfer

Conjugative junctions are regions of tightly appressed membranes between donor and recipient cells which appear to contain the conjugative pore. The application of cell biology techniques, specifically the combination of the GFP-LacI probe and the membrane stain FM4-64, allowed the differentiation of donor, recipients and transconjugants. This novel approach enabled the first visualization of successful, individual mating pairs, as defined as a donor and transconjugant shortly after transfer. A survey of successful mating pairs demonstrated that close physical contact between donor and recipient bacteria is required for DNA transfer. In addition, regions of intimate contact representing conjugative junctions can occur at any location on the donor or recipient cell membrane. This observation demonstrates that the conjugative pore can be located at any region of the donor membrane, which is consistent with the location of Mpf/T4SS proteins (63, 69). Although it is not known how the DNA transverses the recipient membrane, these observations imply that the DNA entry point can be at any region of the recipient.

5.2.5 Establishment of Transferred Strand

Establishment of the transferred plasmid in the recipient requires the termination of transfer, producing a circular DNA molecule, and complementary strand synthesis. Complementary strand synthesis has been proposed to occur concurrently with transfer into the recipient cell, as this would minimize the exposure of the single-stranded DNA to irreparable breaks (218). Complementary strand synthesis occurs by lagging strand synthesis and therefore requires DNA primase, either host- or plasmid-encoded, as well

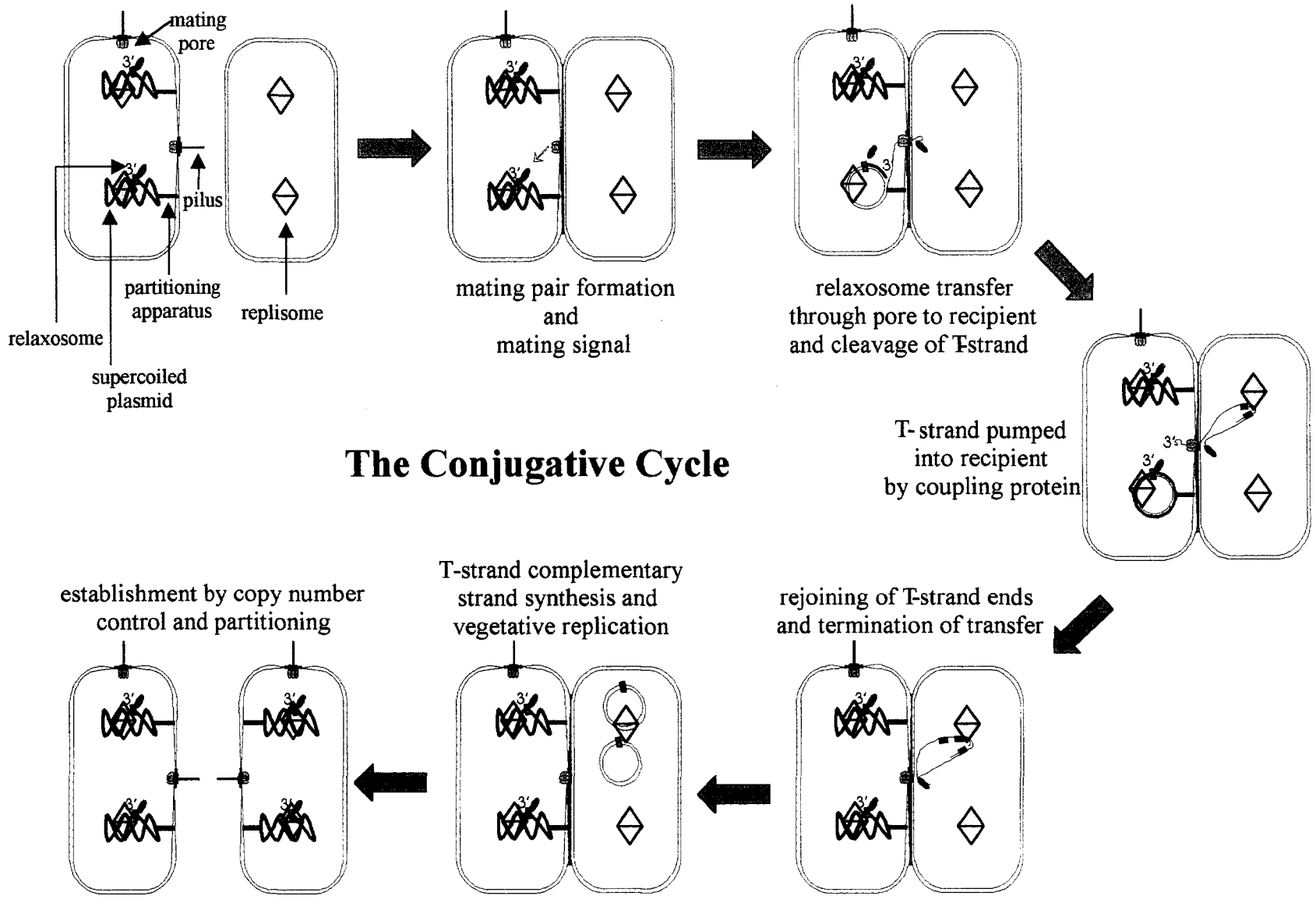
as the host replication machinery (106). IncP, IncI and IncQ plasmids encode their own primases, whereas it is presumed that the host-encoded primase primes lagging strand synthesis for plasmids which do not encode their own. Lagging strand synthesis is dependent on the host replisome, which is located at a fixed position at either the mid- or quarter-cell positions.

Monitoring the establishment of R751 with the GFP-LacI probe provided a unique opportunity to correlate known biochemical reactions (priming and replication) with cellular location. The transferred DNA is positioned at the characteristic mid- or quarter-cell position after being converted to a double-stranded molecule in the recipient cell. The maximum distance between the mating pore and the host-replisome is $\sim 0.5 \mu\text{m}$ (cell pole to quarter-cell position of $2 \mu\text{m}$ cell), which is estimated to be about 1.5 kb of DNA. It is possible that as the single-stranded DNA is entering the recipient, the DNA could also be in contact with the host replisome. Therefore, it would be physically possible for DNA entry and complementary strand synthesis to be coupled. Initial duplication of plasmids often results in an asymmetric distribution of plasmid foci, which is indicative of partitioning-deficient plasmids. Symmetric localization (either at the center or at $1/4$ and $3/4$ cell lengths) occurs only after a significant lag, presumably reflecting the time required to synthesize the plasmid-encoded partitioning proteins. At this time the plasmid is partitioning-proficient and has re-entered the vegetative cycle. The conjugative cycle would therefore be complete.

5.3 The Conjugative Cycle

The conjugative cycle (Figure 5-6) presented here applies to both narrow and broad host-range conjugative plasmids that are partitioning proficient, such as those from the IncHI1, IncP, IncF and IncW plasmid groups, transferring between *E. coli* donor and recipient cells. Such plasmids within *E. coli* encode for a partitioning apparatus, relaxosomes, conjugative pores, and conjugative pili, which distinguish donor from recipient cells in Figure 5-6. During vegetative growth, plasmids reside at the mid- and quarter- cell regions of donor cells, ensuring their vertical transmission. The role of the partitioning apparatus appears to position the plasmids near the replisome to provide

Figure 5-6. Model representing the conjugative cycle of a gram-negative bacterial plasmid transferring between *E. coli* donor and recipient bacteria. See text for details.



The Conjugative Cycle

plasmids with continuous access to replication, undoubtedly the most important aspect of the plasmid life cycle. This part of the plasmid life cycle is referred to as the vegetative cycle.

Conjugative pores appear to be present randomly within the donor cell envelope and all are potentially viable. For example, donor cells containing RP4 possess 25 conjugative pores (41) which is 3-4-fold more in number than the plasmid molecules under laboratory growth conditions. As bacteria may encounter each other in a variety of spatial relationships, the presence of multiple, randomly dispersed pores increases the likelihood of a conjugative pore interacting with a recipient. Upon contact of the conjugative pilus with a suitable recipient, a proposed "mating signal" triggers unwinding of the T-strand, resulting in the production of the T-strand, and conjugal DNA synthesis, replacing the T-strand. This event would be the initial stage of the conjugative cycle. Initial contact between pili and recipient cells is subsequently followed by the formation of mating pairs/aggregates. The region of intimate contact between a donor and a recipient cell is the conjugative junction. Since conjugative junctions are 200 nm long (177), it is likely that multiple conjugative pores could fit within one junction. This is assuming that the width of the conjugative pore is comparable to the size of known secretins (20-30 nm). Transfer systems containing the H/F-like T4SS encode mating pair stabilization proteins, which facilitate the stability of mating pairs in liquid environments. Mating pair stabilization functions are not encoded by P-like T4SS.

The model shown in Figure 5-6 predicts relaxase transfer into the recipient. Although the relaxase interacts with the coupling protein, it is not known if relaxase transfer occurs. The relaxase could guide the single-stranded DNA into the recipient, serving as a "pilot" protein. Single-stranded DNA (1 nm) could potentially fit through the coupling protein pore (2 nm) and the central lumen of the pilus (2 nm), however if the relaxase is to fit through the pore the relaxase must be 2 nm or less in diameter. Given the structural similarities between the coupling protein and DNA ring helicases, it has been proposed that the coupling protein uses ATP hydrolysis to energize the pumping of single-stranded DNA into the recipient (122). The reconstituted *oriT* needs to be cleaved to release the T-strand from the replacement strand. An attractive explanation is that the reconstituted *oriT* is cleaved by a second relaxosome within the donor. Cleavage by the

second relaxosome would replace the transferred relaxosome, re-establishing the superhelical nature of the plasmid. Release of the 3' end of the T-strand by the second cleavage event would facilitate the formation of a "peg" structure via an inverted repeat located, immediately upstream of the *nic* site, the last region to enter the recipient. The inverted repeat is recognized by the relaxase, which rejoins the 5' and 3' ends of the T-strand and terminates transfer.

As the single-stranded DNA is entering the recipient, possibly even before termination, it is likely targeted to the host replisome to begin complementary strand synthesis. Double-stranded DNA is expected to enter into vegetative replication and begin expressing important establishment proteins, such as the partitioning proteins. This will result in the formation of the partitioning apparatus. At this time the plasmid molecules are partitioning proficient, marking the end of the conjugative cycle. Expression of transfer proteins results in the creation of the conjugative apparatus, which results in disaggregation of mating pairs/aggregates.

5.4 Conclusions and Future Directions

The most interesting questions in bacterial conjugation revolve around the T4SS apparatus. The fact that T4SS are central to the virulence of several bacterial pathogens means that general mechanisms/themes discovered from different T4SS model systems may be combined for a fuller understanding of the biology of T4SS. Paramount to such an approach is a comprehensive phylogenetic analysis of the individual components from the T4SS subfamilies. Cao and Saier (27) have recently performed such an analysis on the P/VirB T4SS subfamily. A phylogenetic analysis of the H/F T4SS subfamily is the logical next step and will lend credence to the T4SS subfamily proposal. Verification of the conserved T4SS components and the non-conserved subfamily components with a phylogenetic analysis will provide a foundation for studying the T4SS core and the specialized functions of each T4SS subfamily.

Perhaps we now have a route through which macromolecules could transverse the donor envelope using T4SS (i.e. the conjugative pore). However, much work remains to be done to before a clear understanding of the structure and function of the T4SS

apparatus is available and an appreciation of how DNA enters the recipient. Structural determination of key transfer proteins will undoubtedly provide valuable insight into the nature of T4SS apparatus, which cannot be taken from comparisons of transfer proteins to databases. For example, the crystal structure of the coupling protein TrwB identified structural homologies to DNA ring helicases and therefore a mechanism by which single-stranded DNA could be actively pumped through the conjugative pore. As more structural studies are performed, it will be of interest to know if the ring structure theme is ubiquitous to the T4SS components.

The determination of the structure of the putative T4SS secretin will be necessary to confirm the bioinformatic observation described in this thesis (Figure 2-5). Secretins from Type II (34, 151, 181) and Type III (37) secretion systems and the filamentous phage ϕ 1 (120) have been purified in their multimeric form. Secretin multimers are resistant to 4% sodium dodecyl sulfate at temperatures up to 65°C and this property has been exploited during the purification of secretins in the multimeric form. When viewed with transmission electron microscopy and negative staining secretins appear as ring structures with a central channel. Therefore, well-established purification and diagnostic methods exist for secretins, which can easily be applied to TrhK and TraK-like proteins. The confirmation of a T4SS secretin will certainly be exciting, as a conjugative secretin would allow the passage of both the conjugative pilus and the T-strand across the donor outer membrane. The next logical question would be: do they pass through the secretin individually or together (i.e. T-strand through the pilus)?

One of the objectives of this thesis was to visually document conjugative transfer. The *lacO*/GFP-LacI system has proved to be very useful in documenting the stages of conjugation during which the transferring plasmid is in the double-stranded form. These observations, along with the visualization of individual mating pairs, allowed for speculation on the route by which the single-stranded DNA transfers. Therefore, there is still much more to be seen during conjugation, but it will not be with the *lacO*/GFP-LacI method as I believe I have exhausted this method in this context. Direct visualization of the single-stranded plasmid during transfer should be the next goal. Fortunately, there are sensitive and imaginative methods being developed to visualize macromolecules in living cells in real-time (184, 219). Application of such methods to bacterial conjugation

would require their adaptation for the labeling of the relaxase or the T-strand with fluorescent probes. Innovative fluorescence microscopy technologies combined with a plasmid biologist's creativity could lead to breakthroughs in visualizing the entire conjugative cycle in real-time.

Under laboratory conditions the conjugative cycle occurs at a high frequency and takes only minutes. This is known because bacterial conjugation has been well studied under controlled, simple environments. Conjugative transfer in Nature deserves more investigation, as an understanding of transfer in the natural setting is required if one were to attempt to intervene with conjugation and reduce the spread of antibiotic resistance. Indeed, it does happen quite often in Nature, as gauged by the rapid and widespread occurrence of antibiotic resistance via conjugative plasmids (198). Important antibiotic resistance plasmids have been sequenced and comparisons between plasmid genomes have demonstrated that successful plasmids, as defined by their prevalence, have conserved backbone components. As noted in the Introduction, R751 and RP4 are IncP plasmids which contain a completely conserved backbone. As an even more profound example, both R27 (180 kb), which was isolated from *S. typhi* in 1961, and pHCM1 (220 kb), which was isolated from *S. typhi* in 1993, share a backbone that is 99% identical at the DNA level (165). The difference is 50 kb inserted at two locations of pHCM1 which encode for resistance to first line antibiotics. Because of examples like these and the concept of the plasmid life cycle, I believe that the success of IncHI1 and IncP plasmids, and conjugative plasmids in general, has been dictated by their collective backbone components.

6 Bibliography

1. **Abdel-Monem, M., H. F. Lauppe, J. Kartenbeck, H. Durwald, and H. Hoffmann-Berling.** 1977. Enzymatic unwinding of DNA. III. Mode of action of *Escherichia coli* DNA unwinding enzyme. *J Mol Biol.* **110(4):667-685.**
2. **Achtman, M., N. Kennedy, and R. Skurray.** 1977. Cell-cell interactions in conjugating *Escherichia coli*: role of traT protein in surface exclusion. *Proc Natl Acad Sci U S A.* **74(11):5104-5108.**
3. **Alt-Morbe, J., J. L. Stryker, C. Fuqua, P. L. Li, S. K. Farrand, and S. C. Winans.** 1996. The conjugal transfer system of *Agrobacterium tumefaciens* octopine-type Ti plasmids is closely related to the transfer system of an IncP plasmid and distantly related to Ti plasmid vir genes. *J Bacteriol.* **178(14):4248-4257.**
4. **Altschul, S. F., W. Gish, W. Miller, E. W. Myers, and D. J. Lipman.** 1990. Basic local alignment search tool. *J Mol Biol.* **215(3):403-410.**
5. **Altschul, S. F., T. L. Madden, A. A. Schaffer, J. Zhang, Z. Zhang, W. Miller, and D. J. Lipman.** 1997. Gapped BLAST and PSI-BLAST: a new generation of protein database search programs. *Nucleic Acids Res.* **25(17):3389-3402.**
6. **Anderson, E. S.** 1975. Viability of, and transfer of a plasmid from, *E. coli* K12 in human intestine. *Nature.* **255(5508):502-504.**
7. **Anthony, K. G., W. A. Klimke, J. Manchak, and L. S. Frost.** 1999. Comparison of proteins involved in pilus synthesis and mating pair stabilization from the related plasmids F and R100-1: insights into the mechanism of conjugation. *J Bacteriol.* **181(17):5149-5159.**
8. **Austin, S., and K. Nordstrom.** 1990. Partition-mediated incompatibility of bacterial plasmids. *Cell.* **60(3):351-354.**
9. **Backert, S., E. Ziska, V. Brinkmann, U. Zimny-Arndt, A. Fauconnier, P. R. Jungblut, M. Naumann, and T. F. Meyer.** 2000. Translocation of the *Helicobacter pylori* CagA protein in gastric epithelial cells by a type IV secretion apparatus. *Cell Microbiol.* **2(2):155-164.**
10. **Baron, C., O. C. D., and E. Lanka.** 2002. Bacterial secrets of secretion: EuroConference on the biology of type IV secretion processes. *Mol Microbiol.* **43(5):1359-1365.**

11. **Baron, C., Y. R. Thorstenson, and P. Zambryski.** 1997. The lipoprotein VirB7 interacts with VirB9 in the membranes of *Agrobacterium tumefaciens*. *J Bacteriol.* **179**(4):1211-1218.
12. **Beaber, J. W., B. Hochhut, and M. K. Waldor.** 2002. Genomic and functional analyses of SXT, an integrating antibiotic resistance gene transfer element derived from *Vibrio cholerae*. *J Bacteriol.* **184**(15):4259-4269.
13. **Becker, E. C., and R. Meyer.** 1997. Acquisition of resistance genes by the IncQ plasmid R1162 is limited by its high copy number and lack of a partitioning mechanism. *J Bacteriol.* **179**(18):5947-5950.
14. **Becker, E. C., and R. J. Meyer.** 2000. Recognition of oriT for DNA processing at termination of a round of conjugal transfer. *J Mol Biol.* **300**(5):1067-1077.
15. **Bhattacharjee, M. K., and R. J. Meyer.** 1993. Specific binding of MobA, a plasmid-encoded protein involved in the initiation and termination of conjugal DNA transfer, to single-stranded *oriT* DNA. *Nucleic Acids Res.* **21**(19):4563-4568.
16. **Bignell, C. R., A. S. Haines, D. Khare, and C. M. Thomas.** 1999. Effect of growth rate and *incC* mutation on symmetric plasmid distribution by the IncP-1 partitioning apparatus. *Mol Microbiol.* **34**(2):205-216.
17. **Bingle, L. E., and C. M. Thomas.** 2001. Regulatory circuits for plasmid survival. *Curr Opin Microbiol.* **4**(2):194-200.
18. **Bohne, J., A. Yim, and A. N. Binns.** 1998. The Ti plasmid increases the efficiency of *Agrobacterium tumefaciens* as a recipient in VirB-mediated conjugal transfer of an IncQ plasmid. *Proc Natl Acad Sci U S A.* **95**(12):7057-7062.
19. **Bolland, S., M. Llosa, P. Avila, and F. de la Cruz.** 1990. General organization of the conjugal transfer genes of the IncW plasmid R388 and interactions between R388 and IncN and IncP plasmids. *J Bacteriol.* **172**(10):5795-5802.
20. **Boltner, D., C. MacMahon, J. T. Pembroke, P. Strike, and A. M. Osborn.** 2002. R391: a Conjugative Integrating Mosaic Comprised of Phage, Plasmid, and Transposon Elements. *J Bacteriol.* **184**(18):5158-5169.
21. **Bradley, D. E.** 1980. Morphological and serological relationships of conjugative pili. *Plasmid.* **4**(2):155-169.

22. **Bradley, D. E., D. E. Taylor, and D. R. Cohen.** 1980. Specification of surface mating systems among conjugative drug resistance plasmids in *Escherichia coli* K-12. *J Bacteriol.* **143**(3):1466-1470.
23. **Bradley, D. E., D. E. Taylor, and D. R. Cohen.** 1980. Specification of surface mating systems among conjugative drug resistance plasmids in *Escherichia coli* K-12. *J Bacteriol.* **143**(3):1466-1470.
24. **Byrd, D. R., and S. W. Matson.** 1997. Nicking by transesterification: the reaction catalysed by a relaxase. *Mol Microbiol.* **25**(6):1011-1022.
25. **Byrd, D. R., J. K. Sampson, H. M. Ragonese, and S. W. Matson.** 2002. Structure-Function Analysis of *Escherichia coli* DNA Helicase I Reveals Non-overlapping Transesterase and Helicase Domains. *J Biol Chem.* **277**(45):42645-42653.
26. **Cabezon, E., J. I. Sastre, and F. de la Cruz.** 1997. Genetic evidence of a coupling role for the TraG protein family in bacterial conjugation. *Mol Gen Genet.* **254**(4):400-406.
27. **Cao, T. B., and M. H. Saier, Jr.** 2001. Conjugal type IV macromolecular transfer systems of Gram-negative bacteria: organismal distribution, structural constraints and evolutionary conclusions. *Microbiology.* **147**(12):3201-3214.
28. **Chalfie, M., Y. Tu, G. Euskirchen, W. W. Ward, and D. C. Prasher.** 1994. Green fluorescent protein as a marker for gene expression. *Science.* **263**(5148):802-805.
29. **Chattoraj, D. K.** 2000. Control of plasmid DNA replication by iterons: no longer paradoxical. *Mol Microbiol.* **37**(3):467-476.
30. **Christie, P. J.** 2001. Type IV secretion: intercellular transfer of macromolecules by systems ancestrally related to conjugation machines. *Mol Microbiol.* **40**(2):294-305.
31. **Christie, P. J., and J. P. Vogel.** 2000. Bacterial type IV secretion: conjugation systems adapted to deliver effector molecules to host cells. *Trends Microbiol.* **8**(8):354-360.
32. **Clewell, D. B., and D. R. Helinski.** 1969. Supercoiled circular DNA-protein complex in *Escherichia coli*: purification and induced conversion to an open circular DNA form. *Proc Natl Acad Sci U S A.* **62**(4):1159-1166.
33. **Collet, J. F., and J. C. Bardwell.** 2002. Oxidative protein folding in bacteria. *Mol Microbiol.* **44**(1):1-8.

34. **Collins, R. F., L. Davidsen, J. P. Derrick, R. C. Ford, and T. Tonjum.** 2001. Analysis of the PilQ secretin from *Neisseria meningitidis* by transmission electron microscopy reveals a dodecameric quaternary structure. *J Bacteriol.* **183**(13):3825-3832.
35. **Couturier, M., F. Bex, P. L. Bergquist, and W. K. Maas.** 1988. Identification and classification of bacterial plasmids. *Microbiol Rev.* **52**(3):375-395.
36. **Covacci, A., and R. Rappuoli.** 1993. Pertussis toxin export requires accessory genes located downstream from the pertussis toxin operon. *Mol Microbiol.* **8**(3):429-434.
37. **Crago, A. M., and V. Koronakis.** 1998. Salmonella InvG forms a ring-like multimer that requires the InvH lipoprotein for outer membrane localization. *Mol Microbiol.* **30**(1):47-56.
38. **Datta, N.** 1975. Epidemiology and classification of plasmids, p. 9-15. *In* D. Schlessinger (ed.), *Microbiology*. American Society for Microbiology, Washington.
39. **Datta, N.** 1985. Plasmids as organisms, p. 1-22. *In* D. R. Helinski, S. N. Cohen, D. B. Clewell, D. A. Jackson, and A. Hollaender (ed.), *Plasmids in Bacteria*. Plenum Press, New York.
40. **Datta, N.** 1984. Plasmids of enteric bacteria, p. 487-496. *In* L. E. Bryan (ed.), *Antimicrobial Drug Resistance*. Academic Press Inc., London, U. K.
41. **Daugelavicius, R., J. K. Bamford, A. M. Grahn, E. Lanka, and D. H. Bamford.** 1997. The IncP plasmid-encoded cell envelope-associated DNA transfer complex increases cell permeability. *J Bacteriol.* **179**(16):5195-5202.
42. **Davis, M. A., K. A. Martin, and S. J. Austin.** 1992. Biochemical activities of the ParA partition protein of the P1 plasmid. *Mol Microbiol.* **6**(9):1141-1147.
43. **del Solar, G., R. Giraldo, M. J. Ruiz-Echevarria, M. Espinosa, and R. Diaz-Orejas.** 1998. Replication and control of circular bacterial plasmids. *Microbiol Mol Biol Rev.* **62**(2):434-464.
44. **Durrenberger, M. B., W. Villiger, and T. Bachi.** 1991. Conjugational junctions: morphology of specific contacts in conjugating *Escherichia coli* bacteria. *J Struct Biol.* **107**(2):146-156.
45. **Ebersbach, G., and K. Gerdes.** 2001. The double par locus of virulence factor pB171: DNA segregation is correlated with oscillation of ParA. *Proc Natl Acad Sci U S A.* **98**(26):15078-15083.

46. **Edgar, R., D. K. Chatteraj, and M. Yarmolinsky.** 2001. Pairing of P1 plasmid partition sites by ParB. *Mol Microbiol.* **42(5):**1360-1370.
47. **Eisenbrandt, R., M. Kalkum, E. M. Lai, R. Lurz, C. I. Kado, and E. Lanka.** 1999. Conjugative pili of IncP plasmids, and the Ti plasmid T pilus are composed of cyclic subunits. *J Biol Chem.* **274(32):**22548-22555.
48. **Eisenbrandt, R., M. Kalkum, R. Lurz, and E. Lanka.** 2000. Maturation of IncP pilin precursors resembles the catalytic Dyad-like mechanism of leader peptidases. *J Bacteriol.* **182(23):**6751-6761.
49. **Erickson, M. J., and R. J. Meyer.** 1993. The origin of greater-than-unit-length plasmids generated during bacterial conjugation. *Mol Microbiol.* **7(2):**289-298.
50. **Ermolaeva, M. D., O. White, and S. L. Salzberg.** 2001. Prediction of operons in microbial genomes. *Nucleic Acids Res.* **29(5):**1216-1221.
51. **Espinosa, M., S. Cohen, M. Couturier, G. del Solar, R. Diaz-Orejas, R. Giraldo, L. Janniere, C. Miller, M. Osborn, and C. M. Thomas.** 2000. Plasmid Replication and Copy Number Control, p. 1-47. *In* C. M. Thomas (ed.), *The Horizontal Gene Pool*. Harwood Academic Publishers, Amsterdam.
52. **Farrand, S. K., I. Hwang, and D. M. Cook.** 1996. The Tra region of the nopaline-type Ti plasmid is a chimera with elements related to the transfer systems of RSF1010, RP4, and F. *J Bacteriol.* **178(14):**4233-4247.
53. **Fica, A., M. E. Fernandez-Beros, L. Aron-Hott, A. Rivas, K. D'Ottone, J. Chumpitaz, J. M. Guevara, M. Rodriguez, and F. Cabello.** 1997. Antibiotic-resistant *Salmonella typhi* from two outbreaks: few ribotypes and IS200 types harbor Inc HI1 plasmids. *Microb Drug Resist.* **3(4):**339-343.
54. **Firth, N., K. Ippen-Ihler, and R. A. Skurray.** 1996. Structure and function of the F-factor and mechanism of conjugation, p. 2377-2401. *In* F. C. Neidhardt (ed.), *Escherichia coli and Salmonella Cellular and Molecular Biology*, Second ed, vol. 1. ASM Press, Washington D.C.
55. **Firth, N., and R. Skurray.** 1992. Characterization of the F plasmid bifunctional conjugation gene, *traG*. *Mol Gen Genet.* **232(1):**145-153.

56. **Frost, L. S., K. Ippen-Ihler, and R. A. Skurray.** 1994. Analysis of the sequence and gene products of the transfer region of the F sex factor. *Microbiol Rev.* **58(2):**162-210.
57. **Gabant, P., A. O. Chahdi, and M. Couturier.** 1994. Nucleotide sequence and replication characteristics of RepHI1B: a replicon specific to the IncHI1 plasmids. *Plasmid.* **31(2):**111-1120.
58. **Gabant, P., P. Newnham, D. Taylor, and M. Couturier.** 1993. Isolation and location on the R27 map of two replicons and an incompatibility determinant specific for IncHI1 plasmids. *J Bacteriol.* **175(23):**7697-7701.
59. **Gerdes, K., and S. Molin.** 1986. Partitioning of plasmid R1. Structural and functional analysis of the parA locus. *J Mol Biol.* **190(3):**269-279.
60. **Gerdes, K., J. Moller-Jensen, and R. Bugge-Jensen.** 2000. Plasmid and chromosome partitioning: surprises from phylogeny. *Mol Microbiol.* **37(3):**455-466.
61. **Giebelhaus, L. A., L. Frost, E. Lanka, E. P. Gormley, J. E. Davies, and B. Leskiw.** 1996. The Tra2 core of the IncP(alpha) plasmid RP4 is required for intergeneric mating between *Escherichia coli* and *Streptomyces lividans*. *J Bacteriol.* **178(21):**6378-6381.
62. **Gilmour, M. W., J. E. Gunton, T. D. Lawley, and D. E. Taylor.** 2003. Interaction between the IncHI1 plasmid R27 coupling protein and a component of the R27 Type IV secretion system: TraG associates with the coiled-coil mating pair formation protein TrhB. *Mol Microbiol.* **In Revision.**
63. **Gilmour, M. W., T. D. Lawley, M. M. Rooker, P. J. Newnham, and D. E. Taylor.** 2001. Cellular location and temperature-dependent assembly of IncHI1 plasmid R27-encoded TrhC-associated conjugative transfer protein complexes. *Mol Microbiol.* **42(3):**705-715.
64. **Gomis-Ruth, F. X., G. Moncalian, F. de la Cruz, and M. Coll.** 2002. Conjugative plasmid protein TrwB, an integral membrane type IV secretion system coupling protein. Detailed structural features and mapping of the active site cleft. *J Biol Chem.* **277(9):**7556-7566.

65. **Gomis-Ruth, F. X., G. Moncalian, R. Perez-Luque, A. Gonzalez, E. Cabezon, F. de la Cruz, and M. Coll.** 2001. The bacterial conjugation protein TrwB resembles ring helicases and F1-ATPase. *Nature*. **409**(6820):637-641.
66. **Gordon, G. S., D. Sitnikov, C. D. Webb, A. Teleman, A. Straight, R. Losick, A. W. Murray, and A. Wright.** 1997. Chromosome and low copy plasmid segregation in *E. coli*: visual evidence for distinct mechanisms. *Cell*. **90**(6):1113-1121.
67. **Gordon, G. S., and A. Wright.** 2000. DNA segregation in bacteria. *Annu Rev Microbiol*. **54**:681-708.
68. **Gormley, E. P., and J. Davies.** 1991. Transfer of plasmid RSF1010 by conjugation from *Escherichia coli* to *Streptomyces lividans* and *Mycobacterium smegmatis*. *J Bacteriol*. **173**(21):6705-6708.
69. **Grahn, A. M., J. Haase, D. H. Bamford, and E. Lanka.** 2000. Components of the RP4 conjugative transfer apparatus form an envelope structure bridging inner and outer membranes of donor cells: implications for related macromolecule transport systems. *J Bacteriol*. **182**(6):1564-1574.
70. **Grandoso, G., P. Avila, A. Cayon, M. A. Hernando, L. Llosa, and F. de la Cruz.** 2000. Two active-site tyrosyl residues of protein TrwC act sequentially at the origin of transfer during plasmid R388 conjugation. *J Mol Biol*. **295**(5):1163-1172.
71. **Grandoso, G., M. Llosa, J. C. Zabala, and F. de la Cruz.** 1994. Purification and biochemical characterization of TrwC, the helicase involved in plasmid R388 conjugal DNA transfer. *Eur J Biochem*. **226**(2):403-412.
72. **Guilvout, I., K. R. Hardie, N. Sauvonnnet, and A. P. Pugsley.** 1999. Genetic dissection of the outer membrane secretin PulD: are there distinct domains for multimerization and secretion specificity? *J Bacteriol*. **181**(23):7212-7220.
73. **Guiney, D. G.** 1993. Broad host range conjugative and mobilizable plasmids in gram-negative bacteria, p. 75-104. *In* C. M. Thomas (ed.), *Bacterial Conjugation*. Plenum Press, New York.
74. **Guiney, D. G.** 1984. Promiscuous transfer of drug resistance in gram-negative bacteria. *J Infect Dis*. **149**(3):320-329.

75. **Guzman, L. M., D. Belin, M. J. Carson, and J. Beckwith.** 1995. Tight regulation, modulation, and high-level expression by vectors containing the arabinose pBAD promoter. *J Bacteriol.* **177**(14):4121-4130.
76. **Haase, J., R. Lurz, A. M. Grahn, D. H. Bamford, and E. Lanka.** 1995. Bacterial conjugation mediated by plasmid RP4: RSF1010 mobilization, donor-specific phage propagation, and pilus production require the same Tra2 core components of a proposed DNA transport complex. *J Bacteriol.* **177**(16):4779-4791.
77. **Hamilton, C. M., H. Lee, P. L. Li, D. M. Cook, K. R. Piper, S. B. von Bodman, E. Lanka, W. Ream, and S. K. Farrand.** 2000. TraG from RP4 and TraG and VirD4 from Ti plasmids confer relaxosome specificity to the conjugal transfer system of pTiC58. *J Bacteriol.* **182**(6):1541-1548.
78. **Hamilton, H. L., K. J. Schwartz, and J. P. Dillard.** 2001. Insertion-duplication mutagenesis of neisseria: use in characterization of DNA transfer genes in the gonococcal genetic island. *J Bacteriol.* **183**(16):4718-4726.
79. **Harnett, N., S. McLeod, Y. AuYong, J. Wan, S. Alexander, R. Khakhria, and C. Krishnan.** 1998. Molecular characterization of multiresistant strains of *Salmonella typhi* from South Asia isolated in Ontario, Canada. *Can J Microbiol.* **44**(4):356-363.
80. **Harrington, L. C., and A. C. Rogerson.** 1990. The F pilus of *Escherichia coli* appears to support stable DNA transfer in the absence of wall-to-wall contact between cells. *J Bacteriol.* **172**(12):7263-7264.
81. **Harris, R. L., V. Hombs, and P. M. Silverman.** 2001. Evidence that F-plasmid proteins TraV, TraK and TraB assemble into an envelope-spanning structure in *Escherichia coli*. *Mol Microbiol.* **42**(3):757-766.
82. **Harris, R. L., K. A. Sholl, M. N. Conrad, M. E. Dresser, and P. M. Silverman.** 1999. Interaction between the F plasmid TraA (F-pilin) and TraQ proteins. *Mol Microbiol.* **34**(4):780-791.
83. **Heim, R., A. B. Cubitt, and R. Y. Tsein.** 1995. Improved green fluorescence. *Nature.* **373**(6516):663-664.
84. **Heinemann, J. A., and G. F. Sprague.** 1989. Bacterial conjugative plasmids mobilize DNA transfer between bacteria and yeast. *Nature.* **340**(6230):205-209.

85. **Henderson, D., and R. Meyer.** 1999. The MobA-linked primase is the only replication protein of R1162 required for conjugal mobilization. *J Bacteriol.* **181**(9):2973-2978.
86. **Hiraga, S.** 2000. Dynamic localization of bacterial and plasmid chromosomes. *Annu Rev Microbiol.* **34**:21-59.
87. **Ho, T. Q., Z. Zhong, S. Aung, and J. Pogliano.** 2002. Compatible bacterial plasmids are targeted to independent cellular locations in *Escherichia coli*. *EMBO J.* **21**(7):1864-1872.
88. **Hofreuter, D., S. Odenbreit, and R. Haas.** 2001. Natural transformation competence in *Helicobacter pylori* is mediated by the basic components of a type IV secretion system. *Mol Microbiol.* **41**(2):379-391.
89. **Howard, E. A., J. R. Zupan, V. Citovsky, and P. C. Zambryski.** 1992. The VirD2 protein of *A. tumefaciens* contains a C-terminal bipartite nuclear localization signal: implications for nuclear uptake of DNA in plant cells. *Cell.* **68**(1):109-118.
90. **Ippen-Ihler, K., and R. A. Skurray.** 1993. Genetic organization of transfer-related determinants of the sex factor F and related plasmids, p. 23-52. *In* D. B. Clewell (ed.), *Bacterial Conjugation*. Plenum Press, New York.
91. **Ireton, K., N. W. Gunther, and A. D. Grossman.** 1994. spo0J is required for normal chromosome segregation as well as the initiation of sporulation in *Bacillus subtilis*. *J Bacteriol.* **176**(17):5320-5329.
92. **Ivanoff, B., and M. M. Levine.** 1997. Typhoid fever: continuing challenges from a resilient bacterial foe. *Bull. Inst. Pasteur.* **95**:129-142.
93. **Jensen, J. B., M. Dam, and K. Gerdes.** 1994. Partitioning of plasmid R1. The parA operon is autoregulated by ParR and its transcription is highly stimulated by a downstream activating element. *J Mol Biol.* **236**(5):1299-1309.
94. **Jensen, J. B., and K. Gerdes.** 1997. Partitioning of plasmid R1. The ParM protein exhibits ATPase activity and interacts with the centromere-like ParR-parC complex. *J Mol Biol.* **269**(4):505-513.
95. **Jensen, R. B., and K. Gerdes.** 1999. Mechanism of DNA segregation in prokaryotes: ParM partitioning protein of plasmid R1 co-localizes with its replicon during the cell cycle. *EMBO J.* **18**(14):4076-4084.

96. **Jensen, R. B., R. Lurz, and K. Gerdes.** 1998. Mechanism of DNA segregation in prokaryotes: replicon pairing by *parC* of plasmid R1. *Proc Natl Acad Sci U S A.* **95(15):8550-8555.**
97. **Jin, Q., and S. Y. He.** 2001. Role of the Hrp pilus in type III protein secretion in *Pseudomonas syringae*. *Science.* **294(5551):2556-2558.**
98. **Jin, Q., W. Hu, I. Brown, G. McGhee, P. Hart, A. L. Jones, and S. Y. He.** 2001. Visualization of secreted Hrp and Avr proteins along the Hrp pilus during type III secretion in *Erwinia amylovora* and *Pseudomonas syringae*. *Mol Microbiol.* **40(5):1129-1139.**
99. **Jones, G. W., D. K. Rabert, D. M. Svinarich, and H. J. Whitfield.** 1982. Association of adhesive, invasive, and virulent phenotypes of *Salmonella typhimurium* with autonomous 60-megadalton plasmids. *Infect Immun.* **38(2):476-486.**
100. **Kingsman, A., and N. Willetts.** 1978. The requirements for conjugal DNA synthesis in the donor strain during flac transfer. *J Mol Biol.* **122(3):287-300.**
101. **Kleckner, N., J. Bender, and S. Gottesman.** 1991. Uses of transposons with emphasis on *Tn10*. *Methods Enzymol.* **204:139-180.**
102. **Klimke, W.** 2002. University of Alberta, Edmonton.
103. **Klimke, W. A., and L. S. Frost.** 1998. Genetic analysis of the role of the transfer gene, *traN*, of the F and R100-1 plasmids in mating pair stabilization during conjugation. *J Bacteriol.* **180(16):4036-4043.**
104. **Komano, T., S. R. Kim, T. Yoshida, and T. Nisioka.** 1994. DNA rearrangement of the shufflon determines recipient specificity in liquid mating of IncII plasmid R64. *J Mol Biol.* **243(1):6-9.**
105. **Komano, T., T. Yoshida, K. Narahara, and N. Furuya.** 2000. The transfer region of IncII plasmid R64: similarities between R64 *tra* and legionella *icm/dot* genes. *Mol Microbiol.* **35(6):1348-1359.**
106. **Lanka, E., and B. M. Wilkins.** 1995. DNA processing reactions in bacterial conjugation. *Annu Rev Biochem.* **64:141-169.**
107. **Lawley, T. D., V. Burland, and D. E. Taylor.** 2000. Analysis of the complete nucleotide sequence of the tetracycline-resistance transposon *Tn10*. *Plasmid.* **43(3):235-239.**

108. **Lawley, T. D., M. W. Gilmour, J. E. Gunton, L. J. Standeven, and D. E. Taylor.** 2002. Functional and mutational analysis of conjugative transfer region 1 (Tra1) from the IncHI1 plasmid R27. *J Bacteriol.* **184**(8):2173-2180.
109. **Lawley, T. D., M. W. Gilmour, J. E. Gunton, D. M. Tracz, and D. E. Taylor.** 2003. Functional and mutational analysis of the conjugative transfer region 2 (Tra2) of the IncHI1 plasmid R27. *J Bacteriol.* **185**(2).
110. **Lawley, T. D., G. S. Gordon, A. Wright, and D. E. Taylor.** 2002. Bacterial conjugative transfer: visualization of successful mating pairs and plasmid establishment in live *Escherichia coli*. *Mol Microbiol.* **44**(4):947-956.
111. **Lawley, T. D., B. M. Wilkins, and L. S. Frost.** 2003. Bacterial conjugation in gram-negative bacteria. In G. Phillips and B. Funnel (ed.), *Biology of Plasmids*. ASM Press, Washington. In Press.
112. **Lebaron, P., V. Roux, M. C. Lett, and B. Baleux.** 1993. Effects of pili rigidity and energy availability on conjugative plasmid transfer in aquatic environments. *Microb Releases.* **2**(3):127-133.
113. **Lemon, K. P., and A. D. Grossman.** 1998. Localization of bacterial DNA polymerase: evidence for a factory model of replication. *Science.* **282**(5393):1516-1519.
114. **Lemon, K. P., and A. D. Grossman.** 2000. Movement of replicating DNA through a stationary replisome. *Mol Cell.* **6**(6):1321-1330.
115. **Lessl, M., D. Balzer, R. Lurz, V. L. Waters, D. G. Guiney, and E. Lanka.** 1992. Dissection of IncP conjugative plasmid transfer: definition of the transfer region Tra2 by mobilization of the Tra1 region in trans. *J Bacteriol.* **174**(8):2493-2500.
116. **Lessl, M., D. Balzer, W. Pansegrau, and E. Lanka.** 1992. Sequence similarities between the RP4 Tra2 and the Ti VirB region strongly support the conjugation model for T-DNA transfer. *J Biol Chem.* **267**(28):20471-20480.
117. **Lessl, M., D. Balzer, K. Weyrauch, and E. Lanka.** 1993. The mating pair formation system of plasmid RP4 defined by RSF1010 mobilization and donor-specific phage propagation. *J Bacteriol.* **175**(20):6415-6425.
118. **Lessl, M., W. Pansegrau, and E. Lanka.** 1992. Relationship of DNA-transfer-systems: essential transfer factors of plasmids RP4, Ti and F share common sequences. *Nucleic Acids Res.* **20**(22):6099-6100.

119. **Linderoth, N., P. Model, and M. Russel.** 1996. Essential role of a sodium dodecyl sulfate-resistant protein IV multimer in assembly-export of filamentous phage. *J. Bacteriol.* **178**(7):1962-1970.
120. **Linderoth, N. A., M. N. Simon, and M. Russel.** 1997. The filamentous phage pIV multimer visualized by scanning transmission electron microscopy. *Science.* **278**(5343):1635-1638.
121. **Llosa, M., S. Bolland, and F. de la Cruz.** 1991. Structural and functional analysis of the origin of conjugal transfer of the broad-host-range IncW plasmid R388 and comparison with the related IncN plasmid R46. *Mol Gen Genet.* **226**(3):473-483.
122. **Llosa, M., F. X. Gomis-Ruth, M. Coll, and F. de la Cruz.** 2002. Bacterial conjugation: a two-step mechanism for DNA transport. *Mol Microbiol.* **45**(1):1-8.
123. **Llosa, M., G. Grandoso, M. A. Hernando, and F. de la Cruz.** 1996. Functional domains in protein TrwC of plasmid R388: dissected DNA strand transferase and DNA helicase activities reconstitute protein function. *J Mol Biol.* **264**(1):56-67.
124. **Lu, J., J. Manchak, W. Klimke, C. Davidson, N. Firth, R. Skurray, and L. Frost.** 2002. Analysis and characterization of the IncFV plasmid pED208 transfer region. *Plasmid.* **48**(1):24.
125. **Macartney, D. P., D. R. Williams, T. Stafford, and C. M. Thomas.** 1997. Divergence and conservation of the partitioning and global regulation functions in the central control region of the IncP plasmids RK2 and R751. *Microbiology.* **143**(7):2167-2177.
126. **Maher, D., R. Sherburne, and D. E. Taylor.** 1991. Bacteriophages for incompatibility group H plasmids: morphological and growth characteristics. *Plasmid.* **26**(2):141-146.
127. **Maher, D., R. Sherburne, and D. E. Taylor.** 1993. H-pilus assembly kinetics determined by electron microscopy. *J Bacteriol.* **175**(8):2175-2183.
128. **Maher, D., and D. E. Taylor.** 1993. Host range and transfer efficiency of incompatibility group HI plasmids. *Can J Microbiol.* **39**(6):581-587.
129. **Majdalani, N., and K. Ippen-Ihler.** 1996. Membrane insertion of the F-pilin subunit is Sec independent but requires leader peptidase B and the proton motive force. *J Bacteriol.* **178**(13):3742-3747.

130. **Majdalani, N., D. Moore, S. Maneewannakul, and K. Ippen-Ihler.** 1996. Role of the propilin leader peptide in the maturation of F pilin. *J Bacteriol.* **178**(13):3748-3754.
131. **Manchak, J., K. G. Anthony, and L. S. Frost.** 2002. Mutational analysis of F-pilin reveals domains for pilus assembly, phage infection and DNA transfer. *Mol Microbiol.* **43**(1):195-205.
132. **Maneewannakul, K., S. Maneewannakul, and K. Ippen-Ihler.** 1993. Synthesis of F pilin. *J Bacteriol.* **175**(5):1384-1391.
133. **Maneewannakul, S., P. Kathir, and K. Ippen-Ihler.** 1992. Characterization of the F plasmid mating aggregation gene *traN* and of a new F transfer region locus *trbE*. *J Mol Biol.* **225**(2):299-311.
134. **Manwaring, N.** 2001. University of Sydney, Sydney.
135. **Matson, S. W., J. K. Sampson, and D. R. Byrd.** 2001. F plasmid conjugative DNA transfer: the TraI helicase activity is essential for DNA strand transfer. *J Biol Chem.* **267**(4):2372-2379.
136. **Mazodier, P., and J. Davies.** 1991. Gene transfer between distantly related bacteria. *Annu Rev Genet.* **25**:147-171.
137. **Merz, A. J., M. So, and M. P. Sheetz.** 2000. Pilus retraction powers bacterial twitching motility. *Nature.* **407**(6800):98-102.
138. **Mirza, S., S. Kariuki, K. Z. Mamum, N. J. Beeching, and C. A. Hart.** 2000. Analysis of plasmid and chromosomal DNA of multidrug-resistant *Salmonella enterica* serovar Typhi from Asia. *J Clin Microbiol.* **38**(4):1449-1452.
139. **Mohl, D. A., and J. W. Grober.** 1997. Cell cycle-dependent polar localization of chromosome partitioning proteins in *Caulobacter crescentus*. *Cell.* **88**(5):675-684.
140. **Moller-Jensen, J., R. B. Jensen, and K. Gerdes.** 2000. Plasmid and chromosome segregation in prokaryotes. *Trends Microbiol.* **8**(7):313-320.
141. **Moller-Jensen, J., R. B. Jensen, J. Lowe, and K. Gerdes.** 2002. Prokaryotic DNA segregation by an actin-like filament. *EMBO J.* **21**(12):3119-3127.
142. **Moore, D., K. Maneewannakul, S. Maneewannakul, J. H. Wu, K. Ippen-Ihler, and D. E. Bradley.** 1990. Characterization of the F-plasmid conjugative transfer gene *traU*. *J Bacteriol.* **172**(8):4263-4270.

143. **Moore, D., B. A. Sowa, and K. Ippen-Ihler.** 1981. Location of an F-pilin pool in the inner membrane. *J Bacteriol.* **146**(1):251-259.
144. **Murata, T., M. Ohnishi, T. Ara, J. Kaneko, C. G. Han, Y. F. Li, K. Takashima, H. Nojima, K. Nakayama, A. Kaji, Y. Kamio, T. Miki, H. Mori, E. Ohtsubo, Y. Terawaki, and T. Hayashi.** 2002. Complete nucleotide sequence of plasmid Rts1: implications for evolution of large plasmid genomes. *J Bacteriol.* **184**(12):3194-3202.
145. **Newnham, P.** 1995. University of Alberta, Edmonton.
146. **Newnham, P. J., and D. E. Taylor.** 1990. Genetic analysis of transfer and incompatibility functions within the IncHI plasmid R27. *Plasmid.* **23**(2):107-118.
147. **Newnham, P. J., and D. E. Taylor.** 1994. Molecular analysis of RepHI1A, a minimal replicon of the IncHI1 plasmid R27. *Mol Microbiol.* **11**(4):757-768.
148. **Niki, H., and S. Hiraga.** 1997. Subcellular distribution of actively partitioning F plasmid during the cell division cycle in *E. coli*. *Cell.* **90**(5):951-957.
149. **Nordstrom, K., and S. Austin.** 1993. Cell-cycle-specific initiation of replication. *Mol Microbiol.* **10**(3):457-463.
150. **Nouwen, N., N. Ranson, H. Saibil, B. Wolpensinger, A. Engel, A. Ghazi, and A. P. Pugsley.** 1999. Secretin PulD: association with pilot PulS, structure, and ion-conducting channel formation. *Proc Natl Acad Sci U S A.* **96**(14):8173-8177.
151. **Nouwen, N., H. Stahlberg, A. P. Pugsley, and A. Engel.** 2000. Domain structure of secretin PulD revealed by limited proteolysis and electron microscopy. *EMBO J.* **19**(10):2229-2236.
152. **Novick, R. P.** 1987. Plasmid incompatibility. *Microbiol Rev.* **51**(4):381-395.
153. **Novotny, C. P., and P. Fives-Taylor.** 1978. Effects of high temperature on *Escherichia coli* F pili. *J Bacteriol.* **133**(2):459-464.
154. **Novotny, C. P., and P. Fives-Taylor.** 1974. Retraction of F pili. *J Bacteriol.* **117**(3):1306-1311.
155. **Page, D. T., K. F. Whelan, and E. Colleran.** 1999. Mapping studies and genetic analysis of transfer genes of the multi-resistant IncHI2 plasmid, R478. *FEMS Microbiol Lett.* **179**(1):21-29.

156. **Pansegrau, W., D. Balzer, V. Krufft, R. Lurz, and E. Lanka.** 1990. In vitro assembly of relaxosomes at the transfer origin of plasmid RP4. *Proc Natl Acad Sci U S A.* **87(17):6555-6559.**
157. **Pansegrau, W., and E. Lanka.** 1996. Mechanisms of initiation and termination reactions in conjugative DNA processing. Independence of tight substrate binding and catalytic activity of relaxase (TraI) of IncPalph α plasmid RP4. *J Biol Chem.* **271(22):13068-13076.**
158. **Pansegrau, W., E. Lanka, P. T. Barth, D. H. Figurski, D. G. Guiney, D. Haas, D. R. Helinski, H. Schwab, V. A. Stanisich, and C. M. Thomas.** 1994. Complete nucleotide sequence of Birmingham IncP alpha plasmids. Compilation and comparative analysis. *J Mol Biol.* **239(5):623-663.**
159. **Pansegrau, W., W. Schroder, and E. Lanka.** 1994. Concerted action of three distinct domains in the DNA cleaving-joining reaction catalyzed by relaxase (TraI) of conjugative plasmid RP4. *J Biol Chem.* **269(4):2782-2789.**
160. **Pansegrau, W., W. Schroder, and E. Lanka.** 1993. Relaxase (TraI) of IncP alpha plasmid RP4 catalyzes a site-specific cleaving-joining reaction of single-stranded DNA. *Proc Natl Acad Sci U S A.* **90(7):2925-2929.**
161. **Pansegrau, W., G. Ziegelin, and E. Lanka.** 1990. Covalent association of the *traI* gene product of plasmid RP4 with the 5'-terminal nucleotide at the relaxation nick site. *J Biol Chem.* **265(18):10637-10644.**
162. **Pansegrau, W., G. Ziegelin, and E. Lanka.** 1988. The origin of conjugative IncP plasmid transfer: interaction with plasmid-encoded products and the nucleotide sequence at the relaxation site. *Biochim Biophys Acta.* **951(2-3):365-374.**
163. **Paranchych, W., and L. S. Frost.** 1988. The physiology and biochemistry of pili. *Adv Microb Physiol.* **29:53-114.**
164. **Parker, C., and R. Meyer.** 2002. Selection of plasmid molecules for conjugative transfer and replacement strand synthesis in the donor. *Mol Microbiol.* **46(3):761-768.**
165. **Parkhill, J., G. Dougan, K. D. James, N. R. Thomson, D. Pickard, J. Wain, C. Churcher, K. L. Mungall, S. D. Bentley, M. T. Holden, M. Sebaihia, S. Baker, D. Basham, K. Brooks, T. Chillingworth, P. Connerton, A. Cronin, P. Davis, R. M. Davies, L. Dowd, N. White, J. Farrar, T. Feltwell, N. Hamlin, A. Haque, T. T. Hien,**

- S. Holroyd, K. Jagels, A. Krogh, T. S. Larsen, S. Leather, S. Moule, P. O'Gaora, C. Parry, M. Quail, K. Rutherford, M. Simmonds, J. Skelton, K. Stevens, S. Whitehead, and B. G. Barrell. 2001. Complete genome sequence of a multiple drug resistant *Salmonella enterica* serovar Typhi CT18. *Nature*. **413**(6858):848-852.
166. Pogliano, J., T. Q. Ho, Z. Zhong, and D. R. Helinski. 2001. Multicopy plasmids are clustered and localized in *Escherichia coli*. *Proc Natl Acad Sci U S A*. **98**(8):4486-4491.
167. Preston, G. M., N. Bertrand, and P. B. Rainey. 2001. Type III secretion in plant growth-promoting *Pseudomonas fluorescens* SBW25. *Mol Microbiol*. **41**(5):999-1014.
168. Pukall, R., H. Tschape, and K. Smalla. 1996. Monitoring the spread of broad host and narrow host range plasmids in soil microcosms. *FEMS Microbiology Ecology*. **20**:53-66.
169. Radnedge, L., B. Youngren, M. Davis, and S. Austin. 1998. Probing the structure of complex macromolecular interactions by homolog specificity scanning: the P1 and P7 plasmid partition systems. *EMBO J*. **17**(20):6076-6085.
170. Raskin, D. M., and P. A. de Boer. 1999. Rapid pole-to-pole oscillation of a protein required for directing division to the middle of *Escherichia coli*. *Proc Natl Acad Sci U S A*. **96**(9):4971-4979.
171. Rawlings, D. E., and E. Tietze. 2001. Comparative biology of IncQ and IncQ-like plasmids. *Microbiol Mol Biol Rev*. **65**(4):481-496.
172. Rees, C. E., and B. M. Wilkins. 1990. Protein transfer into the recipient cell during bacterial conjugation: studies with F and RP4. *Mol Microbiol*. **4**(7):1199-1205.
173. Rodionov, O., M. Lobočka, and M. Yarmolinsky. 1999. Silencing of genes flanking the P1 plasmid centromere. *Science*. **283**(5401):546-549.
174. Romine, M. F., L. C. Stillwell, K. K. Wong, S. J. Thurston, E. C. Sisk, C. Sensen, T. Gaasterland, J. K. Fredrickson, and J. D. Saffer. 1999. Complete sequence of a 184-kilobase catabolic plasmid from *Sphingomonas aromaticivorans* F199. *J Bacteriol*. **181**(5):1585-1602.
175. Rooker, M. M., C. Sherburne, T. D. Lawley, and D. E. Taylor. 1999. Characterization of the Tra2 region of the IncHI1 plasmid R27. *Plasmid*. **41**(3):226-239.

176. **Sambrook, J., and D. W. Russell.** 2001. Molecular cloning: a laboratory manual, 3rd ed. Cold Spring Harbor Laboratory Press, Cold Spring Harbor.
177. **Samuels, A. L., E. Lanka, and J. E. Davies.** 2000. Conjugative junctions in RP4-mediated mating of *Escherichia coli*. J Bacteriol. **182**(10):2709-2715.
178. **Sastre, J. I., E. Cabezon, and F. de la Cruz.** 1998. The carboxyl terminus of protein TraD adds specificity and efficiency to F-plasmid conjugative transfer. J Bacteriol. **180**(22):6039-6042.
179. **Schandel, K. A., S. Maneewannakul, K. Ippen-Ihler, and R. E. Webster.** 1987. A *traC* mutant that retains sensitivity to fl bacteriophage but lacks F pili. J Bacteriol. **169**(7):3151-3159.
180. **Schandel, K. A., M. M. Muller, and R. E. Webster.** 1992. Localization of TraC, a protein involved in assembly of the F conjugative pilus. J Bacteriol. **174**(11):3800-3806.
181. **Schmidt, S. A., D. Bieber, S. W. Ramer, J. Hwang, C. Y. Wu, and G. Schoolnik.** 2001. Structure-function analysis of BfpB, a secretin-like protein encoded by the bundle-forming-pilus operon of enteropathogenic *Escherichia coli*. J Bacteriol. **183**(16):4848-4859.
182. **Schroder, G., S. Krause, E. L. Zechner, B. Traxler, H. J. Yeo, R. Lurz, G. Waksman, and E. Lanka.** 2002. TraG-like proteins of DNA transfer systems and of the *Helicobacter pylori* type IV secretion system: inner membrane gate for exported substrates? J Bacteriol. **184**(10):2767-2779.
183. **Segal, E. D., J. Cha, J. Lo, S. Falkow, and L. S. Tompkins.** 1999. Altered states: involvement of phosphorylated CagA in the induction of host cellular growth changes by *Helicobacter pylori*. Proc Natl Acad Sci U S A. **96**(25):14559-14564.
184. **Seisenberger, G., M. U. Ried, T. Endreb, H. Buning, M. Hallek, and C. Brauchle.** 2001. Real-time single-molecule imaging of the infection pathway of an adeno-associated virus. Science. **294**(5548):1929-1932.
185. **Shanahan, P. M., M. V. Jesudason, C. J. Thomson, and S. G. Amyes.** 1998. Molecular analysis of and identification of antibiotic resistance genes in clinical isolates of *Salmonella typhi* from India. J Clin Microbiol. **36**(6):1595-1600.

186. **Shanahan, P. M., K. A. Karamat, C. J. Thomson, and S. G. Amyes.** 2000. Characterization of multi-drug resistant *Salmonella typhi* isolated from Pakistan. *Epidemiol Infect.* **124**(1):9-16.
187. **Sherburne, C. K., T. D. Lawley, M. W. Gilmour, F. R. Blattner, V. Burland, E. Grotbeck, D. J. Rose, and D. E. Taylor.** 2000. The complete DNA sequence and analysis of R27, a large IncHI plasmid from *Salmonella typhi* that is temperature sensitive for transfer. *Nucleic Acids Res.* **28**(10):2177-2186.
188. **Shirasu, K., and C. I. Kado.** 1993. Membrane location of the Ti plasmid VirB proteins involved in the biosynthesis of a pilin-like conjugative structure on *Agrobacterium tumefaciens*. *FEMS Microbiol Lett.* **111**(2-3):287-294.
189. **Shoemaker, N. B., G. R. Wang, and A. A. Salyers.** 2000. Multiple gene products and sequences required for excision of the mobilizable integrated *Bacteroides* element NBU1. *J Bacteriol.* **182**(4):928-936.
190. **Skerker, J. M., and H. C. Berg.** 2001. Direct observation of extension and retraction of type IV pili. *Proc Natl Acad Sci U S A.* **98**(12):6901-6904.
191. **Smith, H. W.** 1974. Letter: Thermosensitive transfer factors in chloramphenicol-resistant strains of *Salmonella typhi*. *Lancet.* **2**(7875):281-282.
192. **Sourjik, V., and H. C. Berg.** 2000. Localization of components of the chemotaxis machinery of *Escherichia coli* using fluorescent protein fusions. *Mol Microbiol.* **37**(4):740-751.
193. **Stein, M., R. Rappuoli, and A. Covacci.** 2000. Tyrosine phosphorylation of the *Helicobacter pylori* CagA antigen after cag-driven host cell translocation. *Proc Natl Acad Sci U S A.* **97**(3):1263-1268.
194. **Straight, A. F., A. S. Belmont, C. C. Robinett, and A. W. Murray.** 1996. GFP tagging of budding yeast chromosomes reveals that protein-protein interactions can mediate sister chromatid cohesion. *Curr Biol.* **6**(12):1599-1608.
195. **Szpirer, C. Y., M. Faelen, and M. Couturier.** 2000. Interaction between the RP4 coupling protein TraG and the pBHR1 mobilization protein Mob. *Mol Microbiol.* **37**(6):1283-1292.

196. **Taylor, D. E.** 1989. General properties of resistance plasmids, p. 325-357. *In* L. E. Bryan (ed.), *Handbook of Experimental Pharmacology*, vol. 91. Springer-Verlag, Berlin.
197. **Taylor, D. E., and E. C. Brose.** 1988. Modified Birnboim-Doly method for rapid detection of plasmid copy number. *Nucleic Acids Res.* **16**(18):9056.
198. **Taylor, D. E., A. Gibreel, T. D. Lawley, and D. M. Tracz.** 2003. Antibacterial resistance mechanisms. *In* G. Philips and B. Funnel (ed.), *Biology of Plasmids*. ASM Press, Washington. In Press.
199. **Taylor, D. E., and J. G. Levine.** 1980. Studies of temperature-sensitive transfer and maintenance of H incompatibility group plasmids. *J Gen Microbiol.* **116**(2):475-484.
200. **Taylor, D. E., M. Rooker, M. Keelan, L. Ng, I. Martin, N. T. Perna, V. Burland, and F. R. Blattner.** 2002. Genomic variability of O islands encoding tellurite resistance in enterohemorrhagic *Escherichia coli* O157:H7 isolates. *J Bacteriol.* **184**(17):4690-4698.
201. **Thorsted, P. B., D. P. Macartney, P. Akhtar, A. S. Haines, N. Ali, P. Davidson, T. Stafford, M. J. Pocklington, W. Pansegrau, B. M. Wilkins, E. Lanka, and C. M. Thomas.** 1998. Complete sequence of the IncPbeta plasmid R751: implications for evolution and organisation of the IncP backbone. *J Mol Biol.* **282**(5):969-990.
202. **Tobe, T., T. Hayashi, C. G. Han, G. K. Schoolnik, E. Ohtsubo, and C. Sasakawa.** 1999. Complete DNA sequence and structural analysis of the enteropathogenic *Escherichia coli* adherence factor plasmid. *Infect Immun.* **67**(10):5455-5462.
203. **Top, E. M., Y. Moenne-Loccoz, T. Pembroke, and C. M. Thomas.** 2000. Phenotypic traits conferred by plasmids, p. 249-285. *In* C. M. Thomas (ed.), *The Horizontal Gene Pool*. Harwood Academic Publishers, Amsterdam.
204. **Tsien, R. Y.** 1998. The green fluorescent protein. *Annu Rev Biochem.* **67**:509-544.
205. **van Elsas, J. D., J. Fry, P. Hirsch, and S. Molin.** 2000. Ecology of plasmid transfer and spread, p. 175-206. *In* C. M. Thomas (ed.), *The Horizontal Gene Pool*. Harwood Academic Publishers, Amsterdam.

206. **Watanabe, E., M. Wachi, M. Yamasaki, and K. Nagai.** 1992. ATPase activity of SopA, a protein essential for active partitioning of F plasmid. *Mol Gen Genet.* **234(3):346-352.**
207. **Waters, V. L.** 2001. Conjugation between bacterial and mammalian cells. *Nat Genet.* **29(4):375-376.**
208. **Waters, V. L., K. H. Hirata, W. Pansegrau, E. Lanka, and D. G. Guiney.** 1991. Sequence identity in the nick regions of IncP plasmid transfer origins and T-DNA borders of *Agrobacterium* Ti plasmids. *Proc Natl Acad Sci U S A.* **88(4):1456-1460.**
209. **Waters, V. L., B. Strack, W. Pansegrau, E. Lanka, and D. G. Guiney.** 1992. Mutational analysis of essential IncP alpha plasmid transfer genes *traF* and *traG* and involvement of *traF* in phage sensitivity. *J Bacteriol.* **174(20):6666-6673.**
210. **Webb, C. D., A. Teleman, S. Grodon, A. Straight, A. Belmont, D. C. Lin, A. D. Grossman, A. Wright, and R. Losick.** 1997. Bipolar localization of the replication origin regions of chromosomes in vegetative and sporulating cells of *B. subtilis*. *Cell.* **88(5):667-674.**
211. **Weiss, A. A., F. D. Johnson, and D. L. Burns.** 1993. Molecular characterization of an operon required for pertussis toxin secretion. *Proc Natl Acad Sci U S A.* **90(7):2970-2974.**
212. **Whelan, K. F., D. Maher, E. Colleran, and D. E. Taylor.** 1994. Genetic and nucleotide sequence analysis of the gene *htdA*, which regulates conjugal transfer of IncHI plasmids. *J Bacteriol.* **176(8):2242-2251.**
213. **Willetts, N.** 1993. Bacterial conjugation: a historical perspective, p. 1-22. *In* D. B. Clewell (ed.), *Bacterial Conjugation*. Plenum Press, New York.
214. **Willetts, N., and B. M. Wilkins.** 1984. Processing of plasmid DNA during bacterial conjugation. *Microbiol Rev.* **48(1):24-41.**
215. **Winans, S. C., and G. C. Walker.** 1985. Conjugal transfer system of the IncN plasmid pKM101. *J Bacteriol.* **161(1):402-410.**
216. **Wolkow, C. A., R. T. DeBoy, and N. L. Craig.** 1996. Conjugating plasmids are preferred targets for Tn7. *Genes Dev.* **10(17):2145-2157.**

217. **Yu, D., H. M. Ellis, E. C. Lee, N. A. Jenkins, N. G. Copeland, and D. L. Court.** 2000. An efficient recombination system for chromosome engineering in *Escherichia coli*. *Proc Natl Acad Sci U S A.* **97**(11):5978-5983.
218. **Zechner, E. L., F. de la Cruz, R. Eisenbrandt, A. M. Grahn, G. Koraimann, E. Lanka, G. Muth, W. Pansegrau, C. M. Thomas, B. M. Wilkins, and M. Zatyka.** 2000. Conjugative-DNA transfer processes, p. 87-174. *In* C. M. Thomas (ed.), *The Horizontal Gene Pool*. Harwood Academic Publishers, Amsterdam.
219. **Zhang, J., R. E. Campbell, A. Y. Ting, and R. Y. Tsien.** 2002. Creating new fluorescent probes for cell biology. *Nat Rev Mol Cell Biol.* **3**(12):906-918.
220. **Zhu, J., P. M. Oger, B. Schrammeijer, P. J. Hooykaas, S. K. Farrand, and S. C. Winans.** 2000. The bases of crown gall tumorigenesis. *J Bacteriol.* **182**(14):3885-3895.